VAASA UNIVERSITY

FACULTY OF TECHNOLOGY

DEPARTMENT OF ELECTRICAL ENGINEERING AND AUTOMATION

Jani Ahvonen

DESIGN AND IMPLEMENTATION OF NEAR-FIELD MEASUREMENT PROBES

Master´s thesis for the degree of Master of Science in Technology submitted for inspection in Vaasa, 21th of November 2011.

Inspector	D.Sc (Tech) Timo Vekara
Evaluator	M.Sc (Tech) Maarit Vesapuisto
Instructor	M.Sc (Tech) Santiago Chavez

ACKNOWLEDGEMENTS

I will thank D.Sc Timo Vekara, M.Sc Maarit Vesapuisto and M.Sc Santiago Chavez for good and professional advices during the work.

I want to thank my lovely wife Katherine del Carpio Ahvonen for support and encouragement during this work.

In addition, I would like to thank Master student Daniel Tizda proofreading of this report.

TABLE OF CONTENTS

ABBREVIATIONS AND SYMBOLS

Abbreviations

BNC	Bayonet Neill-Concelman
EC	European commission
EM	Electromagnetic
EMC	Electromagnetic compatibility
EMI	Electromagnetic interference
EU	European Union
EUT	Equipment under test
ICD	Implantable cardioverter defibrillator
OATS	Open area test site
PCB	Printed circuit board
RMS	Root mean square
SA	Spectrum analyser
TTL	Transistor-transistor logic

Symbols

$\boldsymbol{A}$	Magnetic vector potential [Vs/m]
$\boldsymbol{B}$	Magnetic flux density [Vs/m^2]
C	Capacitance [As/V]
c	The speed of light $300 \cdot 10^6$ m/s
c_0	Fourier series DC-component
c_n	Fourier series harmonic number n
$\boldsymbol{D}$	Electric flux density [As/m^2]
d_{loop}	Diameter of loop antenna [m]
d_{wire}	Diameter of wire [m]
$\boldsymbol{E}$	Electric field strength [V/m]
$\boldsymbol{e}_z$	Unit vector (direction z)
f	Frequency [1/s]
$\boldsymbol{H}$	Magnetic field strength [A/m]

h_e	Effective length of the antenna [m]
I	Current (RMS) [A]
I_{CM}	Common-mode current (RMS) [A]
I_m	Antenna maximum current (amplitude) [A]
$\hat{\imath}$	Current (amplitude) [A]
j	Imaginary unit
$\boldsymbol{J}_C$	Conduction current density [A/m^2]
$\boldsymbol{J}_D$	Displacement current density [A/m^2]
k_1	Correction factor $0.8 \cdot 10^6$ [Am/Vs]
k_2	Correction factor $10.6 \cdot 10^{-3}$ [A/V]
L,l	Length [m]
L_e	External Inductance [Vs/A]
r	Distance [m]
R_L	Ohmic losses of an antenna [V/A]
R_r	Radiation resistance [V/A]
S	Surface area [m^2]
s	Side length of the magnetic field probe [m]
T	Period time [s]
t	Time [s]
t_f	Fall time [s]
t_r	Rise time [s]
$\hat{u}$	Voltage (amplitude) [V]
V_{OC}	Open circuit voltage (amplitude) [V]
X	Reactance [V/A]
$x(t)$	Function of time
X_a	Reactance (antenna) [V/A]
Z	Impedance [V/A]
Z_0	Characteristic impedance [V/A]
Z_{LOAD}	Load impedance [V/A]
Z_T	Transfer impedance [V/A]
V	Volume [m^3]

Greek

η_0	Wave impedance [V/A]
β	Phase shift constant [1/m]
λ	Wavelength [m]
μ_0	Permeability of vacuum [Vs/Am]
μ_r	Relative permeability
ρ_V	Volume charge density [As/m^2]
σ_{CU}	Conductivity of copper [A/Vm]
τ	Time constant [s]
ϕ	Magnetic flux [Vs]
ω	Angular frequency [rad/s]
ω_0	Angular frequency of fundamental frequency f [rad/s]
ε_0	Permittivity of vacuum [As/Vm]
ε_r	Relative permittivity
ε_{rad}	Radiation efficiency
∇	Nabla

UNIVERSITY OF VAASA
Faculty of technology
Author: Jani Ahvonen
Topic of the Thesis: Designing and implementation of near-field measurement probes
Supervisor: Timo Vekara
Evaluator: Maarit Vesapuisto
Instructor: Santiago Chavez
Degree: Master of Science in Technology
Major of Subject: Electrical Engineering
Year of Entering the University: 2004
Year of Completing the Thesis: 2011
Pages: 120

ABSTRACT

The problems of electronics product because of electromagnetic incompatibility are increasing constantly. To end this incompatibility the European Union (EU) has decided to empower the Directive 2004/108/EC so devices could operate close to each other properly.

The product manufacturers are required to make standardized tests to verify that the product is compliant with the Directive 2004/108/EC. Many times the designer uses a lot of time to design product functions and uses project time for verification of these functions. However, the final product should be tested in according the most recent electromagnetic standards and one of these many tests is the radio disturbance test as a function of frequency and for this disturbance the standard states limit values.

This thesis is intended to bring out some phenomena by using calculations to show that how these limit values are easily broken if the product contains some design faults for example in the printed circuit board. The main focus is to design a near-field measurement probes which are electric field probes, magnetic field probes and a high-frequency current probe.

The standardized test is done in the far field, and sometimes for the designer it is very difficult to spot the origin of interference. According the measurement results of this thesis the designed and implemented near-field probes can be used efficiently to locate the origin of interference. The magnetic field probe and electric field probe can be used to spot interference source from the printed circuit board (PCB) and high-frequency current probe can be used to search product external cable which carries common-mode current. According the calculations of this thesis the common-mode current is most problematic radiator from electronic product cabling.

KEYWORDS: near-field probe, receiving loop antenna, receiving dipole antenna, current probe.

1 INTRODUCTION

The purpose of this work is to develop a concrete near-field measurement probes which can be used to measure electromagnetic interferences at different frequencies. This kinds of measurement probes can be purchased from many different manufacturers but those probes are relatively expensive. The near-field measurement probes, are made from different kind of small antennas and high-frequency current probes which are quite simple and cheap to implement for the purposes of qualitative measurements because near-field magnitudes are not easily comparable with far field values. This is a quantitative research where subject is a near-field measurement probes and other subject is electromagnetic phenomena.

Field theory has been used to find interference problems, like electromagnetic radiation caused problems, and some phenomena are tested in test bench. The focus is to search interference source from product which contains electronics like microprocessors. To ensure that electromagnetic field theories apply in electronic device, the concrete measurements were done with near-field measurement probes. As references of this study are the latest electromagnetic compatibility books, antenna books, publications, documents from various component manufacturers and various measurement equipment manufacturers.

2 ELECTROMAGNETICS

2.1 Maxwell equations

James Clerk Maxwell's equations of electromagnetism can be thought of as 1800-century greatest achievements and these equations are comparable to Isaac Newton's achievements in mechanics. Maxwell equations can be used as a macroscopic level and equations can be taught as axiom which can be used describing for example antenna radiation. (Lehto 2006: 56-57)

History contains many people who were involved with electromagnetics. These are the main researchers who influenced to James Clerk Maxwell equations; Andre Marie Ampere (1775–1836), Michael Faraday (1791–1867), Johann Carl Friedrich Gauss (1777–1855) and James Clerk Maxwell (1831–1879). Maxwell equations in Table 1. (Hyper-Jeff Network 2010)

Table 1. Maxwell equations (Edminister 1993, 208)

Equation	**Point Form**	**Integral Form**
Ampére's law	$\nabla \times \boldsymbol{H} = \boldsymbol{J}_{\mathrm{C}} + \frac{\partial \boldsymbol{D}}{\partial t}$	$\oint \boldsymbol{H} \cdot \mathrm{d}\boldsymbol{l} = \int_S \left(\boldsymbol{J}_{\mathrm{C}} + \frac{\partial \boldsymbol{D}}{\partial t} \right) \cdot \mathrm{d}\boldsymbol{S}$
Faraday's law	$\nabla \times \boldsymbol{E} = -\frac{\partial \boldsymbol{B}}{\partial t}$	$\oint \boldsymbol{E} \cdot \mathrm{d}\boldsymbol{l} = \int_S \left(-\frac{\partial \boldsymbol{B}}{\partial t} \right) \cdot \mathrm{d}\boldsymbol{S}$
Gauss' law	$\nabla \cdot \boldsymbol{D} = \rho_V$	$\oint_S \boldsymbol{D} \cdot \mathrm{d}\boldsymbol{S} = \int_V \rho_V \ \mathrm{d}V$
Nonexistence of monopole	$\nabla \cdot \boldsymbol{B} = 0$	$\oint \boldsymbol{B} \cdot \mathrm{d}\boldsymbol{S} = 0$

2.1.1 Ampére's law

The original Ampére's (discoverer Andre Marie Ampére) equation where $\boldsymbol{H}$ is magnetic field strength and $\boldsymbol{J}_C$ is conduction current density,

$$\nabla \times \boldsymbol{H} = \boldsymbol{J}_C. \tag{1}$$

This equation one was modified by (equation 2) Maxwell when he introduced the displacement current density $\boldsymbol{J}_D$

$$\nabla \times \boldsymbol{H} = \boldsymbol{J}_C + \boldsymbol{J}_D = \boldsymbol{J}_C + \frac{\partial \boldsymbol{D}}{\partial t}. \tag{2}$$

Where t is time and $\boldsymbol{D}$ is electric flux density. One example of displacement current is that a magnetic field is generated during the charge or discharge of a capacitor. By using this fact and by using Faraday's law, Maxwell was able to draw a conclusion for the wave equations. (Huang & Boyle 2008, 18)

Figure 1 describes how time-varying electric current density $\boldsymbol{J}$ on a linear antenna produces a circulating and time-varying magnetic field $\boldsymbol{H}$ (Ampére's law), which through Faraday's law generates a circulating electric field $\boldsymbol{E}$, which through Ampére's law generates a magnetic field, and this combination continues. The cross-linked electric and magnetic fields propagate away from antenna. (Orfanidis 2008, 2)

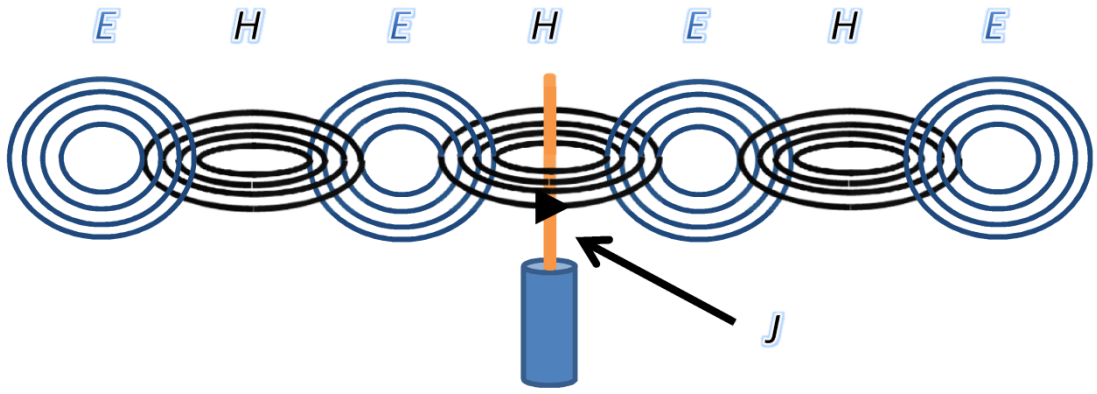

Figure 1. The basic principle of an antenna radiation. (Orfanidis 2008: 2)

2.1.2 Faraday's law

Magnetic induction in equation 3 is an effect discovered by Michael Faraday and this effect connects electricity and magnetism

$$\oint \boldsymbol{E} \cdot \mathrm{d}\boldsymbol{l} = \int_S \left(-\frac{\partial \boldsymbol{B}}{\partial t} \right) \cdot \mathrm{d}\boldsymbol{S} = -\frac{\partial \phi}{\partial t}. \tag{3}$$

Where $\boldsymbol{E}$ is electric field, l is length, $\boldsymbol{S}$ is surface area and ϕ is flux and equation (Crowell 2010: 78). This equation 3 simply means that the induced voltage is proportional to the rate of change of the magnetic flux through a loop

$$\nabla \times \boldsymbol{E} = -\frac{\partial \boldsymbol{B}}{\partial t}. \tag{4}$$

Where $\boldsymbol{B}$ is magnetic flux density. It is obvious from this equation 4 that a time-varying magnetic field will generate an electric field. If the magnetic field is not function of time, it will not generate an electric field and vice versa. (Huang & Boyle 2008: 17)

Changing flux ϕ (blue arrows) in Figure 2 induces the voltage to the loop and induced voltage has a polarity such that the current (red arrow) established in a closed path gives rise to a flux which opposes the change in flux. (Edminister 1993:194)

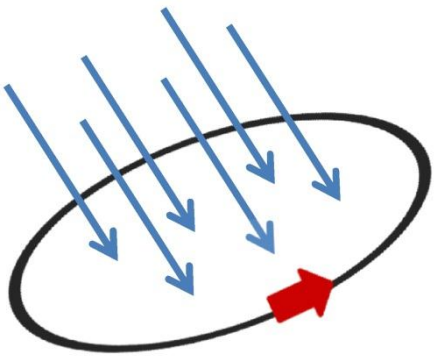

Figure 2. Time varying flux induces voltage which causes a current to the loop.

2.1.3 Gauss' law

Gauss' (discoverer Johann Carl Friedrich Gauss) law states that the total flux out of a closed surface is equal to the net charge within the surface where ρ_V is volume charge (Edminister 1993, 34):

$$\nabla \cdot \boldsymbol{D} = \rho_V . \tag{5}$$

This equation 5 is the electrostatic application of Gauss's theorem, gives the equivalence relation between electric flux flowing out of any closed surface and the result of inner sources and sinks, such as electric charges enclosed within the closed surface. It is not possible for electric fields to form a closed loop. Since $\boldsymbol{D} = \varepsilon \boldsymbol{E}$, it is obvious that charge ρ can generate electric field. (Huang & Boyle 2008: 18)

The surface over which Gauss' law is used must be closed, but it can be made up of many different plates. If these plates can be selected so that $\boldsymbol{D}$ is either tangential or normal and if $|\boldsymbol{D}|$ is constant over any plate to which $\boldsymbol{D}$ is normal. Figure 3 contains parallel plate capacitor with electric field (arrows). For example Gauss' law can be used to determine magnitude for electric flux density which is equal to magnitude of the surface charge density. Fringing is neglected. (Edminister 1993: 35, 43, 44)

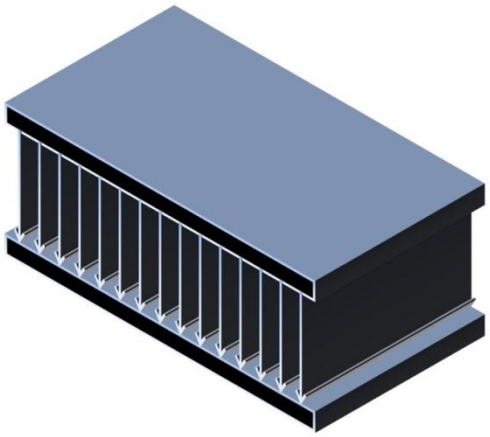

Figure 3. Parallel plate capacitor and electric flux.

2.1.4 Nonexistence of monopole

Equation 6 shows that the divergence of the magnetic field density is always zero, which means that the magnetic field density lines are closed loops and the integral of $\boldsymbol{B}$ over a closed surface is zero (Huang & Boyle 2008: 18):

$$\nabla \cdot \boldsymbol{B} = 0. \tag{6}$$

2.1.5 Heinrich Rudolf Hertz antenna experiment

The first well-known antenna experiment was made by the German physicist Heinrich Rudolf Hertz (1857–1894). The SI frequency unit, the Hertz (Hz), is named after Heinrich Rudolf Hertz. In 1887 Hertz built a system, as shown in Figure 4, to produce and detect radio waves. The original idea of his experiment was to demonstrate the existence of electromagnetic waves. In the transmitter, a variable voltage source was connected to a dipole antenna which is a pair of one-meter wires with two conducting spheres at the ends. The gap between the spheres could be changed for circuit resonance as well as for the generation of sparks. When the voltage was increased to high enough the breakdown discharge was produced. The receiver was a simple loop with two identical conducting spheres. The gap between the spheres was carefully adjusted to receive the spark effectively. Hertz put the apparatus in a darkened box in order to see the spark. During the experiment sparks can be seen in both transmitter and receiver almost at the same time. (Huang & Boyle 2008: 2)

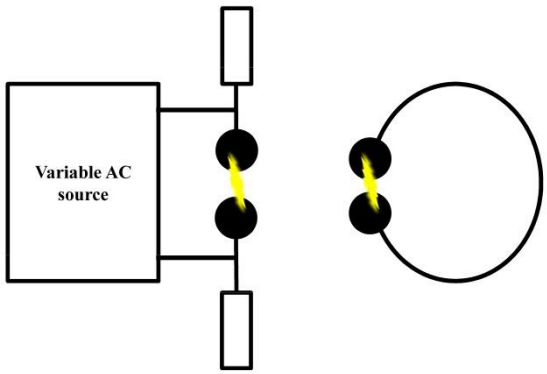

Figure 4. Hertz test equipment consist transmitter and receiver.

2.2 Electromagnetic compatibility

2.2.1 What is electromagnetic compatibility?

The consideration of electromagnetic compatibility during electronic product design will ensure that the product works well in the environment where we want to use it. Electromagnetic compatibility also ensures that product does not unduly generate interfering fields to other systems or devices. These two issues can be found from EU Directive 2004/108/EC and all EU countries must follow this directive. If a product creates electromagnetic (EM) fields which are unwanted then those EM fields are considered as interference. One example of wanted EM field is radio station transmitter fields. Interference can propagate through wires or through air. For example in television (TV) screen interference tracks, radio interference or even computer malfunctions are many times caused by other nearby electric devices. (Tukes 2011)

Amplitude modulation (AM) radio station transmitter is shown as a source box in Figure 5 and it's transmission is picked up by another radio receiver that is tuned to that carrier frequency behaves as wanted emitter. If the same AM radio transmission is received by another radio receiver which is not tuned to the carrier frequency of the transmitter, then the EM waves are unwanted. (Clayton 2006: 3-4)

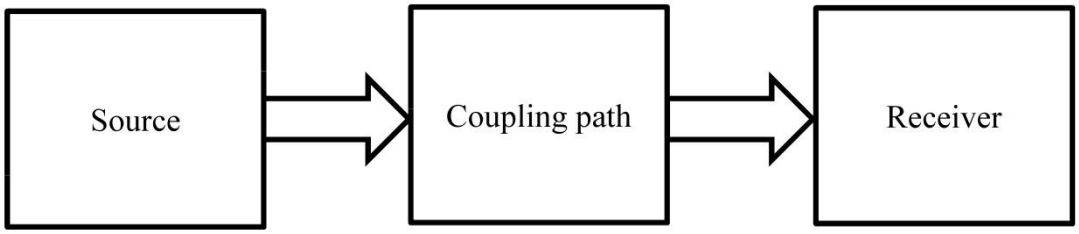

Figure 5. EM-wave travels from source through coupling path to receiver.

2.2.2 Some reported cases in electromagnetic incompatibility

B-52 Missile Interface Unit problem

When making the aircraft bomber B-52 missile interface unit test, an unwanted missile launch was given. One of the contributing factors was near-field coupling in the system wiring. Another factor was that the designers do not pay attention to the electromagnetic compatibility (EMC) control plan requirements. Because of this the project needs an extra year-long redesign and test effort. (Nasa 1995)

H.M.S Sheffield Catastrophe

Falklands War (war between Argentina and Great Britain) was in 1982 and the British Royal Navy warship H.M.S. Sheffield sank with many casualties after being hit by a French made Exocet missile. The Sheffield warship has the most advanced antimissile defence system available. This antimissile system creates electromagnetic interference to ship radio communications and this causes communication problems with Harrier jets. While the Harrier aircraft land and take took off, the antimissile defence system was disengaged to allow communications with the Harrier jets and this method provides a time window of opportunity to the Exocet missile to hit. (Nasa 1995)

Safety critical control systems

New electronics of embedded systems contain increasing amount of microcontrollers and circuit boards and also the microcontroller clock frequencies increase every year, which might interfere with safety-critical control systems. (University of Toulouse 2007) Examples of safety critical-control systems are car anti-lock braking system (ABS) or electric wheel chairs. Electromagnetic compatibility directive makes possible that these safety-critical control systems can be used without interference problems and for example radio traffic with mobile phones can be used without interference problems. Free operation is possible because the EU has set emission limits for radiation from equipments and in Finland these limits are monitored by Tukes (Finnish safety and chemicals agency) and Ficora (Finnish communication regulatory authority). (Tukes 2011)

Interference caused by mobile phone

Some cases, a mobile phone could affect an implantable cardioverter defibrillator's (ICD) or pacemaker's operation if the distance is less than 15 cm to the implanted equipment. This interaction is temporary, and moving the mobile phone away from the implanted equipment will return it to proper function. (UNC School of Medicine)

2.2.3 History of electromagnetic compatibility

Military and electromagnetic compatibility

EMC first began to be remarkable in the military environment, especially on-board ships where many types of electronic products had to properly operate in close proximity. In this environment communication, navigation and data processing electronics all need to work at the same time in the presence of strong EM fields. Such EM fields are produced by two-way communications products, radar transmitters and microprocessor controlled equipment. In addition to these EM fields on-board a military ship there are explosives and aircraft fuel. In this environment it is very important that all equipments are electromagnetically compatible with their environment and malfunctions cannot be accepted. Also all equipments added to this milieu cannot unnecessarily or unintentionally radiate EM fields that do not perform any particular function. From the preceding, the origin of the two major phenomena of EMC, emissions and immunity, can be recognized. (Analab 2011)

Electric wheelchair problem

U.S department of health & human services got some reports that electromagnetic interference can cause some manufacturer's battery powered wheelchairs to move unexpectedly. The agency has investigated those products and they determined that electromagnetic interference (EMI) can cause unexpected movement in some battery powered wheelchairs when those are turned on. (National Semiconductor 1996)

3 ELECTROMAGNETIC INTERFERENCE

3.1 Some common sources of electromagnetic interference

Digital microcontrollers can be found in nearly every product of modern life. Many consumer and commercial equipments for example almost in every home can be found mobile phones, digital cameras, MP3 players, personal computers, printers, cordless phones, televisions, remote controllers, microwave ovens, washing machines, thermometers and the like are being controlled by digital microcontrollers. Additionally many microcontrollers can be found in industrial products. (Renesas 2007)

The use of microcontroller-based systems increases all the time and especially in such areas as industrial, automotive and consumer applications, where manufacturers focus on to make cost effective products. This means increasing complexity of such systems and highly integrated single chip systems are needed so semiconductor manufacturers have to respond to this need. This also means high operating frequency microcontrollers by using the highest packing density technology possible. The fact is that the higher density and the faster operation of chips means higher EMI level which is generated because of these microcontrollers. (STM Microelectronics 2000)

From the physics point of view electromagnetic radiation is produced by any accelerated or any decelerated charge which means that there has to be time-varying current element. (Nikolova, 2010)

3.2 Common-mode radiation

Common-mode radiation is the result of not desirable inductance, capacitance and resistance in the circuit and results from unwanted voltage losses in the conductors. The normal operation current which is differential mode current in Figure 6 flows through ground impedance and produces a voltage loss in the digital logic ground system. The cables which are connected to the equipment are driven by this common-mode ground

potential and these cables act like antennas which radiate predominately electric fields. (Ott 2009: 464)

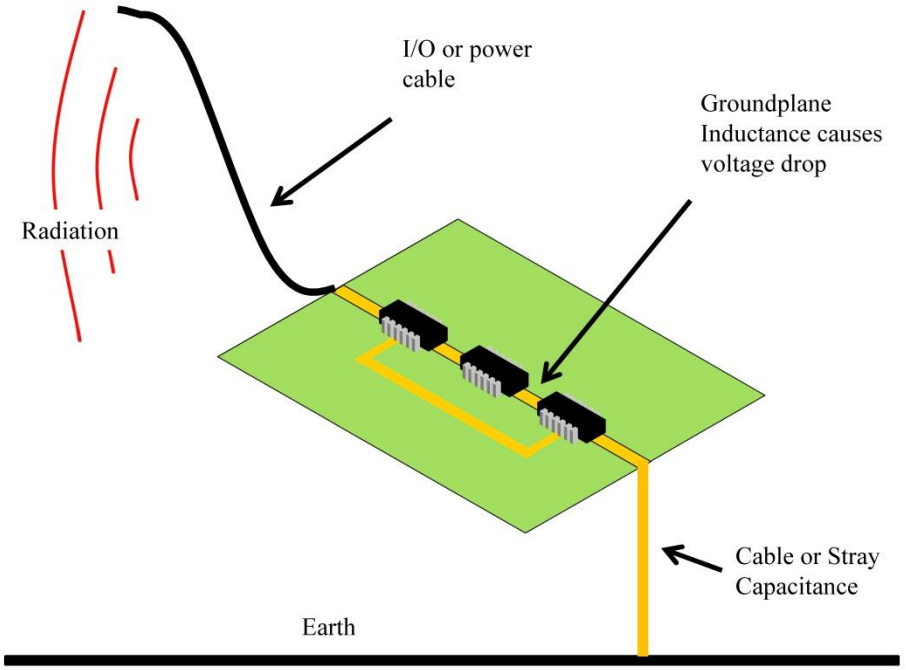

Figure 6. Poor PCB ground causes a voltage drop which causes a common-mode radiation from device external cables. (Willis 2007: 238)

If the person who designs the electronic device understands the antenna theory then the controlling of common-mode radiation becomes a lot easier task. This means that the design engineer should know how a dipole antenna works, and how this antenna operation is related to the common-mode radiation from a product. (Ott 2009: 765)

Antenna is a transformer of current or voltage to a magnetic field or electric field and it can also be considered as a bridge to link the EM wave and the transmission line. (Huang & Boyle 2008: 5)

3.2.1 Electrically small dipole antenna

The electrically small dipole which is also called Hertzian dipole antenna consists of an infinitesimal (infinitesimal means that antenna is so small that there is no way to measure antenna length) current element of length dl carrying a phasor current I that is predicted to be the same in phase and magnitude (same current distribution) at all points along the antenna length, as illustrated in Figure 7. This is because EM waves radiated from antennas at long distances are spherical waves and that's why the spherical coordinate system is commonly used to describe antennas. (Clayton 2006: 422)

There are many thumb rules for considering an antenna to be electrically small. The most used definition is that the longest dimension of the antenna is smaller than $\lambda/10$. Thus, a dipole with a length of $\lambda/10$ or a loop antenna with a diameter of $\lambda/10$ can be considered as electrically small. (High-frequency Design 2007)

Small dipole antenna (Herzian dipole antenna) frequency domain representation for magnetic vector potential in the z direction can be found from equation 7. Antenna is assumed to be in free space, where A_z magnetic vector potential, I is antenna current, r is distance between antenna and observation point, μ_0 is vacuum permeability, j is imaginary unit and β is phase shift constant (Vesapuisto 2009: 30):

$$A_z = \frac{I\,\mu_0 \mathrm{e}^{-\mathrm{j}\beta r}}{4\pi r}\mathrm{d}l. \tag{7}$$

The following equations 8, 9 and 10 show the magnetic vector potential transformation to spherical (r, θ, ϕ) coordinates. Spherical magnetic vector potential is valid also in Figure 7 at the point P, where θ is angle between z-axel and xy-plane in spherical coordinate system (Vesapuisto 2009: 30):

$$A_r = A_z \cos\theta = \frac{I\,\mu_0 \mathrm{e}^{-\mathrm{j}\beta r}}{4\pi r}\mathrm{d}l\cos\theta, \tag{8}$$

$$A_\theta = -A_z \sin\theta = -\frac{I\,\mu_0 \mathrm{e}^{-\mathrm{j}\beta r}}{4\pi r}\mathrm{d}l\sin\theta \quad \text{and} \tag{9}$$

$$A_\varphi = 0. \tag{10}$$

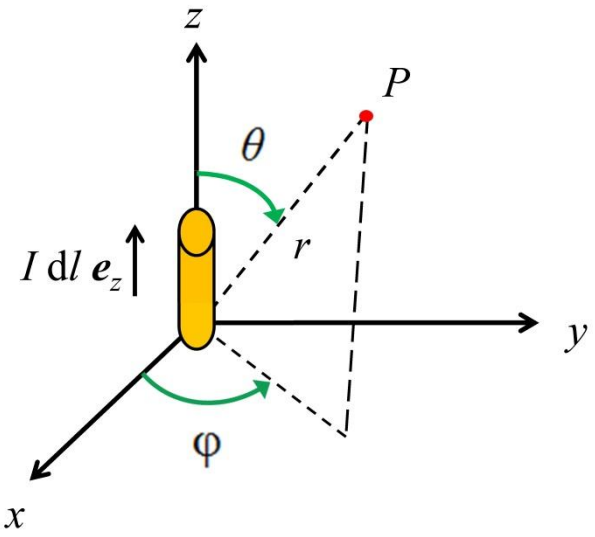

Figure 7. Small dipole antenna represented by using Cartesian coordinates and Spherical coordinates . (Edminister 1993: 294)

The curl of magnetic vector potential ***A*** gives the magnetic field at the point *P*

$$\boldsymbol{H} = \frac{1}{\mu_0} \nabla \times \boldsymbol{A}. \tag{11}$$

The curl of magnetic field ***H*** gives the electric field ***E*** at the point *P* where ω angular frequency and ε_0 is permittivity of vacuum

$$\boldsymbol{E} = \frac{1}{\mathrm{j}\omega\varepsilon_0} \nabla \times \boldsymbol{H}. \tag{12}$$

All in all the magnetic field is present only in ϕ direction and electric field at the direction r and θ and equations 13-15 contain all information regarding the antenna. (Vesapuisto 2009). Where η_0 wave impedance of vacuum,

$$H_{\varphi} = -\frac{I\,\mathrm{d}l}{4\pi}\beta^2 \sin\theta\left[\frac{1}{\mathrm{j}\beta r} + \frac{1}{(\mathrm{j}\beta r)^2}\right]\mathrm{e}^{-j\beta r}, \tag{13}$$

$$E_{r} = -\frac{I\,\mathrm{d}l}{2\pi}\eta_0\beta^2 \cos\theta\left[\frac{1}{(j\beta r)^2} + \frac{1}{(\mathrm{j}\beta r)^3}\right]\mathrm{e}^{-j\beta r} \quad \text{and} \tag{14}$$

$$E_{\theta} = -\frac{I\,\mathrm{d}l}{4\pi}\eta_0\beta^2 \sin\theta\left[\frac{1}{\mathrm{j}\beta r} + \frac{1}{(\mathrm{j}\beta r)^2} + \frac{1}{(\mathrm{j}\beta r)^3}\right]\mathrm{e}^{-j\beta r}. \tag{15}$$

When we make near-field measurements by using near-field probes we are interested in near-field equations. For a small dipole antenna where λ is wavelength and the near-field definition is

$$\beta r = \frac{2\pi r}{\lambda} << 1 \rightarrow \frac{\lambda}{2\pi} >> r. \tag{16}$$

If multiplier $e^{-j\beta r} = 1 - 1/\beta r + 1/(\beta r)^2 + \ldots \approx 1$ then the equation 13 for the near-field can be calculated and equation 17 shows that magnetic field decreases rapidly, inversely in proportion to the square of distance

$$H_{\varphi} = \frac{I\,\mathrm{d}l}{4\pi r^2}\sin\theta. \tag{17}$$

Near electric field functions decrease as a function of distance even more rapidly than magnetic field function and now the frequency is inversely proportional to the electric field amplitude, where *f* is frequency and electric fields are (Vesapuisto 2009):

$$E_{r} = -\mathrm{j}\frac{I\,\mathrm{d}l}{4\pi^2 f\,\varepsilon_0 r^3}\cos\theta \quad \text{and} \tag{18}$$

$$E_{\theta} = -\mathrm{j}\frac{I\,\mathrm{d}l}{8\pi^2 f\,\varepsilon_0 r^3}\sin\theta. \tag{19}$$

The equations 20 and 21 contain the far field functions and it is interesting to see that frequency has directional proportion to the magnetic field amplitude and the electric

field amplitude. This means from a practical point of view that radiation increases from small dipole antenna when frequency is increased, where c is the speed of light and the equations are (Clayton 2006: 423):

$$H_{\varphi} = \mathrm{j}\frac{I\,\mathrm{d}l\,f\,\mu_0}{2\,r\,\eta_0}\sin\theta\,\mathrm{e}^{-\mathrm{j}\left[\frac{2\pi\,f\,r}{c}\right]} \quad \text{and} \tag{20}$$

$$E_{\theta} = \mathrm{j}\frac{I\,\mathrm{d}l\,f\,\mu_0}{2\,r}\sin\theta\,\mathrm{e}^{-\mathrm{j}\left[\frac{2\pi\,f\,r}{c}\right]}. \tag{21}$$

When dipole antenna is used as a radiator we want to know the antenna's electric field or magnetic field at some distance. The radiation resistance R_r is defined as the equivalent resistor that would dissipate a power equal to the power radiated by the antenna when fed by the current I. If we have dl = 10 mm antenna, frequency f of interest is in range 80 MHz to 1000 MHz, frequency dependent resistance for losses R_L (conductivity for copper σ_{CU} = 57 MS/m), antenna radius (0.5 mm), θ = 90°, distance 3 m and needed electric field for standardized industry immunity test $|E|$ = 10 V/m. (IEC61000-6-2: 21)

We want to know current I (and efficiency ε_rad) which have to flow through the antenna to produce 10 V/m at the distance of 3 m. Antenna length dl is very small compared to the wavelength λ >> dl = 0.01 m so we can assume that the current distribution in the antenna is almost uniform. So we can use small dipole equations which are the same as for the Hertzian dipole antenna. (Clayton 2006: 14, 425)

Equations 22, 23 and 24 have to be used to calculate current and efficiency, where R_r is the radiation resistance of the antenna, R_L is ohmic losses of the antenna, I_m is the maximum current (amplitude value of current) of the antenna, ε_rad is radiation efficiency of the antenna and equations are (Edminister 1993: 294, 303):

$$R_\mathrm{r} = \frac{2\pi\eta_0}{3}\left(\frac{f\,\mathrm{d}l}{c}\right)^2, \tag{22}$$

$$I_\mathrm{m} = \frac{2\,r\,|E|\,c}{\eta_0\;\;f\,\mathrm{d}l\sin(\theta)} \quad \text{and} \tag{23}$$

$$\varepsilon_{\text{rad}} = \frac{R_{\text{r}}}{\left(R_{\text{r}} + R_{\text{L}}\right)}. \tag{24}$$

Figure 8 shows an antenna equivalent circuit diagram which applies to all dipole antennas. Voltage source can be either unwanted interference source or wanted transmitter amplifier. (Edminister 1993: 300) (Clayton 2006: 436, 438, 439)

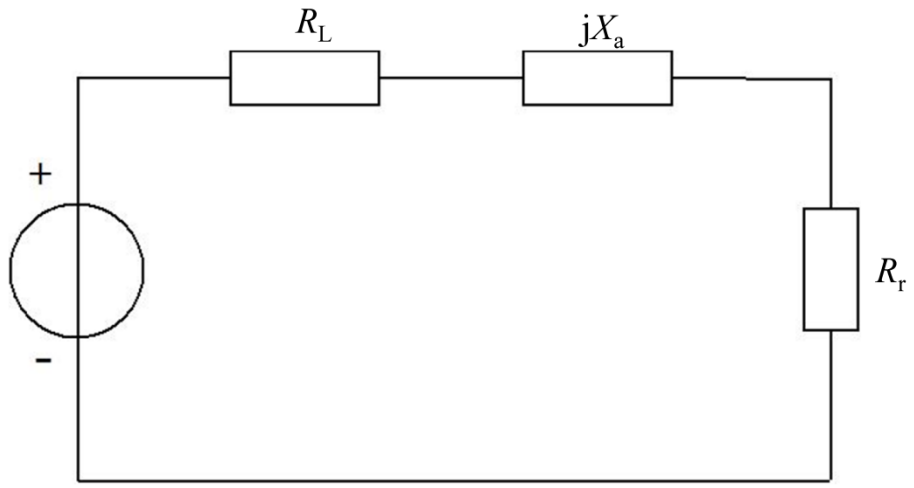

Figure 8. Transmitter dipole antenna equivalent circuit.

Antennas are reciprocal so same circuit can be used when antenna is used as a receiving antenna and now the voltage source V_{OC} is the received voltage and maximum power to the load Z_{LOAD} in Figure 9 can be delivered when $Z_{\text{LOAD}} = (R_{\text{r}} + \text{j}X_{\text{a}})^*$ which means that the antenna's reactance X_{a} component disappears and only R_{r} and R_{L} are in series with the load Z_{LOAD}. (Edminister 1993: 300)

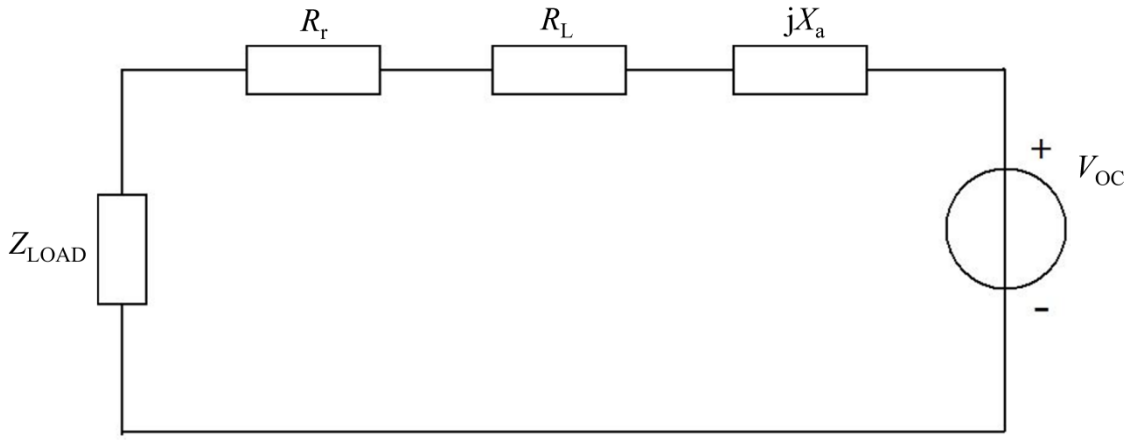

Figure 9. Receiver dipole antenna equivalent circuit.

Table 2 shows some calculated results. The high current value I_m shows that the antenna of length dl = 10 mm is not an efficient radiator at low frequencies and the radiation efficiency ε_{rad} is quite poor, but in high frequencies the antenna is quite efficient radiator. Table 2 means that we need five amps current to achieve 10 V/m electric field at the distance of three meters.

Table 2. Electrically small antenna calculations.

f [MHz]	R_r [Ω]	R_L [Ω]	I_m [A]	ε_{rad} [%]
30	$790 \cdot 10^{-6}$	$4.59 \cdot 10^{-3}$	160	15
80	$5.62 \cdot 10^{-3}$	$7.49 \cdot 10^{-3}$	60	42
500	0.22	$19 \cdot 10^{-3}$	10	92
1000	0.88	$26 \cdot 10^{-3}$	5	97

3.2.2 Electrically long dipole antenna

The electrically small dipole antenna also called Hertzian dipole is impractical antenna for following reasons. First of all, the length of the dipole was predicted to be infinitesimal in order to simplify the calculations of fields. Secondly the current along the small dipole antenna was assumed to be constant along the dipole. This latter assumption states that the current should be nonzero at the endpoints of the antenna which is unrealistic and, moreover, it is impossible in a real world situation because the surrounding

medium and additionally the free space is nonconductive. An electrically long dipole means that the maximum dimension of the antenna is larger than $\lambda/10$ and this will be investigated in this chapter. (Clayton 2006: 22, 429)

In reality, we cannot find such as an electrically small dipole antenna because the antenna current is zero at the ends. As we can see for antennas it is all about the current distribution. When we know the current distribution, other parameters, such as the input impedance and radiation pattern, can be determined. (Huang & Boyle 2008: 146)

Figure 10 contains a transmission line with current distribution shown as blue sine waves and electric field shown as red arrows at the end.

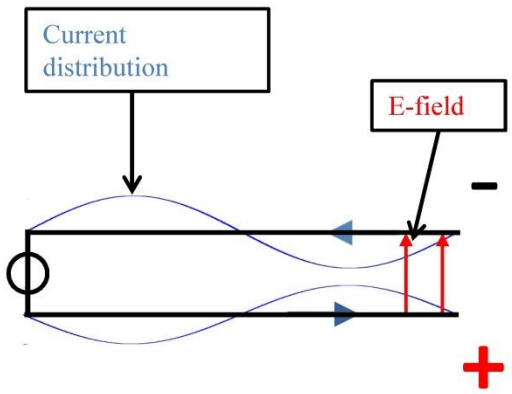

Figure 10. Transmission line current distribution and electric field.

Next the wires of the antenna are twisted in Figure 11 at the point where $\lambda/4$ and transmission line with current distribution (blue sine waves) and electric field (red arrows) at the end. Now wires are separated to 90° degree angle compared to each other.

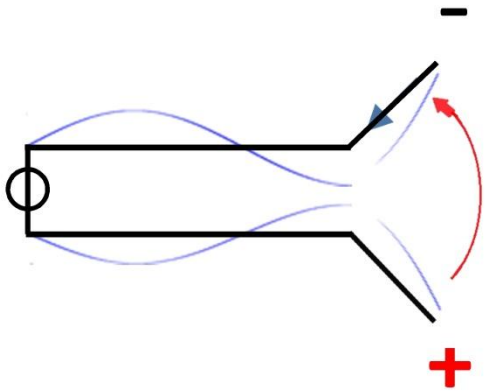

Figure 11. Transmission line with 90° degree wire separation.

Figure 12 contains a transmission line with 180° degree separation. This separation gives the half wavelength dipole antenna and we can see that the electric field goes from positive polarity to negative polarity and the currents at the ends of the antenna are equal to zero. The angle point is the so called feed point for an antenna and a realistic antenna contains a connector to the transmission line at this point.

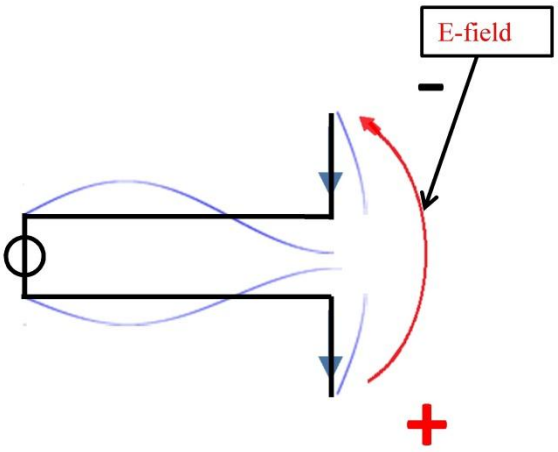

Figure 12. Transmission line with 180° degree wire separation.

An antenna can be described as a complex *RLC* network. At some frequency, it will look like an inductive reactance X_L, and at some other frequency it will look like a capacitive reactance X_C. At one frequency, the inductive reactance and capacitive reactance are equal in magnitude but the signs are different so they cancel out each other $X_L - X_C = 0$. At this frequency, the impedance of an antenna is purely resistive and this is

called the resonant frequency. At the resonant frequency antenna can be matched to the transmission line impedance. (Carr 2001: 143)

The standard CIPSR22 defines the maximum limit for electric field intensity 30 dBμV/m which a device can radiate to the environment at the distance of 10 m. This corresponds to $|E| = 31.6$ μV/m. Table 3 shows the calculated maximum antenna current and radiation efficiency for dipole antennas. This low maximum current value I_m shows that the long dipole antenna is the most problematic radiator from electromagnetic compatibility point of view and it's a much more efficient radiator than the small dipole antenna. The parameters for the antenna and for the test environment are the frequency dependent resistance for losses R_L (conductivity for copper σ_{CU} = 57 MS/m), antenna radius (0.5 mm), pattern angle $\theta = 90°$ and antenna fixed length is three meters. Test is done in far field where $r > 2\pi/\lambda$. (Clayton 2006: 423)

Table 3. Electrically long dipole antenna calculations.

f [MHz]	L = 3 m	R_r [Ω]	R_L [Ω]	I_m [μA]	ε_{rad} [%]
50	$\lambda/2$	73	1.7	5.3	97.6
150	1.5λ	105	3.1	5.3	97.2

Table 3 simply means that as small as five micro amp current in the dipole antenna will radiate more than the emission standard allows.

3.3 Differential mode radiation

Digital electronics can radiate in two ways either in differential mode or in common-mode. Normal operation of the circuit causes differential mode radiation, because of currents flowing around loops. Differential mode radiation in near-field is predominantly magnetic field radiation. These signal loops and power loops are necessary for the circuit operation and their areas and sizes have to be controlled during the design process to reduce the radiation. (Ott: 464)

In most products the primary noise sources are currents flowing in circuits (clock signals, buses like high speed serial data bus, oscillators or impulsive sources) that are in the printed circuit board and it should be remembered that any current can flow only in the loops of the PCB. Some of the electromagnetic energy is radiated from the PCB, which can be modeled as a small loop antenna carrying the rapid current transients like in Figure 13. (Willis 2007: 235)

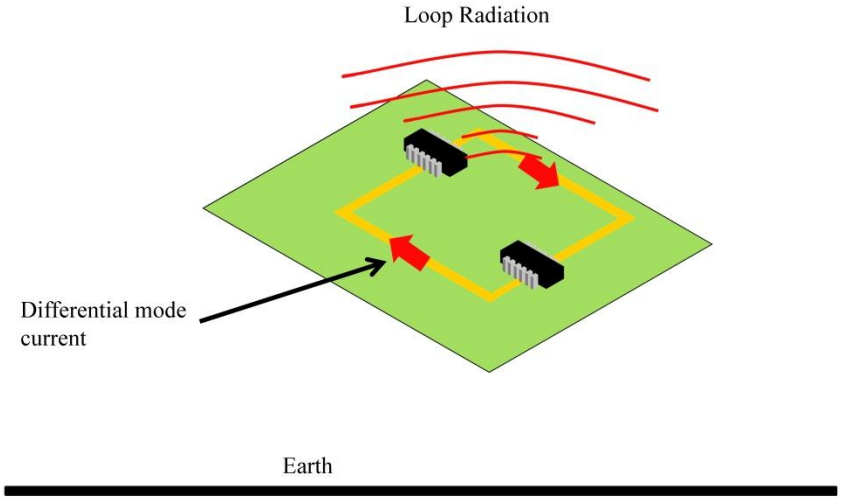

Figure 13. PCB loop causes differential mode radiation. (Willis 2007: 235)

3.3.1 Electrically small loop antenna

The definition for electrically small loop antenna is $2\pi r < \lambda/10$ (r is radius) which means that the circumference is small. Let us consider a 2.5 mm radius loop where we can be sure that almost every PCB contains this kind of loops. Maximum limit for electric field intensity which a device can radiate to the environment at the distance of 10 m is $|E|$ = 31.6 µV/m which is about 30 dBµV/m as in standard CISPR22 which gives limits for commercial products. Table 3 shows calculated maximum antenna current and radiation efficiency for small loop antennas. This low maximum current value I_m shows that the small loop is a quite problematic radiator from the electromagnetic compatibility point of view and it's much more efficient radiator than a small dipole antenna, but less efficient than a long dipole antenna. The parameters for the antenna and for the test environment are the frequency dependent resistance for losses R_L (value for copper σ_{CU} = 57

MS/m), loop is made of 500 μm wide PCB trace which has a thickness of 35 μm and pattern angle θ is 90°. The test is done in far field where $r > 2\pi/\lambda$ (r is distance between antenna and receiver). Loop antenna functions for radiated fields are the same as for a small dipole antenna but directions of ***E*** and ***H*** are interchanged. The reactive part (inductance and capacitance) of the loop are not considered in the calculations in the Table 4. (Clayton 2006: 423,426,428)

Table 4. Electrically small loop antenna calculations.

f [MHz]	R_r [Ω]	R_L [Ω]	I_m [mA]	ε_{rad} [%]
30	$1.2 \cdot 10^{-12}$	$21.2 \cdot 10^{-3}$	1360	$5.7 \cdot 10^{-9}$
80	$60.8 \cdot 10^{-12}$	$34.6 \cdot 10^{-3}$	191	$176 \cdot 10^{-9}$
500	$92.7 \cdot 10^{-12}$	$86.4 \cdot 10^{-3}$	4.9	$107 \cdot 10^{-6}$
1000	$1.5 \cdot 10^{-6}$	$122 \cdot 10^{-3}$	1.2	$1.2 \cdot 10^{-3}$

The equations 25 and 26 are the far field equations for a small loop antenna where the electric field is present only in ϕ direction and magnetic field at the direction θ. The equations show that when frequency is increased the loop radiation increases in proportion to the square of frequency and loop area and loop current have direct proportion to fields (Clayton 2006: 428):

$$E_{\varphi} = \frac{I_m \pi f^2 \mu_0 S}{rc} \sin\theta \, e^{-j\left[\frac{2\pi f r}{c}\right]} \quad \text{and} \tag{25}$$

$$H_{\theta} = \frac{I_m \pi f^2 \mu_0 S}{r \eta_0 c} \sin\theta \, e^{-j\left[\frac{2\pi f r}{c}\right]}. \tag{26}$$

3.3.2 Electrically large loop antenna

There are two forms of loop antennas, large and small. The characteristics of these small and large loops are different with each other. In a small loop antenna the current in the metal wire has the same phase and amplitude at every point in the loop. The current in a large loop varies along the loop wire in a manner similar to the dipole antennas. (Carr 2001: 287)

If a loop antenna cannot be considered small then the current distribution cannot be regarded as constant. The properties of a large loop are different when compared to the small loop. It has been shown that when the circumference of a large loop becomes comparable to the wavelength then the maximum radiation shifts its axis from the center of the loop. This phenomenon is very different from a small loop. There is no simple mathematical expression for the radiated field of such a large loop antenna. (Huang & Boyle 2008: 144)

3.4 Victims of electromagnetic radiation

Many times electronic devices send interferences to the environment and one path for this interference is radiation through EM-waves. These EM-waves can cause malfunctions in the victim equipment. Usually an electronic device contains many loops because of normal functions of the device need these loops and usually the device contains external cables which are made of conductive material. These mentioned loops and cables in the device can act as transmitter antennas or as receiver antennas.

3.4.1 Electrically small loop antenna as receiver

In Figure 2 the loop antenna is in external flux ϕ. The inducted voltage V_{OC} is caused by changing external flux ϕ and induced voltage V_{OC} has a polarity such that the established current in the loop opposes external flux ϕ where $B = \phi/S$ and $H = B/\mu_0$. The circulating electric field $\boldsymbol{E}$ causes current to the loop according to (Edminister 1993: 194):

$$V_{OC} = \oint \boldsymbol{E} \cdot \mathrm{d}\boldsymbol{l} = \int_S \left(-\frac{\partial \boldsymbol{B}}{\partial t} \right) \cdot \mathrm{d}\boldsymbol{S}. \tag{27}$$

If the right side is solved when the flux is perpendicular to the loop surface then equation 28 can be obtained and this is the authors own version of equation 27 because from this form we can see that frequency f, magnetic field H and surface area S have direct

proportion to induced voltage. Appendix 1 contains calculations about loop antenna and final equation is

$$|V_{OC}| = 2\pi f S H \mu_0 . \tag{28}$$

When the electrically small loop having a loop diameter less than $\lambda/10$ is used as a receiving antenna, the voltage induced at the loop antenna open-circuited terminals V_{OC} is proportional to the normal component of the incident flux density of the loop. (McGraw-Hill Professional, Loop antennas: 5) (Miron 2006: 31)

Table 5 contains calculated values for small receiving loop antenna where EM wave is plane wave and $H = E/\eta_0$. This calculation does not consider the reactance (capacitance and inductance of loop) effect of the antenna. In the printed circuit board the loop areas should be kept small to prevent induced voltages. External interfering frequency we cannot affect and here the selected frequency is 500 MHz.

Table 5 Electrically small loop antenna calculations.

f **[MHz]**	***S*** **[cm^2]**	**|*E*|** **[V/m]**	**|*H*|** **[A/m]**	V_{OC} **[mV]**
500	1	10	$26.5 \cdot 10^{-3}$	10.5
500	2.5	10	$26.5 \cdot 10^{-3}$	26.2
500	6	10	$26.5 \cdot 10^{-3}$	62.8
500	80	10	$26.5 \cdot 10^{-3}$	837

3.4.2 Electrically long dipole antenna as receiver

Two dipole antennas are arranged as in Figure 14. This is a normal situation when testing EMC immunity according to IEC 61000-4-3 standard where distance between antennas is three meters. Left side antenna produces electric field 10 V/m and antenna on the right side receives the field.

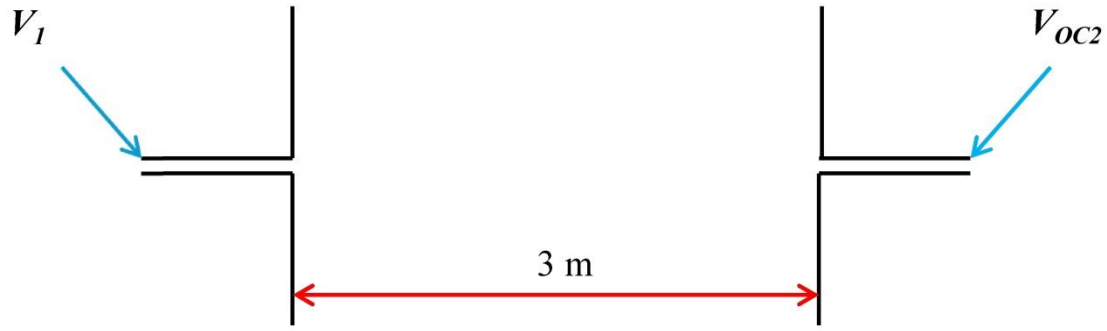

Figure 14. Transmitter dipole antenna and receiver dipole antenna when the distance between antennas is three meters.

The open circuit voltage for half wave dipole antenna 2 can be calculated according to equation 29, where $|E(\theta_1)|$ = 10 V/m, L_2 = 1 m, f = 150 MHz, r = 3 m, $\theta_1 = \theta_2 = 90°$, $c = 300 \cdot 10^6$ m/s, $\beta = 2\pi/\lambda$ and $\lambda = c/f$. By using these values in equation 29 the antenna two's open circuit voltage magnitude $V_{OC2} \approx 6.4$ V (Edminister 1993: 308):

$$|V_{OC2}| = h_e(\theta_2)|E(\theta_1)| = \frac{2}{\beta}\frac{\cos\left(\frac{\pi}{2}\cos\theta_2\right)}{\sin\theta_2}|E(\theta_1)| = \frac{c}{f\,\pi}|E(\theta_1)|. \quad (29)$$

4 ELECTROMAGNETIC EMISSION

4.1 Signal spectra

The signal spectra are the concept which means the relationship between the frequency domain and the time domain. The spectrum or the frequency content of the signal present in electronic equipment is perhaps the most important aspect of the ability of that equipment to not only satisfy electromagnetic compatibility standards but also perform compatibly with other electronic equipment's. (Clayton 2006: 91)

4.1.1 Fourier transform

Basic to an understanding of why electronic circuit causes unwanted interference is the concept of the time domain to frequency domain transform. The mathematical tool which can be used to analyse a known time domain current waveform or time domain voltage waveform in the frequency domain is called the Fourier transform. (Willis 2007: 288)

A French physicist and mathematician Jean Baptiste Joseph Fourier (1768-1830) discovered that periodic functions can be transformed to a series of sines and cosines. (Agilent technologies 2006. Spectrum Analysis Basics: 4)

The Fourier series can be described in complex form which simplifies calculations, where c_0 is Fourier series DC-component magnitude, c_n is the magnitude of Fourier series harmonic number n and $x(t)$ is the time domain function which can be represented by using Fourier series components c_0 and c_n and equations are (Clayton 2006: 97, 98):

$$c_0 = \frac{1}{T}\int_{t_1}^{t_1+T} x(t)\,\mathrm{d}t, \tag{30}$$

$$c_n = \frac{1}{T}\int_{t_1}^{t_1+T} \mathrm{e}^{-\mathrm{j}n\omega_0 t}\, x(t)\,\mathrm{d}t \quad \text{and} \tag{31}$$

$$x(t) = c_0 + \sum_{n=1}^{\infty} 2|c_n|\sin(n\omega_0 t + \angle c_n + 90°). \quad (32)$$

4.1.2 Some common waveforms caused by digital electronics

Ideal square wave time domain representation is in Figure 15 and Fourier transform one-sided magnitude spectrum representation is in Figure 16. Input values for a square wave are period time T = 100 ns (10 MHz), 50 % duty cycle where $\tau = T/2$, u = 2.5V, infinite rising time and infinite falling time, where u is the maximum voltage (amplitude value of voltage) and equation (Clayton 2006: 100):

$$\text{Amplitude}(f) = \frac{2\hat{u}t}{T}\left|\frac{\sin(0.5\pi fT)}{(0.5\pi fT)}\right|. \quad (33)$$

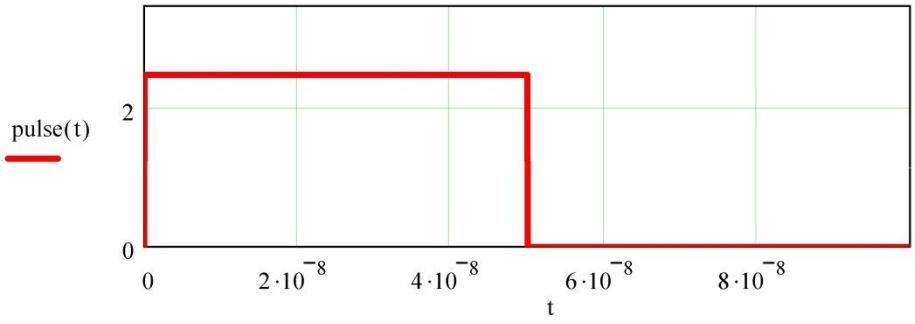

Figure 15. Square-wave voltage as a function of time.

The envelope amplitude representation shows that even harmonics in Figure 16 are all zero when Fourier transform is taken from the ideal square wave. Figure 16 shows that 20 MHz, 40 MHz, 60 MHz, 80 MHz and 100 MHz are all zero.

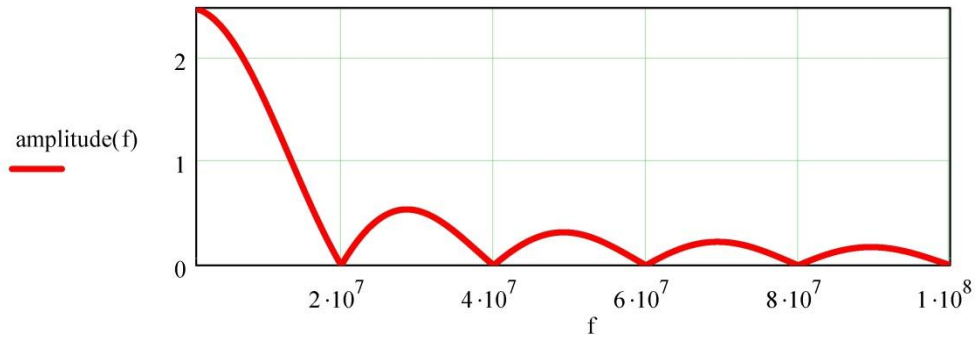

Figure 16. Square-wave voltage amplitude as a function of frequency.

In a realistic PCB the digital circuit switching waveform has to be represented as a trapezoidal waveform as in Figure 17 which is always a square wave with period time T, duty cycle, finite rise time t_r and fall time t_f. (Willis 2007: 289)

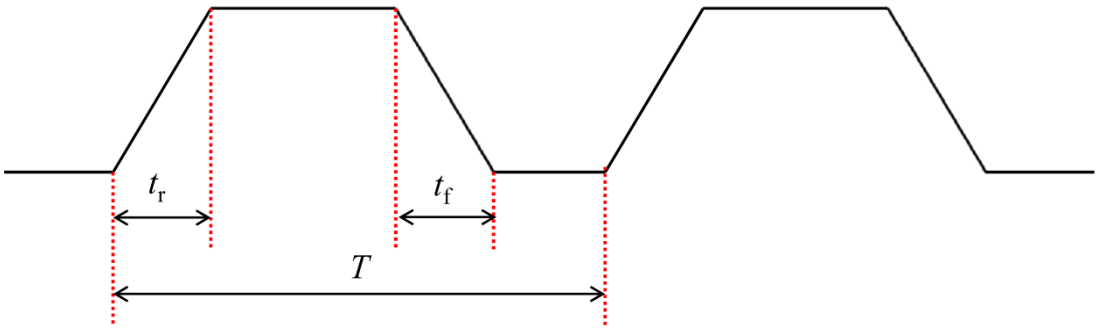

Figure 17. A practical shape of square-wave as a function of time.

The top formula in equation 34 can be used to plot frequency domain harmonic amplitudes where n = 1,2,3. Voltage differences between harmonics can be relatively large so the function is better to plot by using decibel units and in this case dBµV, as in the complete equation 34. This unit dBµV is actually the same unit which is used in conductive emission test standard, where t_r is rise time in Figure 17 and T is period time in Figure 17 and equation is (CISPR22 2008: 12) (Willis 2007: 467):

$$\hat{u}(\mathrm{n}) = 20\log\left(\frac{\left(\frac{2u(t+t_\mathrm{r})}{T}\right)\left(\frac{\sin\left(\frac{\mathrm{n}\pi(t+t_\mathrm{r})}{T}\right)}{\frac{\mathrm{n}\pi(t+t_\mathrm{r})}{T}}\right)\left(\frac{\sin\left(\frac{\mathrm{n}\pi t_\mathrm{r}}{T}\right)}{\frac{\mathrm{n}\pi t_\mathrm{r}}{T}}\right)}{1\cdot 10^{-6}\,\mathrm{V}}\right). \qquad (34)$$

Figure 18 shows that when the duty cycle is 50 %, rise time is 3 ns (rise time equals to fall time) and period time 100 ns (fundamental frequency 10 MHz). From Figure 18 we can see that when duty cycle is 50 % there are no even harmonics, but this result is purely theoretical. A duty cycle in real digital electronics cannot be exactly 50 % and thus there are always some odd harmonics. However, the magnitude of even harmonics gets smaller when the signal duty cycle approaches 50 %. (Clayton 2006: 122)

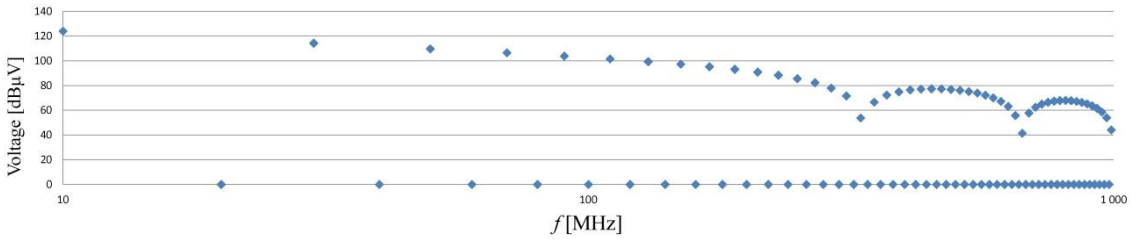

Figure 18. Square wave with duty cycle 50 %, rise time 3 ns and fundamental frequency 10 MHz.

Figure 19 has the same situation but rise time is ten times faster and cycle is 50 %, rise time = 300 ps (rise time = fall time) and period time 100 ns so frequency is 10 MHz. Digital waveform which has short rise time and short fall time will have larger high-frequency spectral content than a signal having longer rise time and fall time. So it is important to realize that if we want to reduce emission of a device then rise time and fall time should be longer. Fast rise time or fast fall time are the primary contributors why device cannot pass the regulator's requirements of radiated or conducted emission. (Clayton 2006: 125)

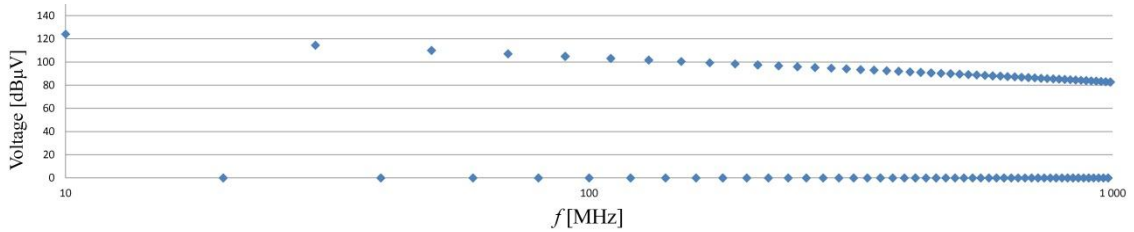

Figure 19. Square wave with duty cycle 50 %, rise time 0.3 ns and fundamental frequency 10 MHz.

These calculated results in Figure 18 and Figure 19 show that there are no even harmonics when the duty cycle is exactly 50 %. During empirical tests the even harmonics can never be completely eliminated because in digital waveform the duty cycle cannot be set to exactly 50 %. This is the problem when we measure two units of the same device and the results are not comparable because a small change in duty cycle (due to variation in individual component tolerances) can be seen in the emission results. Figure 20 shows the results when duty cycle is 30 % : even and odd harmonics are both present. (Clayton 2006: 122)

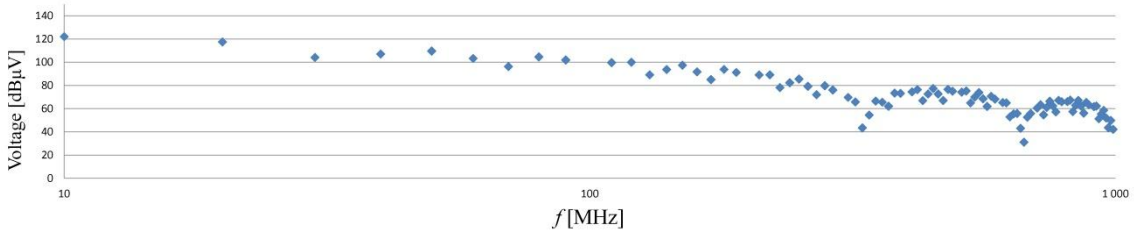

Figure 20. Square wave with duty cycle 30 %, rise time 3 ns and fundamental frequency 10 MHz.

The digital electronics current waveform is shown in Figure 21. For example microcontroller power supply current time domain waveform looks like Figure 21. The input values for the triangle wave are period time T = 100 ns (10 MHz) and $t_r = t_f$ = 10 ns.

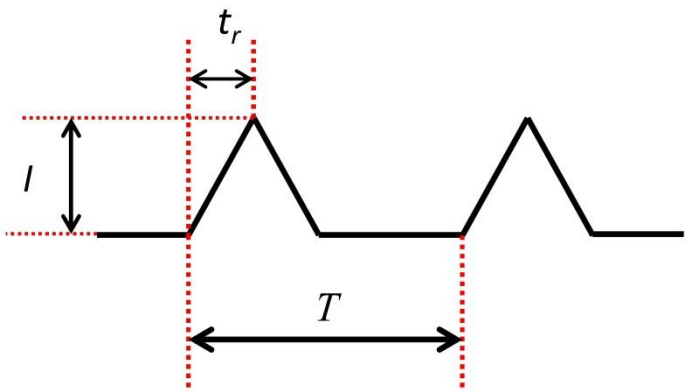

Figure 21. The current waveform of digital electronics as a function of time.

The top formula in equation 35 can be used to plot frequency domain harmonic amplitudes where n = 1,2,3. The result is current *i* as function of frequency by using unit dBμA

$$\hat{i}(\mathrm{n}) = 10\log\left(\frac{\frac{2ut_\mathrm{r}}{T}\left(\frac{\sin\left(\frac{\mathrm{n}\pi t_\mathrm{r}}{T}\right)}{\frac{\mathrm{n}\pi t_\mathrm{r}}{T}}\right)^2}{1\cdot 10^{-6}\,\mathrm{A}}\right). \tag{35}$$

The waveform values are selected on purpose $t_r/T = 0.1$ so the reduction of harmonics levels at the high frequencies can be easily noticed. Both even and odd harmonics can be seen. Higher frequencies than 30 MHz harmonics starts to reduce with a 40 dB per decade rate. This frequency is calculated by $f = 1/\pi t_r \approx 30$ MHz. (Ott 2009: 429)

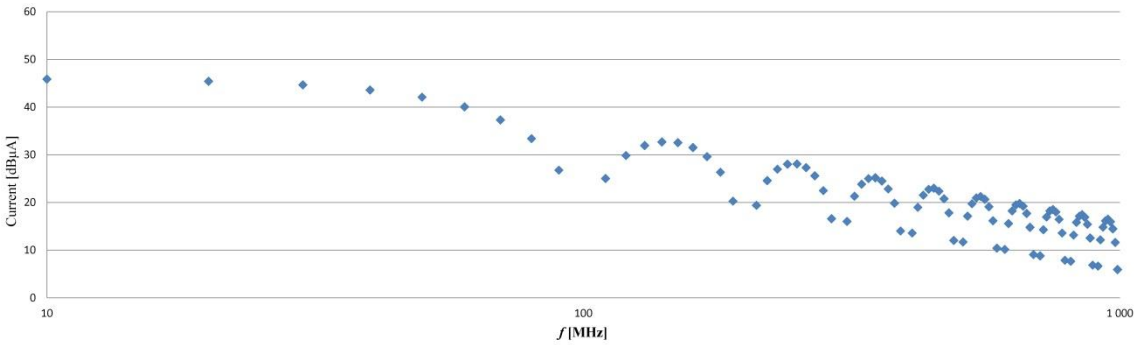

Figure 22. The current harmonics of digital electronics when duty Cycle 50 %, rise time 10 ns and fundamental frequency 10 MHz.

4.1.3 Spectrum analyzer and measuring receiver

The standardized conformance test measurements are taken with an expensive measuring receiver, which is optimized for the purpose of making EMC standardized measurements. A spectrum analyzer (SA) is much cheaper than a measuring receiver and is commonly used to "quick-look" diagnostics and testing for example near-field measurements from a PCB. The spectrum analyzer is not an alternative to a measuring receiver in a full compliance standardized test because of the SA's limited dynamic range and sensitivity and susceptibility to overload. Anyway the SA is very valuable for confirming the frequencies and nature of offending emissions for example in near-field measurements. (Willis 2007: 119)

Most electronics designers are familiar with waveforms in the time domain, as viewed on an oscilloscope, but periodic waveforms can also be investigated in the frequency domain, for which the basic measuring equipment is the SA whereas the oscilloscope shows the time domain. (Willis 2007: 288)

The SA can be described as a voltmeter calibrated to display the root mean square (RMS) value of a sine wave and which has features like frequency-selection and peak-response. Spectrum analyzer is not a power meter which is important to realize even though SA can be used as a power meter. For example if we know peak or average val-

ue of a sine wave and we know the resistance across the spectrum analyzer's input resistor we can calibrate our voltmeter to indicate power. (Agilent technologies 2006: 4)

The peak mode in the SA shows the maximum RMS sinusoidal voltage. A very simple peak detector circuit is shown in Figure 23. In Figure 23 V_{IN} is the measured interference voltage and this voltage feeds the peak detector circuit. The input and output voltage waveforms can be seen in Figure 24 and it shows that peak voltage remains in the capacitor. (Clayton 2006: 146)

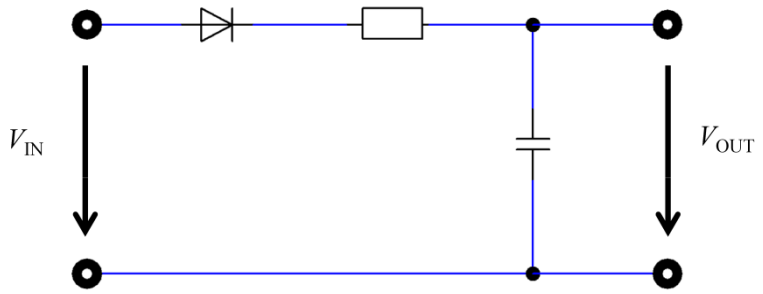

Figure 23. Spectrum analyzer peak-hold circuit which looks like half-wave rectifier combined with low pass *RC*-circuit.

Figure 24 shows that peak detector follows the input signal, where blue waveform is circuit output voltage.

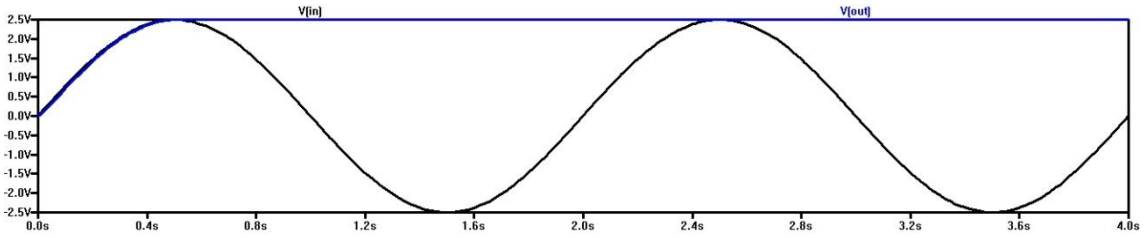

Figure 24. Spectrum analyzer peak-hold circuit connected to sine wave.

However the electromagnetic compatibility standard requires that the interference level that is to be compared with the limit line to determine compliance has to be measured by using a quasi-peak detector. A very simple quasi-peak detector circuit is in Figure 25. The CISPR16 determines quasi-peak charging time constant to one millisecond and

discharge time 550 ms when measurement range is 30 MHz – 1000 MHz. If the measured interference voltage varies slowly compared to the quasi-peak detector time constant then the capacitor will charge but it will also discharge and the quasi-peak detector reading is lower than in the peak-detector as we can see from Figure 26. According to these results the quasi-peak detector will always show less or equal magnitude when compared to peak-detector. (Clayton 2006: 146,147)

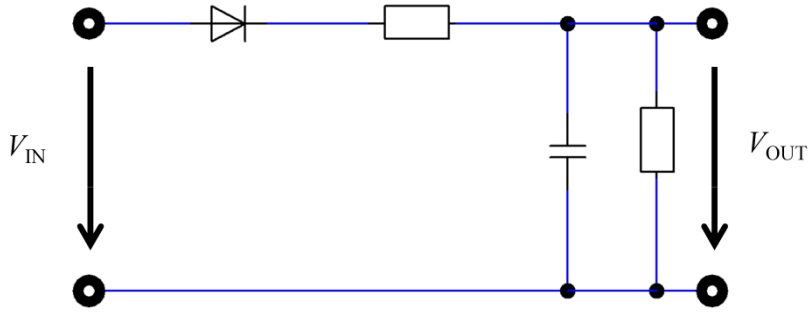

Figure 25. Quasi-peak detector circuit which looks like half-wave rectifier combined with low pass *RC*-circuit and output load resistor.

Figure 26 shows quasi-peak detector value, where blue waveform is circuit output voltage.

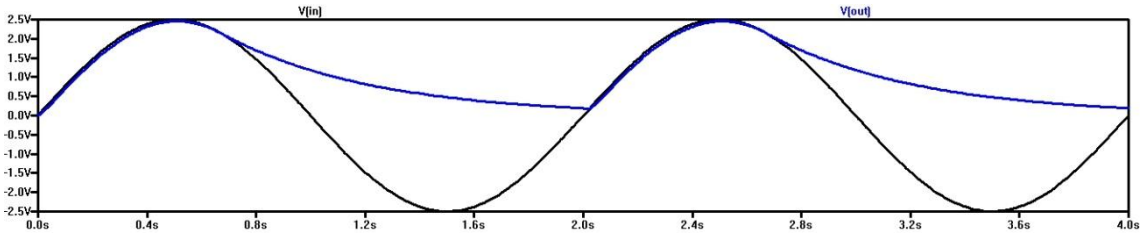

Figure 26. The output waveform of Quasi-peak detector when input signal is sine wave.

If interference is nearly constant then quasi-peak detector output voltage will be higher and get closer to the peak detector value and at some point the interference will be so powerful that the peak detector value is equal to the quasi-peak detector value as in Figure 27.

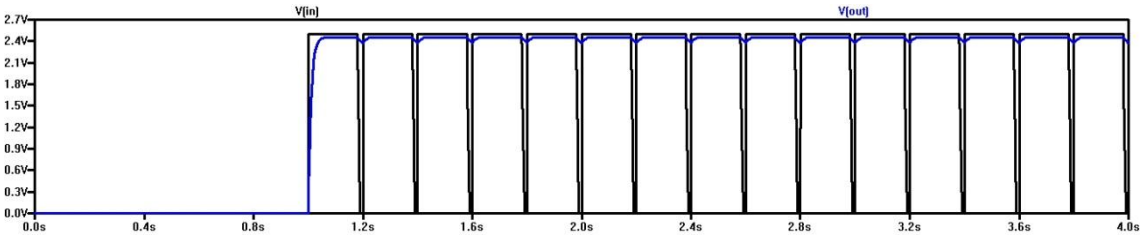

Figure 27. The output waveform of Quasi-peak detector when input signal is pulse wave.

4.2 Standardized far-field measurement and CISPR22 standard

CISPR22 (Information technology equipment-Radio disturbance characteristics-Limits and methods of measurement) emission standard.

> *CISPR 22 applies to information technology equipment (ITE). Procedures are given for the measurement of the levels of spurious signals generated by the ITE and limits are specified for the frequency range 9 kHz to 400 GHz for both class A and class B equipment. No measurements need be performed at frequencies where no limits are specified. The intention of this publication is to establish uniform requirements for the radio disturbance level of the equipment contained in the scope, to fix limits of disturbance, to describe methods of measurement and to standardize operating conditions and interpretation of results.* (CISPR22 2008)

CISPR 22 standard has been used all over the world for many years to determine compliance of ITE equipment. Many parts of the world like Japan, Australia, European Union and New Zealand have empowered CISPR 22, sometimes with some modifications. (Conformity 2007: Standards and Certification)

Figure 28 shows CISPR22 top view of the test setup arrangement. On the left in Figure 28 we can see a measuring receiver and an antenna which is used for measurement purposes. The distance between antenna and equipment under test (EUT) is ten meters. The outer dotted line means that EUT can be measured in an anechoic chamber or at an open area test site (OATS). EUT sends EM waves and these EM waves are measured by an accurate measurement receiver. EUT will be rotated so every corner of the EUT is

measured. Limit lines for household (class B) device field levels are in Table 4. EUT emission should not be more than Table 4 states.

Table 6. Household product electric field limit lines.

f **[MHz]**	***E*** **[dBµV/m]**	***E*** **[µV/m]**
30 - 230	30	31.6
230 - 1000	35	56.2

Figure 28 shows test arrangement according to CISPR22 standard.

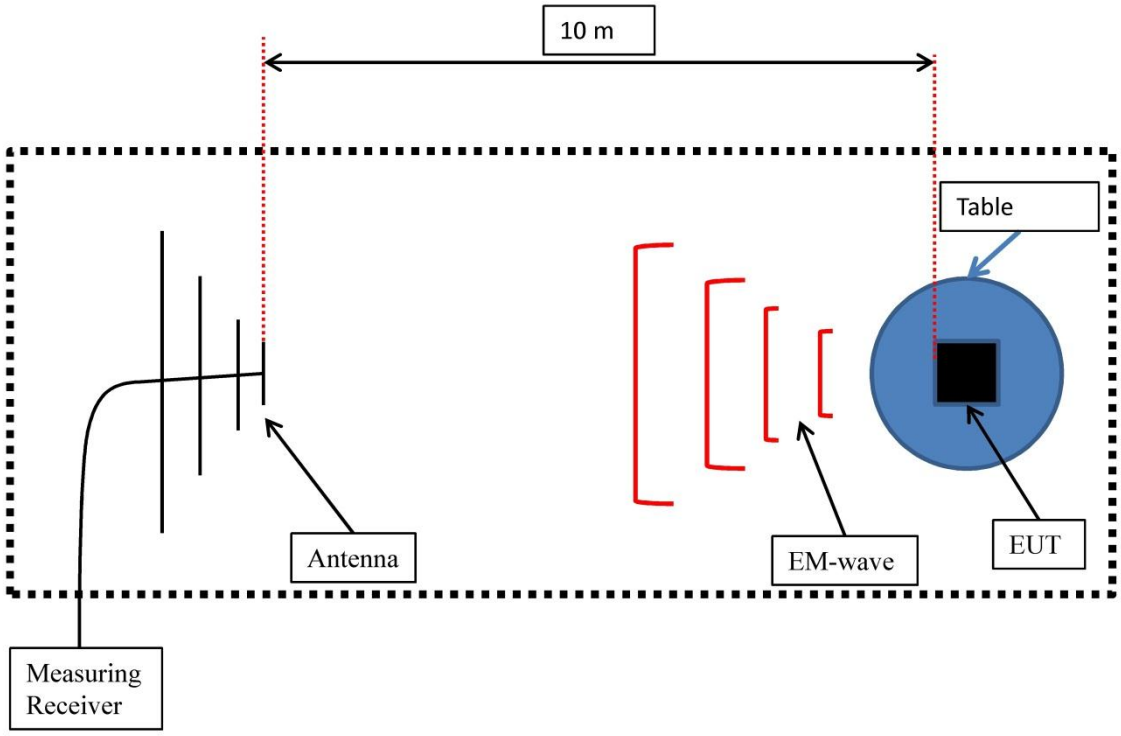

Figure 28. Test arrangement for EUT emission measurement. (CISPR22: 33)

4.3 Why we need non-standardized near-field measurements?

Typical emission measurement is the CISPR22 method. If the device is failing, because of too high emissions then device must be investigated and fixed to make the device radiation lower. To find the EMI-source from the device may require making measurements closer to the EUT and the PCBs of the EUT. These measurements are not possi-

ble using an antenna in far field like in CISPR22. Near-field magnetic field probes and electric field probes let us "sniff" around the PCB and the enclosure to find the radiation source. (Com-power Corporation 2010: Near-field Probes PS-400)

After measurements like CISPR22 the design engineer often notices that the device does not pass the test and some trips have to be made between the test lab and the company's own design facility. In order to minimize the cost of the EMC tests it is wise that a pre-compliance measurement should be done in companies facilities. This pre-compliance phase would use a spectrum analyzer and near-field probes. When the device seems to be electromagnetically quiet it is submitted to the compliance certification laboratory. In this way the test time and money can be saved. The purchase price of the spectrum analyzer can be saved because compliance measurements are quite expensive. (Bk Precision 1996: 1)

The company called Emscan provides near-field measurement systems for PCB and on their webpage they advertise: 'Immediate reduction in outsourced / allocated anechoic chamber costs'. So this is the main reason to make pre-compliance near-field measurements because full compliant anechoic chamber test hours are quite expensive. (Em scan)

5 DESIGN AND IMPLEMENTATION OF NEAR-FIELD PROBES

Figure 29 shows implemented near-field measurement probes. The collection contains two versions of electric-field probes (dipole antenna), five versions of magnetic field probes (loop antenna) and two versions of high-frequency current probes and one type of electric-field probe, one type of magnetic field probe and one type of current probe discussed in this chapter. There are many commercial near-field measurement probes from different manufacturers, but probes can be at home by using coaxial cable, shrinking tube, Bayonet Neill-Concelman (BNC) connector, ferrite ring and copper wire. We should remember that commercial products for example Bk precision PR-261 probes have been tested according to EN 61010-1 standard (Safety requirements for electrical equipment for measurement, control, and laboratory use), but many times self-made (like in Figure 29) probes have not been tested according to this standard and these self-made probes should not be used with non-shielded electric circuits above safety voltage which is in Finland 120 V DC or 50 V AC.

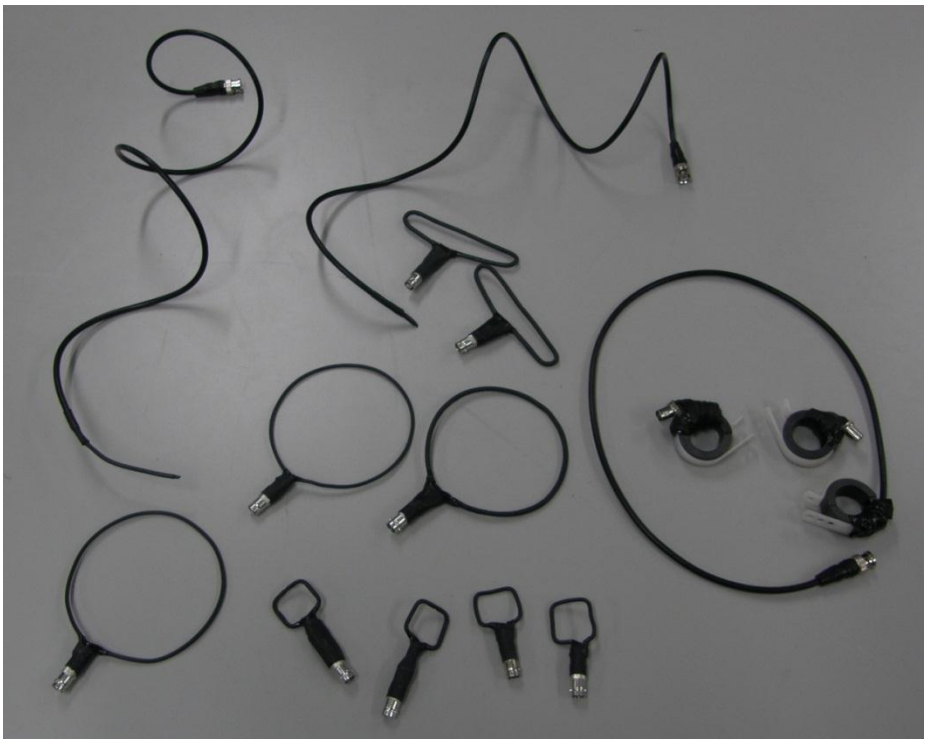

Figure 29. Self-made near-field measurement probes.

In the near-field of an antenna (where $\lambda/2\pi > r$), the magnetic and electric fields are not coupled to the electromagnetic field. The near-field might be predominantly magnetic or predominantly electric. It is important to point out that the fields that determine whether the EUT (equipment under test) passes the standardized test are not near-fields but are measured in far field by the EMC test antenna. Hence near-field magnitudes are not easily comparable with real standardized emission test electric field magnitudes. (Clayton 2006: 848)

5.1 EMI-source

During probe test it is good to have some kind of EMI-source. Figure 30 shows an EMI-source circuit diagram. The system uses +9 V DC batteries and U1 is voltage regulator which lowers the input voltage to +5 V DC. The interference is produced by 5V output transistor-transistor logic (TTL) oscillator which has 10 MHz square wave output (oscillator type MCO-10MHZ). Nowadays 10 MHz data transfer speed is quite common so 10 MHz EMI-source should be very well justified.

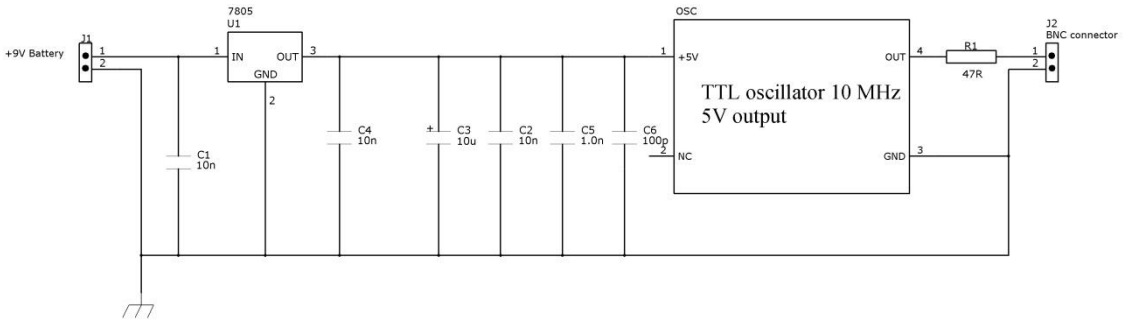

Figure 30. Circuit diagram for the EMI-source.

This EMI-source is assembled to the aluminum box Figure 31 and in this measurement setup the EMI-source is connected to an Agilent oscilloscope through RG-58 coaxial cable which has a length of one meter.

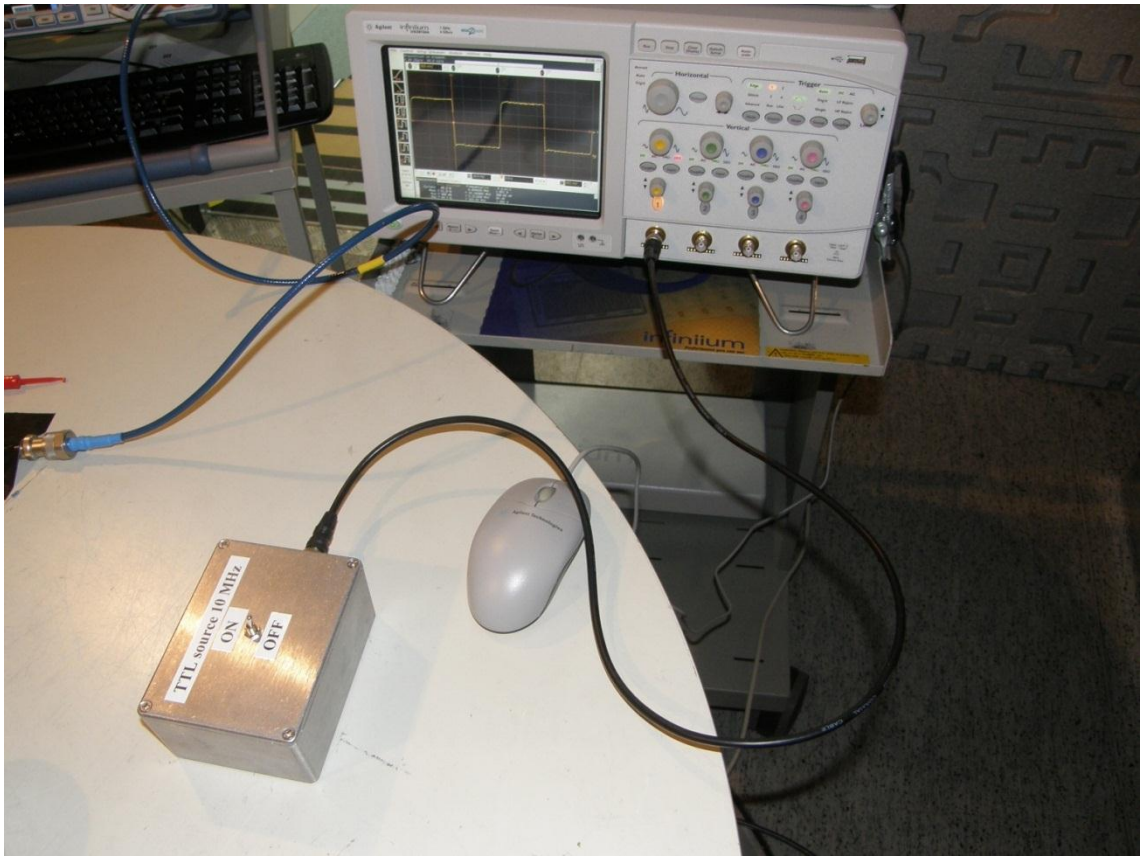

Figure 31. The EMI-source connected to an oscilloscope.

In Figure 32 the RG-58 cable has the characteristic impedance $Z_0 = 50\ \Omega$ and the output resistor in the EMI-source is 47 Ω so there is no significant mismatch between the generator and the coaxial cable. The oscilloscope input impedance is pure resistive 50 Ω load. The oscillator suffers because it is not designed to give high current values (like now $I \approx 5\text{V}/100\Omega \approx 50$ mA), but anyway this source can be used in these measurements because the frequency is about 10 MHz, duty cycle 48.3 %, Fall time 1 ns, Rise time 2.6 ns and the output voltage 2.0 V. Figure 32 shows output voltage waveform from EMI-source.

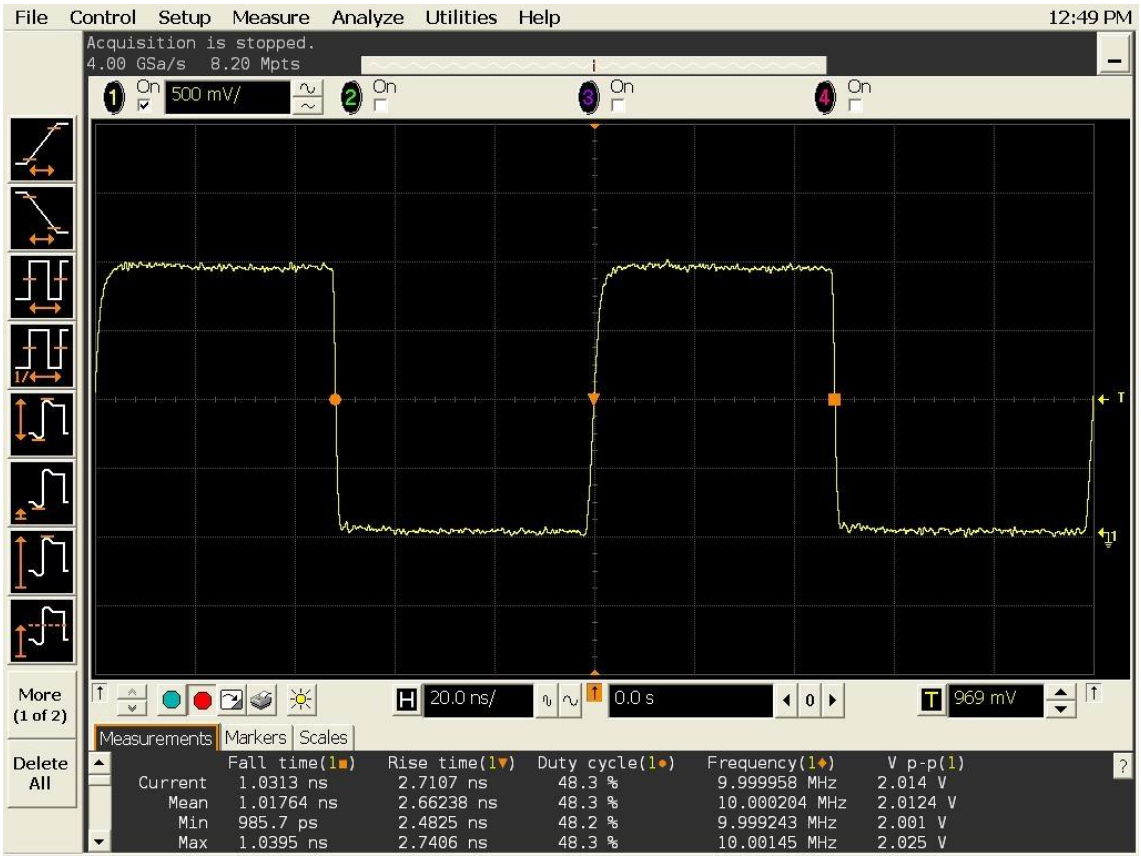

Figure 32. The EMI-source output voltage when EMI-source connected to an oscilloscope and oscilloscope input impedance is 50 Ω.

Figure 33 shows spectrum analyzer measurement result from EMI-source. Spectrum analyzer uses dBµV units because the different frequency components have so different levels that otherwise it is impossible to see the higher frequency components. The frequency 8.992 MHz magnitude is 118.31 dBµV which equals 0.823 V. It can be seen clearly now that the spectrum contains both even and odd harmonics, because the duty cycle is not 50 % and the rise time is not equal to the fall time.

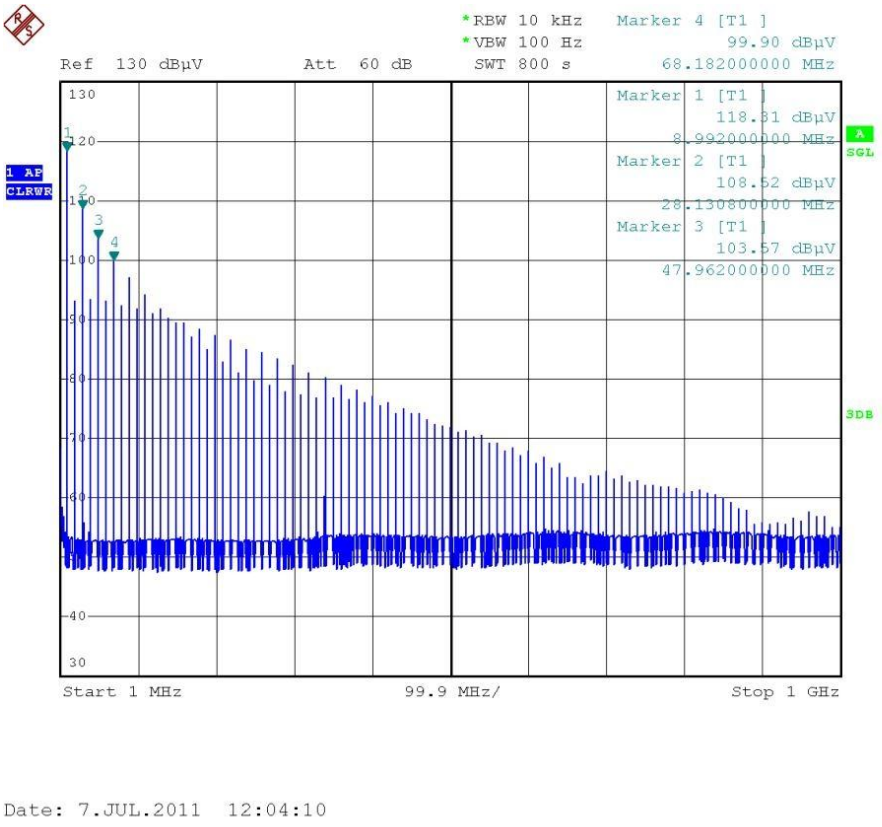

Figure 33. The EMI-source output voltage when EMI-source connected to an spectrum analyzer and spectrum analyzer input impedance is 50 Ω.

Many sources state that when working in the high frequencies the cable should be treated as a transmission line if the cable length is greater than 1/10 of a wavelength at frequency of interest and this can be written $l > v/(10f)$ where v is the electrical velocity in the cable. The digital data transmission should be treated as a transmission line if in the time domain the data rise time is less than twice the propagation delay of the line and this can be written as $t_r < 2l/v$. (Ott 2009: 215)

Propagation velocity v for RG-58/U (0.6·c) cable equals $198 \cdot 10^6$ m/s and the maximum cable length for the fundamental 10 MHz frequency $\lambda/10 = v/(10f) = 198 \cdot 10^6$ m/s / $(10 \cdot 10 \cdot 10^6$ 1/s) ≈ 1.98 m so for the fundamental frequency the cable does not need to be treated as a transmission line but for all the harmonics the cable should be treated as a transmission line because for 20 MHz $\lambda/10 = v/(10f) = 198 \cdot 10^6$ m/s / $(10 \cdot 20 \cdot 10^6$ 1/s) ≈ 0.99 m.

Figure 34 shows oscilloscope result when the oscilloscope input impedance is 1 MΩ. Now the frequency is about 10 MHz, duty cycle 50.5 %, fall time 4 ns, rise time 3.5 ns and peak to peak output voltage 5.56 V. The load voltage is greater than 5 V because of harmonics there is significant positive mismatch at the load end where reflection Γ factor is about 0.999 so value is practically one and where Z_L is load impedance and Z_0 transmission line characteristic impedance and equation is

$$\Gamma = \frac{Z_L - Z_0}{Z_L + Z_0}. \tag{36}$$

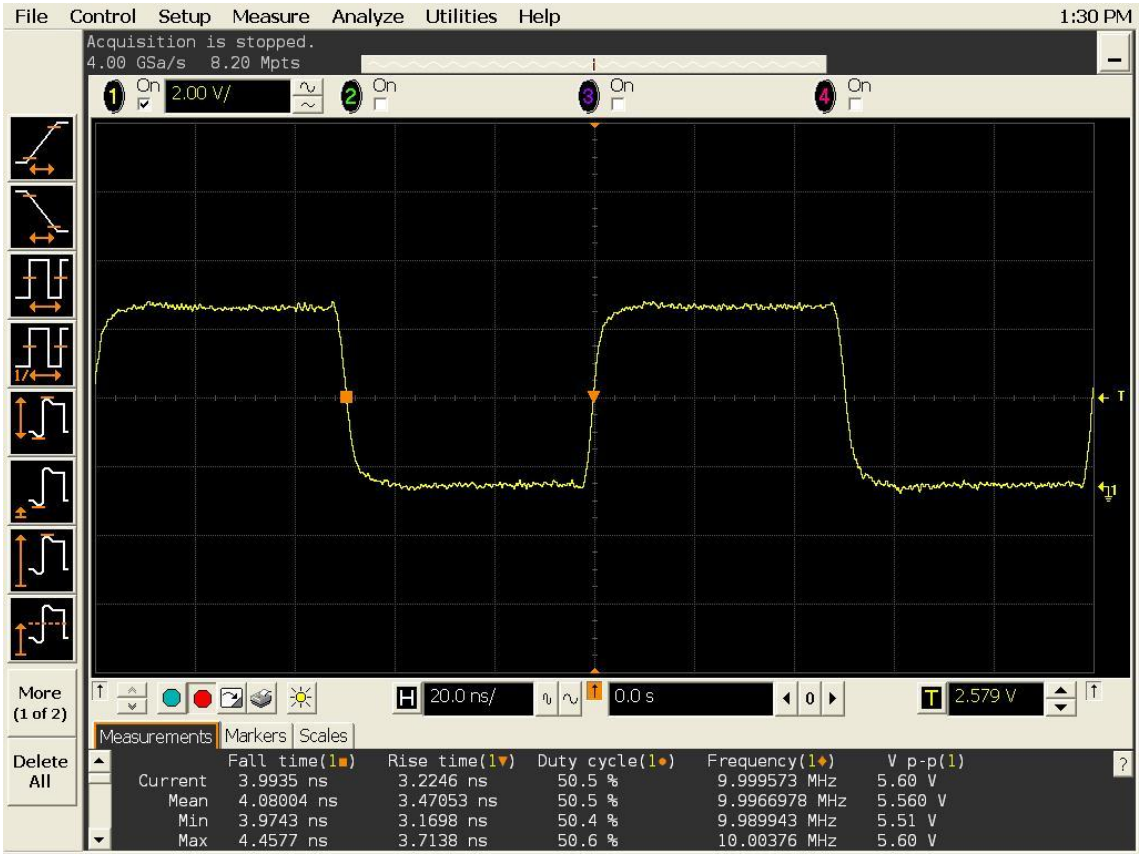

Figure 34. The EMI-source output voltage when EMI-source connected to an oscilloscope and oscilloscope input impedance is 1 MΩ.

5.2 Practical common-mode radiation

Common-mode emission from EUT cables can be modeled as a monopole or dipole antenna. The radiated emissions are determined by the potential difference which is many times the ground voltage like in Figure 6. The frequencies radiated are not related to the wanted signals in the cable. This test has been made to show how the cable shield will effectively reduce the radiation caused by common-mode current when the PCB ground noise voltage in Figure 6 cannot be reduced. Common-mode voltage source is artificially emulated by Figure 31 EMI-source. (Ott 2009: 477, 482) (Institute of telecommunication sciences. Glossary of telecommunication terms)

Figure 35 shows one example how the common-mode voltage source (generated in the poor PCB ground plane which contains inductances) is connected to the cable which contains a data signal and the ground. Equipment chassis is conductive material aluminum. This common-mode voltage which is caused by ground plane inductance can be seen in both output wires. The ground plane connection is made from the easiest point to the metal box chassis which is not a good solution. (Sepponen: 137)

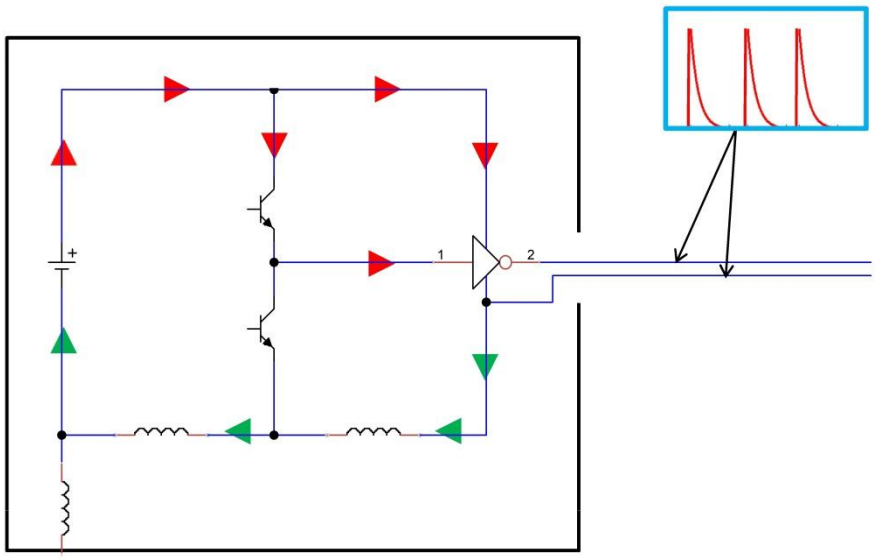

Figure 35. Device without external cable shield and only one PCB point is connected to the device chassis.

Figure 36 shows a better situation than in Figure 35 because now the current has many paths to go back to the source thanks to many PCB to chassis connections, but still there is some inductance between the PCB ground and the metal box.

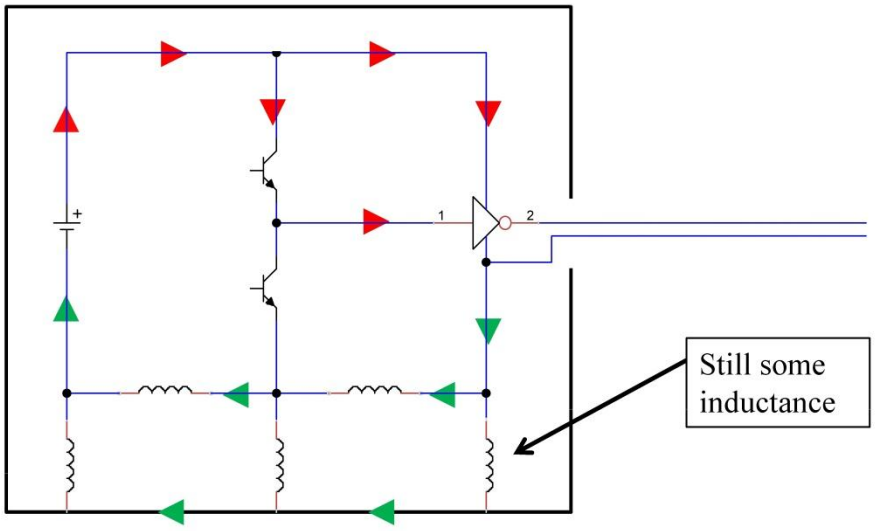

Figure 36. Device without external cable shield and multiple PCB points connected to device chassis.

This modification in Figure 37 assumes that the metal box chassis does not contain inductance and now the cable is shielded and the connection between the aluminum box and the cable is made 360° degrees.

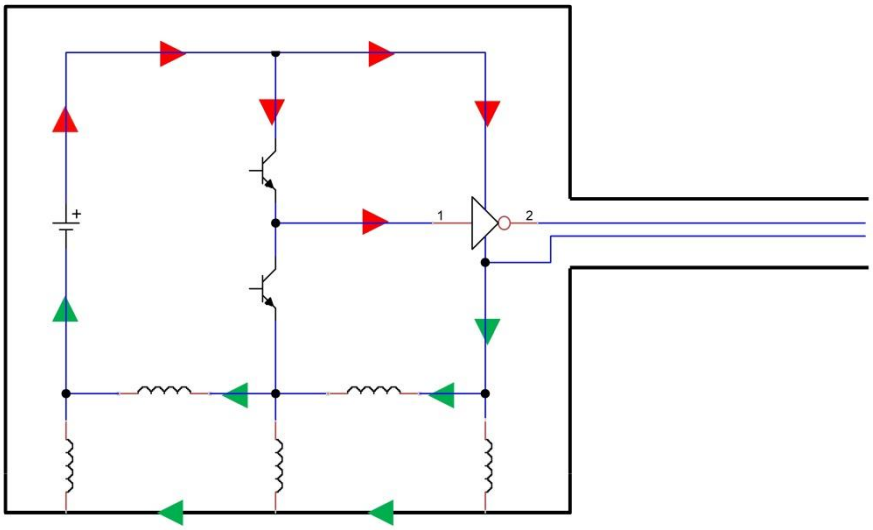

Figure 37. Device with external cable shield and multiple PCB points connected to device chassis.

Figure 38 shows common-mode voltage sources which are actually the ground plane voltages caused by inductance in the ground plane. In the leftmost part of Figure 38 common-mode voltage cause's common-mode current (to the cable) which is shown with red arrows and this current wants to go back to the source (like Kirchoff's law states). There is capacitance between the cable and the EUT chassis where green arrows show the current path back to the source. Same thing happens in the rightmost part of Figure 36 where shielded cable is used, but now the shield effectively reduces the total capacitance between the cable and the EUT chassis. Both enclosures are aluminum. (Ott 2009: 482)

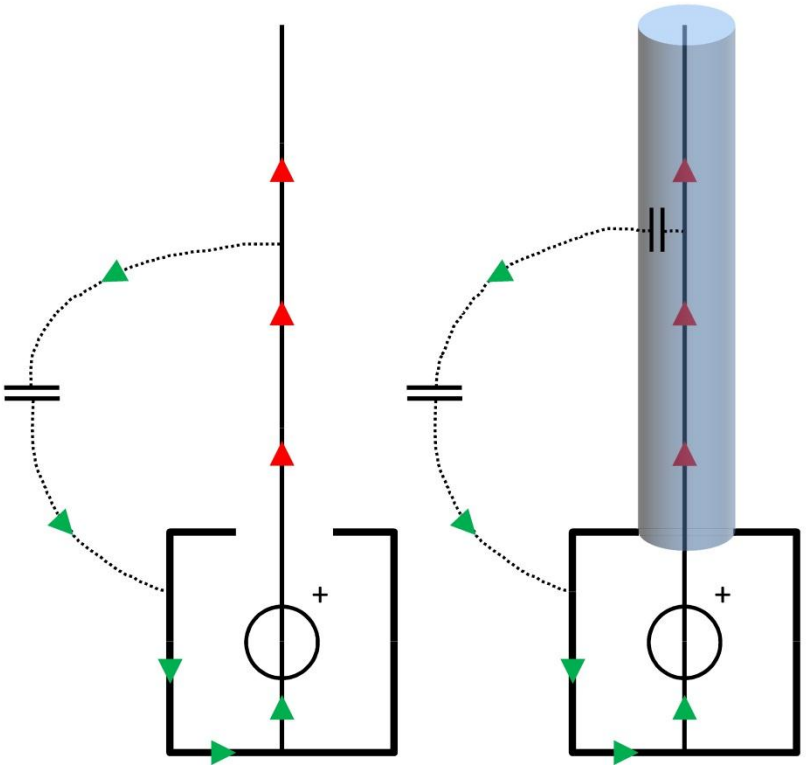

Figure 38. **N**on-shielded cable and shielded cable radiation which is caused by common-mode voltage.

5.2.1 Non-shielded cable

EMI-source has been used in the full anechoic chamber. EMI-source is connected to the 0.2 mm^2 wire positive TTL output in Figure 39. The TTL signal emulates common-mode interference in the cable (real cable contains several wires but functionality is the same) and there are no wanted signals in the test setup. (Ott 2009: 483)

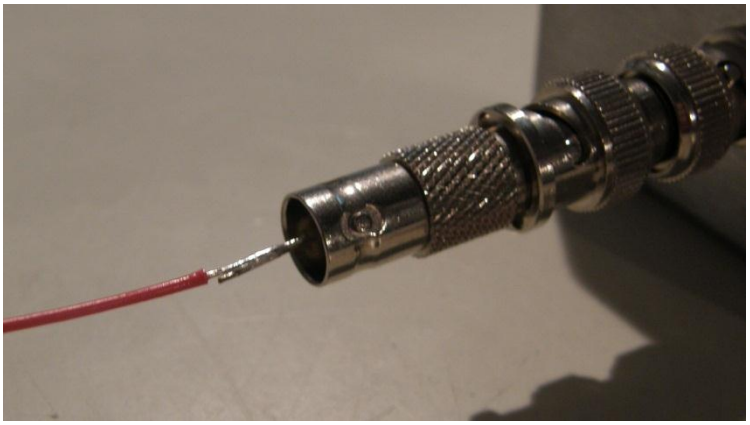

Figure 39. EMI-source connected to the wire (antenna) trough BNC-connector.

The connected red wire is two meters long. There is capacitance between the wire and the chassis of the EMI-source like in Figure 38, where noise current can flow and part of this noise current radiates as electromagnetic field to the receiving antenna. Additionally this wire has been twisted 180° back to the EMI-source which emulates the CISPR22 (Figure 28) cable bundle arrangement. The current distribution in the twisted (Figure 40) cable causes that some frequencies are attenuated and some are amplified because of the magnetic field direction. (Ott 2009: 483)

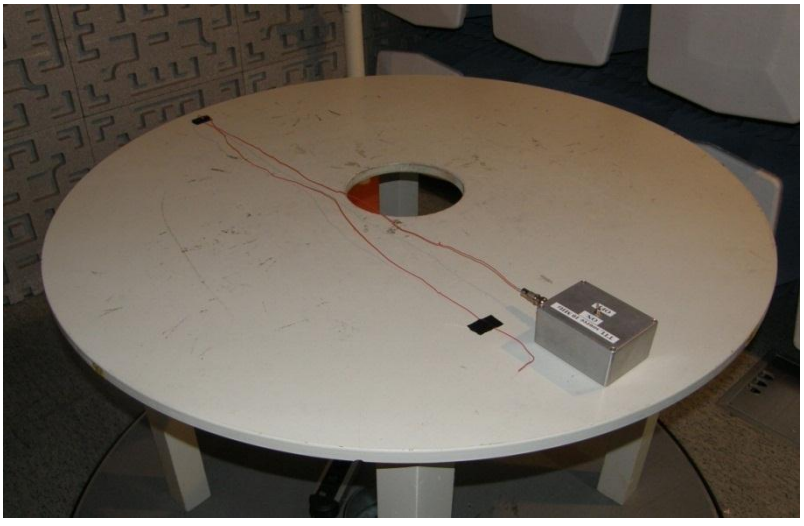

Figure 40. EMI-source connected to the two meter non-shielded wire.

From the results in Figure 41 it can be seen that radiation is very effective. At frequency range 30 MHz – 230 MHz the limit line equals 35 dBµV/m (because measurement distance in full anechoic chamber is three meters) and the highest result is at the frequency 49.98 MHz and this frequency's electric field magnitude is 58.3 dBµV/m which means that interference magnitude is about 15 times higher than allowed in standard CISPR22 and the results show clearly that there are even and odd harmonics. The numeric results can be found in Table 7.

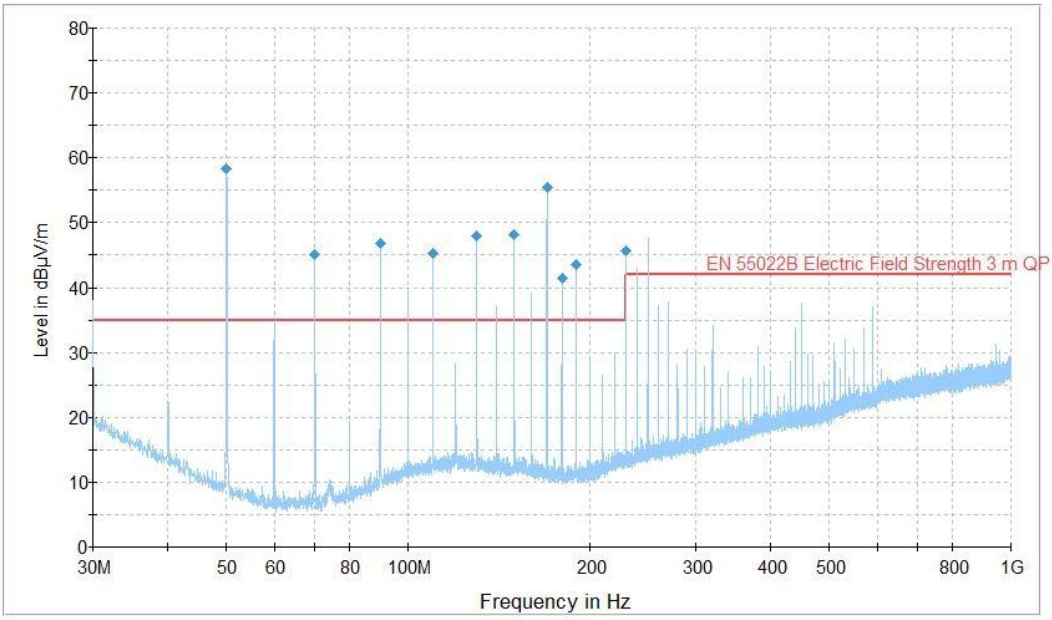

Figure 41. EMI results for non-shielded cable.

Table 7 contains measured frequency [MHz], quasi-peak values [dBµV/m], measurement time [ms], detector bandwidth [Hz], antenna height [m], antenna polarization which can be either horizontal or vertical, turntable position [°], antenna correction factor [dB], margin between limit line and the measured value which is calculated as Limit – Quasipeak = Margin.

Table 7. EMI results for non-shielded cable.

Frequency (MHz)	QuasiPeak (dBµV/m)	Meas. Time (ms)	Bandwidth (kHz)	Antenna height (cm)	Polarity	TurnTable position (deg)	Corr. (dB)	Margin (dB)	Limit (dBµV/m)
49.980000	58.3	1000.000	120.000	155.0	H	-2.0	8.0	-23.3	35.0
70.020000	45.1	1000.000	120.000	155.0	H	-2.0	5.7	-10.1	35.0
90.000000	46.9	1000.000	120.000	155.0	H	-2.0	9.1	-11.9	35.0
109.980000	45.2	1000.000	120.000	155.0	H	-2.0	11.5	-10.2	35.0
130.020000	47.9	1000.000	120.000	155.0	H	-2.0	11.6	-12.9	35.0
150.000000	48.1	1000.000	120.000	155.0	H	-2.0	10.8	-13.1	35.0
169.980000	55.5	1000.000	120.000	155.0	H	-2.0	9.7	-20.5	35.0
180.000000	41.5	1000.000	120.000	155.0	H	-2.0	9.1	-6.5	35.0
190.020000	43.6	1000.000	120.000	155.0	H	-2.0	9.4	-8.6	35.0
229.980000	45.6	1000.000	120.000	155.0	H	-2.0	11.6	-10.6	35.0

5.2.2 Braided Shield cable

Braided shield cable tested in Figure 42 shows the connection to the female BNC-connector. Braid connection to the connector chassis is made by soldering and this kind of long connection, also called pigtail connection, to the BNC-connector chassis is ineffective because of pigtail inductance which means that there is no connection to the connector chassis at high frequencies and also the center wire is exposed to any external electric field. (Willis 2007: 350)

Figure 42. Braided cable soldered to BNC-connector.

Pigtail effect can be removed (Figure 43) where copper tape has been used in 360° over the pigtail and the BNC-connector chassis. Copper tape has really good performance, because the tape glue is electrically conductive.

Figure 43. Pigtail effect removed by using copper foil.

The setup is placed on the measurement chamber Table in Figure 44 by using the same method as for the non-shielded cable.

Figure 44. EMI-source connected to the two meter braided shield cable.

If we compare this Figure 45 result to the non-shielded (Figure 41) cable the reduction of interference is remarkable at every frequency, but still the low commercial limits 35 dBµV/m cannot be fulfilled.

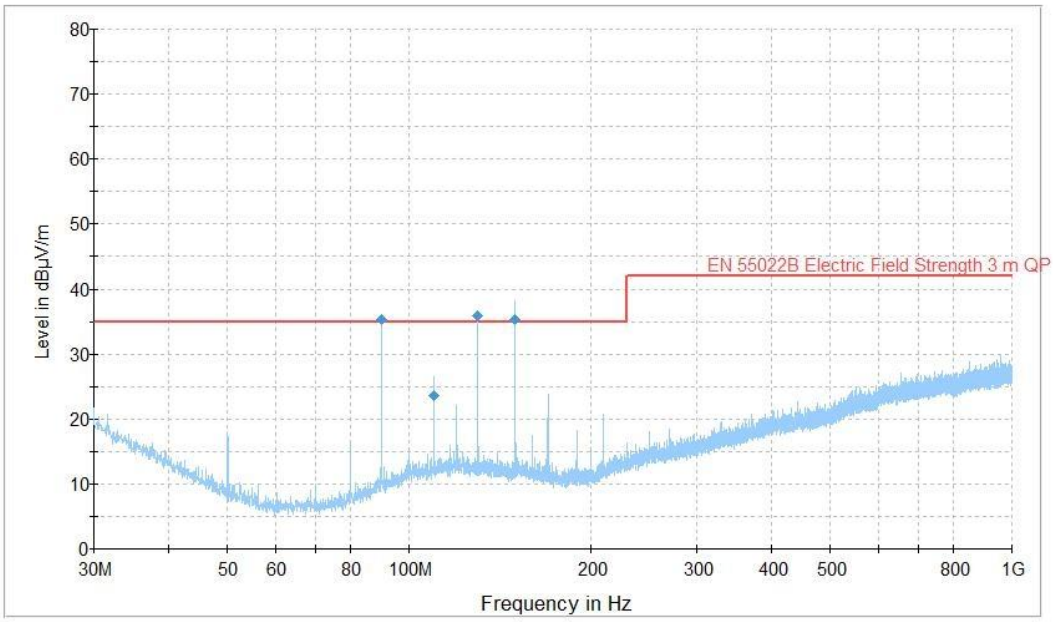

Figure 45. EMI results for braided shield cable.

Table 8 shows that some frequencies are still above limit line 35 dBµV/m.

Table 8. EMI results for braided shield cable.

Frequency (MHz)	QuasiPeak (dBµV/m)	Meas. Time (ms)	Bandwidth (kHz)	Antenna height (cm)	Polarity	TurnTable position (deg)	Corr. (dB)	Margin (dB)	Limit (dBµV/m)
90.000000	35.2	1000.00	120.000	155.0	H	0.0	9.1	-0.2	35.0
109.980000	23.5	1000.00	120.000	155.0	H	0.0	11.5	11.5	35.0
130.020000	35.8	1000.00	120.000	155.0	H	0.0	11.6	-0.8	35.0
150.000000	35.3	1000.00	120.000	155.0	H	0.0	10.8	-0.3	35.0

5.2.3 Single shield low cost coaxial cable

Low cost coaxial cable on the test room table in Figure 46.

Figure 46. EMI-source connected to the two meter low cost single shield coaxial cable.

Common-mode current flows uniformly in the same direction along all wires in the used cable but in this test the cable has only one middle wire because coaxial cable was used. The shield of the coaxial cable is tested for how good the shield attenuation is against high level common-mode interference. The common-mode interference is present now in the middle wire of the coaxial cable and no wanted differential mode signals are present. Real equipment contains many wanted differential mode signal currents which do not return via the cable but leak out through stray capacitance and convert to common-mode current. (Willis 2007: 341)

Figure 47 shows that low cost coaxial cable cannot hold the high interference voltage inside the cable middle wire.

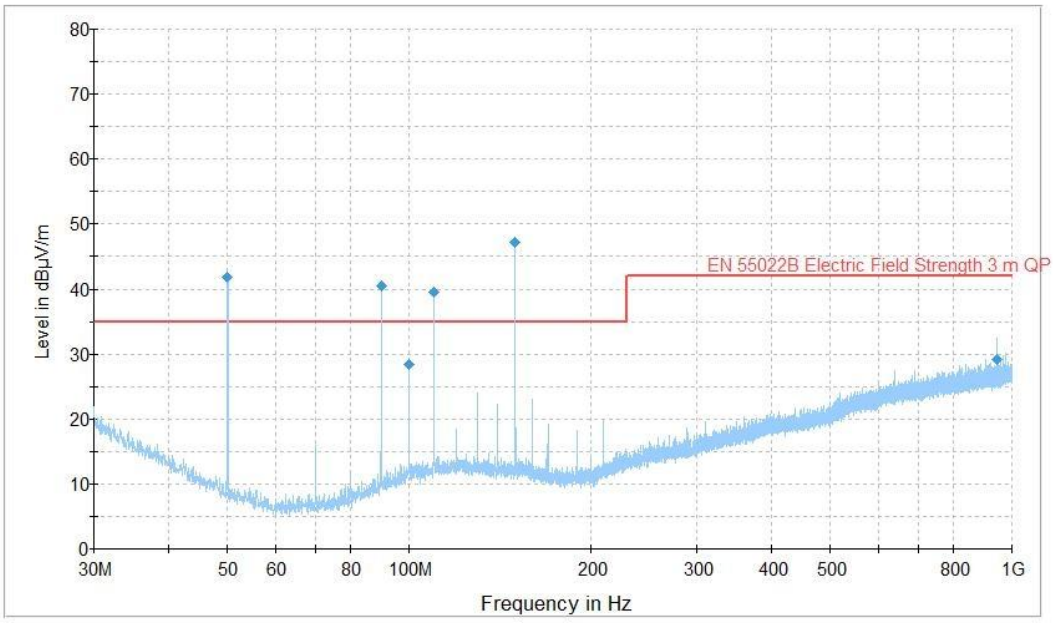

Figure 47. EMI results for low cost single shield coaxial cable.

Table 9 shows that several frequencies are above limit line 35 dBµV/m.

Table 9. EMI results for low cost single shield coaxial cable.

Frequency (MHz)	QuasiPeak (dBµV/m)	Meas. Time (ms)	Bandwidth (kHz)	Antenna height (cm)	Polarity	TurnTable position (deg)	Corr. (dB)	Margin (dB)	Limit (dBµV/m)
49.980000	41.8	1000.000	120.000	155.0	H	0.0	8.0	-6.8	35.0
90.000000	40.4	1000.000	120.000	155.0	H	0.0	9.1	-5.4	35.0
100.020000	28.4	1000.000	120.000	155.0	H	0.0	10.8	6.6	35.0
109.980000	39.4	1000.000	120.000	155.0	H	0.0	11.5	-4.4	35.0
150.000000	47.1	1000.000	120.000	155.0	H	0.0	10.8	-12.1	35.0
944.640000	29.2	1000.000	120.000	155.0	H	0.0	22.8	12.8	42.0

5.2.4 Double shielded coaxial cable

Double shielded high quality coaxial cable on the test room table in Figure 48.

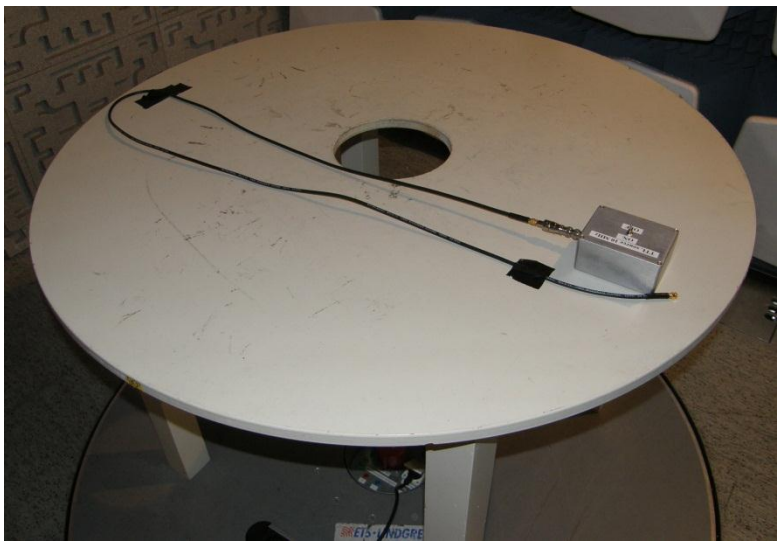

Figure 48. EMI-source connected to the two meter high quality double shield coaxial cable.

As we can see from the results in Figure 49 the radiation reduces when compared to other cables. Now with this double shielded coaxial cable the test is fulfilled and the result it is extremely good. Double shielded cable is a wise try if the design engineer has problems with common-mode currents.

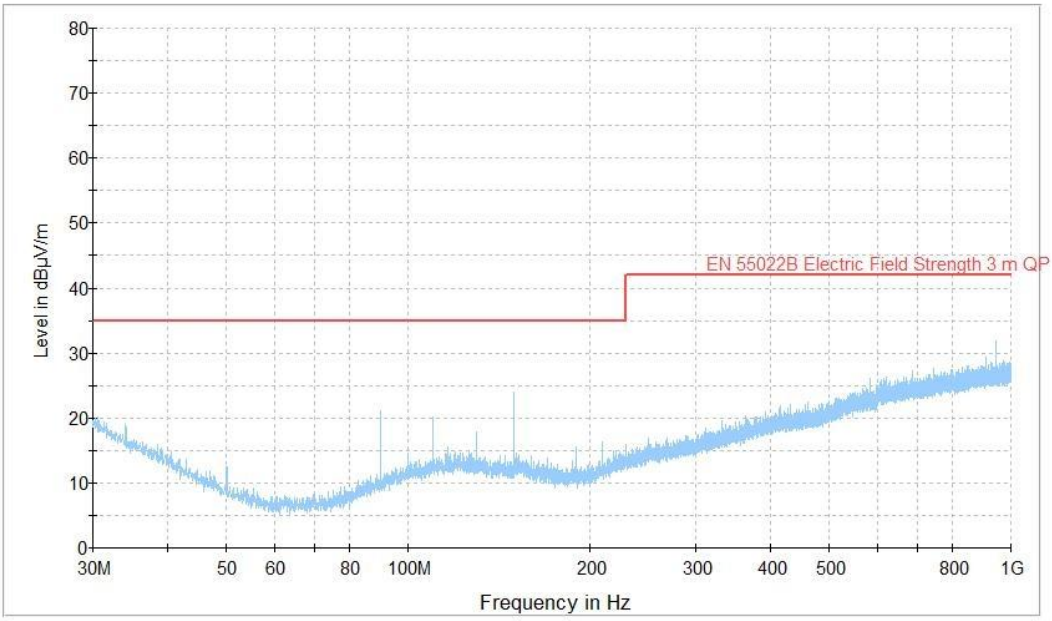

Figure 49. EMI results for high quality double shield coaxial cable.

5.3 Electric field probe (dipole antenna)

Electric field probe can be constructed from RG-58 coaxial cable and it will act like a dipole antenna and is not sensitive to magnetic fields. The intent here is to determine that which part of the EUT radiates to the far field. An electric field probe can be used to measure relative levels of near electric fields and these field levels are not easily comparable with far field levels. (Clayton 2006: 848)

Figure 50 where the coaxial cable middle wire is exposed.

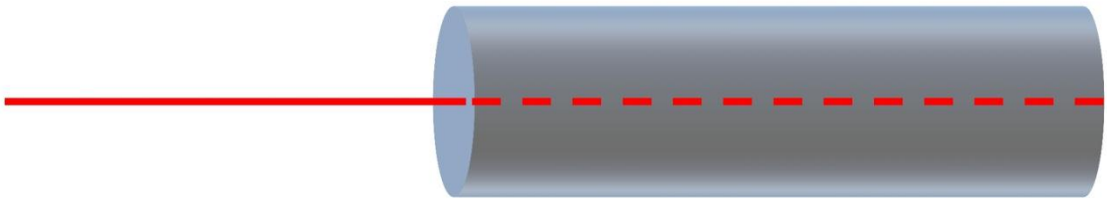

Figure 50. Principle of an electric field probe (dipole antenna).

The manufacturer ETS-lindgren calls this electric field probe a stub probe. ETS-lindgren manual gives the following instructions for using the electric field probe: Select the probe that can be put close to the interfering source. Take the largest probe and begin outside the EUT, then move closer to the source and change to smaller probe to determine the location of the interference. The smallest probe should show exactly the radiation source on a printed circuit board. The radiation source in the PCB can be an integrated circuit or a trace etc. This kind of systematic measurement approach provides the ability to stop the interference at the source rather than shielding an entire EUT. (ETS-Lindgren: 32)

It is important to remember that a high electric field level can be found from a PCB but in fact far field radiation comes from cables which are connected to the EUT because interference from the PCB is coupled via a complex path to the EUT cables. (Willis 2007: 139)

In Figure 51 on the test room table there is the EMI-source which is connected to the RG58 cable (50 Ω characteristic impedance). The ferrite probe is used to remove unwanted coaxial cable common-mode current (leakage field) and the left end of the RG58 cable contains a dipole antenna. The mismatch is very bad for most of the harmonic frequencies and half wave dipole antenna radiation resistance is 73 Ω and the length L = 0.25 m when usable frequency is 600 MHz in Figure 49.

Figure 51. Dipole connected to the EMI-source through large ferrite clamp.

Figure 52 shows that the dipole is made from a female BNC-connector and two connection wires.

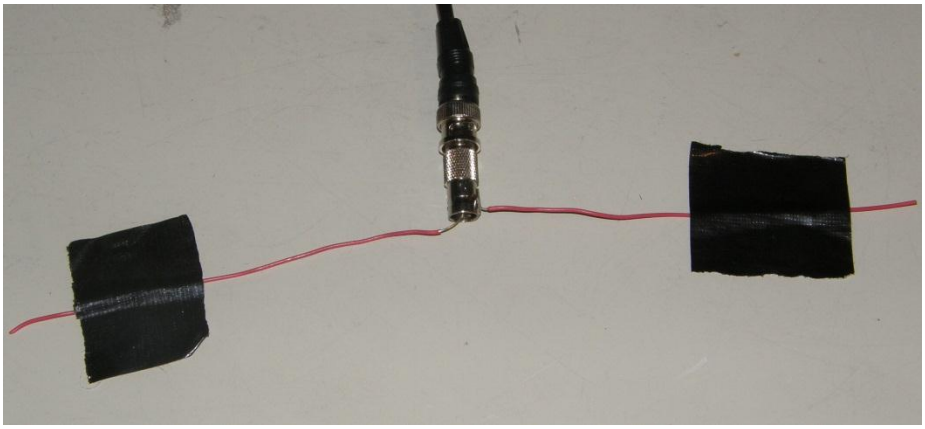

Figure 52. Simple dipole antenna.

Figure 53 shows the measurement antenna and the EMI-source loaded dipole antenna on the test room Table.

Figure 53. Simple dipole antenna and EMC-test room.

The dipole antenna impedance is complex valued which contains a real part and the imaginary part (Figure 8). Figure 54 shows the antenna resistance as a function of frequency and Figure 55 shows the antenna reactance as a function of frequency and these values are the theoretically estimated curves (Clayton 2006: 437) for a dipole which is L = 0.25 m long and antenna wire radius r is 0.25 mm. The radius of the wire is important to know because the imaginary part of the impedance will be determined ρ/λ according to the radius of the wire. We can see from Table 10 that 600 MHz is the frequency at which the antenna is mainly used if it's designed as a transmitter antenna for one frequency (half wavelength dipole), because at this frequency there is only very small reactance. (Edminister 1993: 299)

Table 10. Dipole antenna radiation resistance and reactance.

λ multiplier	**f [MHz]**	**R_a [Ω]**	**X_a [Ω]**
0.2	240	10	-730
0.25	300	15	-590
0.3	360	22	-460
0.35	420	30	-330
0.4	480	40	-190
0.45	540	55	-70
0.5	600	73	43
0.55	660	98	160
0.6	720	132	290

The resistance R_r for dipole antenna in Figure 54.

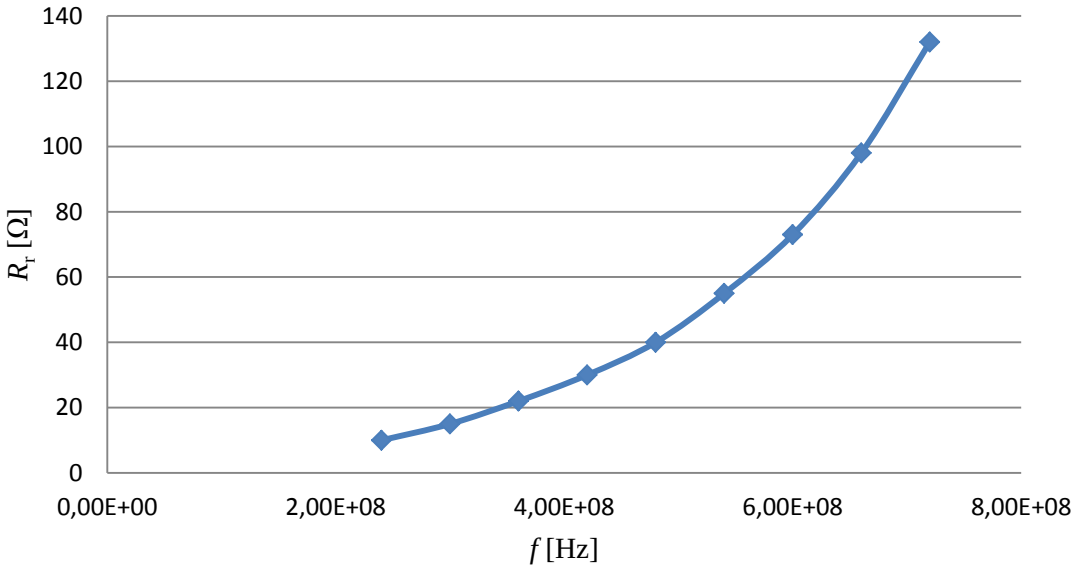

Figure 54. Radiation resistance of dipole antenna which length L is 0.25 m and wire radius r is 0.25 mm.

The reactance X_r for dipole antenna in Figure 55 which has a wire radius r = 0.25 mm.

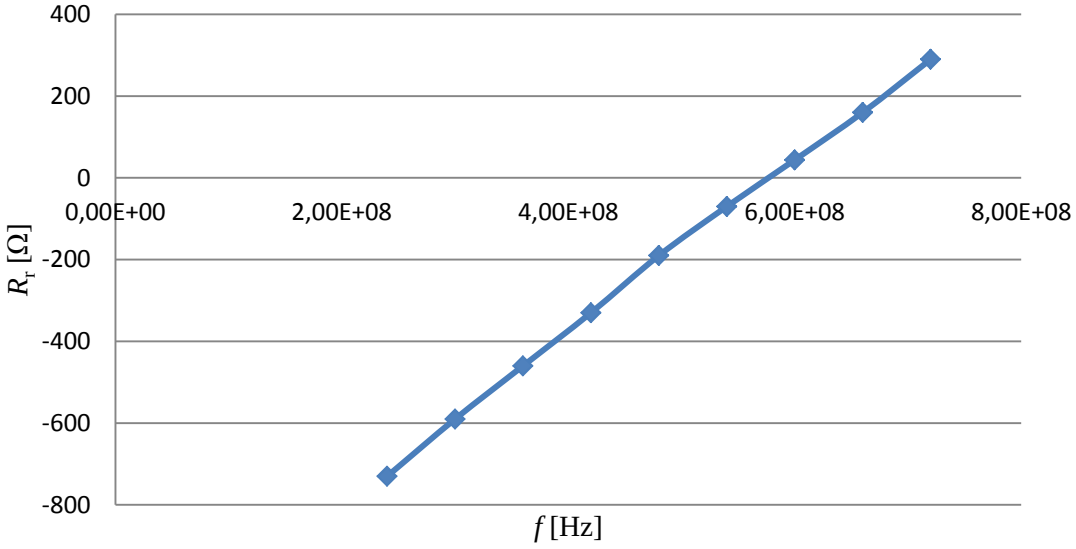

Figure 55. Reactance of dipole antenna which length L is 0.25 m and wire radius r is 0.25 mm.

Figure 56 shows the results when the measurement setup from Figure 53 is used. Radiation is above the limit line. The harmonics (voltages) of the EMI-source are very powerful in smaller frequencies than the antenna half-wave frequency which is about 600 MHz. Because of the antenna parameters R_r and X_a the mismatch between the RG-58 cable and the antenna is significant almost at all harmonic frequencies.

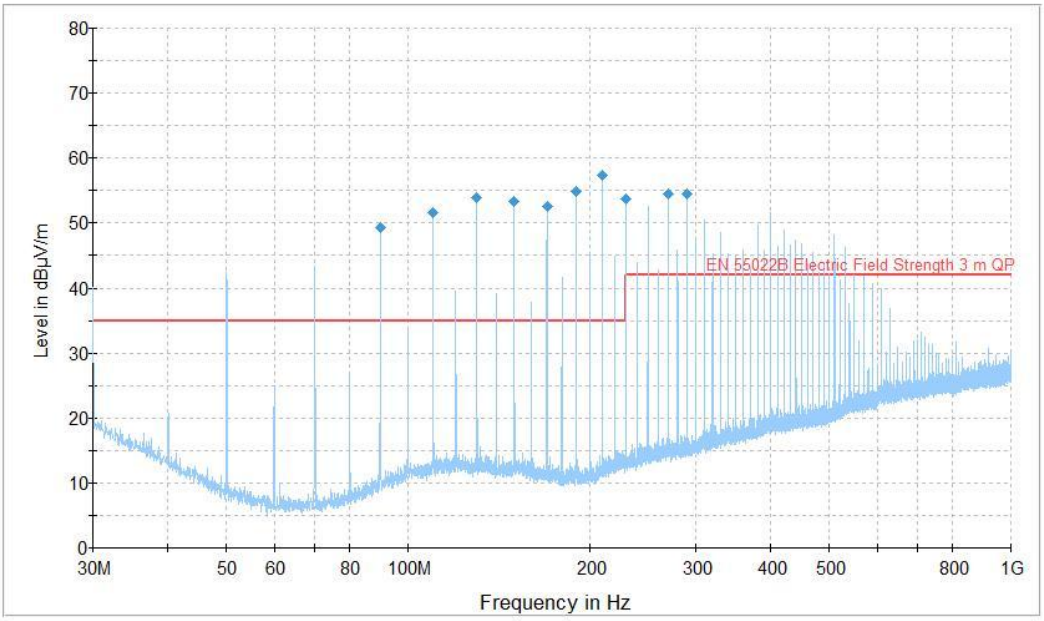

Figure 56. Dipole antenna results.

Table 11 shows that many frequencies are above the limit line.

Table 11. Dipole antenna results.

Frequency (MHz)	QuasiPeak (dBµV/m)	Meas. Time (ms)	Bandwidth (kHz)	Antenna height (cm)	Polarity	TurnTable position (deg)	Corr. (dB)	Margin (dB)	Limit (dBµV/m)
90.000000	49.2	1000.000	120.000	155.0	H	-2.0	9.1	-14.2	35.0
109.980000	51.5	1000.000	120.000	155.0	H	-2.0	11.5	-16.5	35.0
130.020000	53.9	1000.000	120.000	155.0	H	-2.0	11.6	-18.9	35.0
150.000000	53.4	1000.000	120.000	155.0	H	-2.0	10.8	-18.4	35.0
169.980000	52.5	1000.000	120.000	155.0	H	-2.0	9.7	-17.5	35.0
190.020000	54.9	1000.000	120.000	155.0	H	-2.0	9.4	-19.9	35.0
210.000000	57.3	1000.000	120.000	155.0	H	-2.0	10.3	-22.3	35.0
229.980000	53.7	1000.000	120.000	155.0	H	-2.0	11.6	-18.7	35.0
270.000000	54.5	1000.000	120.000	155.0	H	-2.0	13.4	-12.5	42.0
289.980000	54.6	1000.000	120.000	155.0	H	-2.0	13.9	-12.6	42.0

Figure 57 contains the measurement result without the dipole antenna (red wires removed) when the EMI-source, probe and the RG-58 cable are still connected. The result shows that exposing the end of the RG-58 cable to the form of a dipole antenna increases radiation dramatically. According to this result it is clear from the EMC point of view that shielded cable signal wires should never be exposed from the shield.

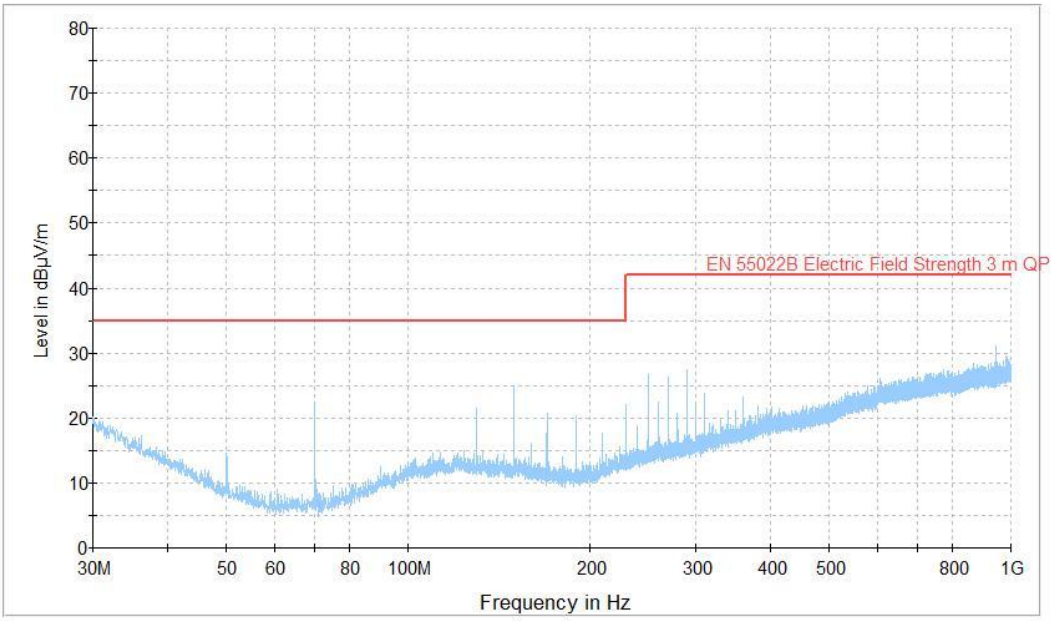

Figure 57. Results without dipole antenna.

RG-58 coaxial cable electric field probe whose center wire is exposed 100 mm and this version is investigated (in the other version the center wire is exposed 10 mm) and insulated with a shrinking tube. The half wave dipole frequency is 750 MHz and the half wave dipole antenna length is L = 0.2 m and then radiation resistance $R_r \approx 73\ \Omega$ and antenna reactance is $jX_a \approx 44\ \Omega$. This antenna equivalent circuit can be found from in Figure 9. Now the load Z_{LOAD} is actually the spectrum analyzer where input impedance is purely resistive 50 Ω and characteristic impedance of the RG-58 is 50 Ω so there is no mismatch between cable and the spectrum analyzer. The electric field probe (antenna) reactance and resistance varies as a function of frequency so at every frequency there is some sort of mismatch situation between the probe and the RG-58 cable but anyway the practical measurements have shown that the electric field probe can be used to search interferences in near-field.

Figure 58. Electric field probe (dipole antenna).

The electric field probe should have high sensitivity according to Bk-precision near-field probe manual. They state that the probe can be used to check screening and to perform pre-compliance testing on a comparative basis. (Bk Precision 1996: 2)

Figure 59 shows the test setup. The spectrum analyzer and the oscilloscope has been used to make measurements. During the measurement the shielded room door was closed so the measurement does not contain any additional external interferences.

Figure 59. Test setup for electric field probe.

Figure 60 shows the test arrangement when a dipole and the electric field probe are placed very close to each other.

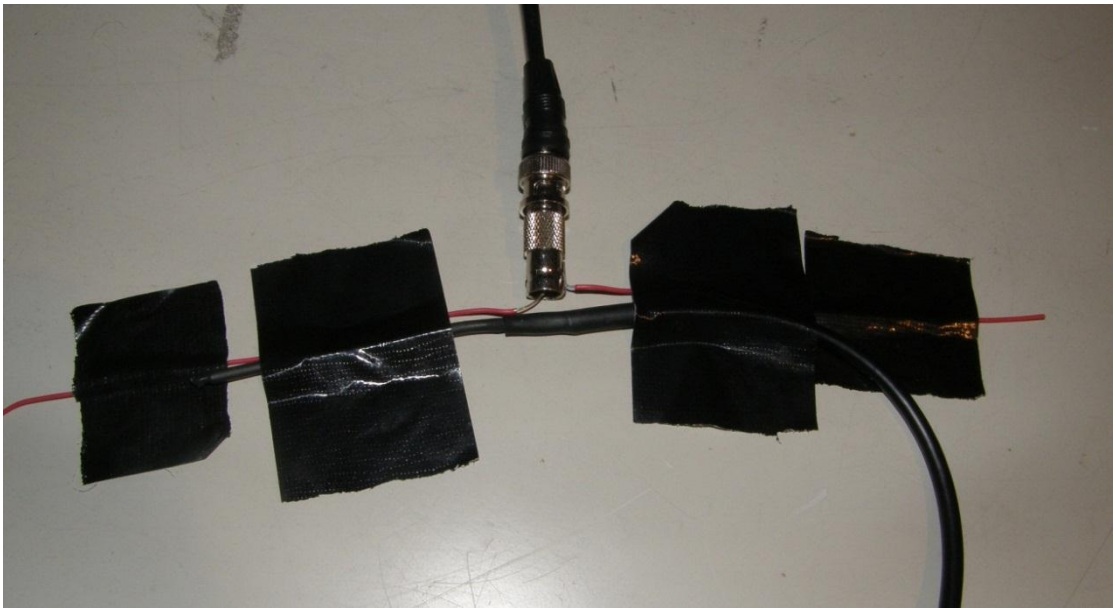

Figure 60. Dipole antenna and electric field probe.

This result shows that only rising and falling edges will cause coupling to the electric field probe. Electric field probe is terminated to impedance of 50 Ω (oscilloscope) when the signal output peak to peak voltage is about 150 mV. The EMI-source fundamental frequency (red dotted line in Figure 61) is 10 MHz which means a period time of 100 ns and if we look at two rising edges of the probe the time between these events are almost exactly 100 ns (one division in oscilloscope is 20 ns).

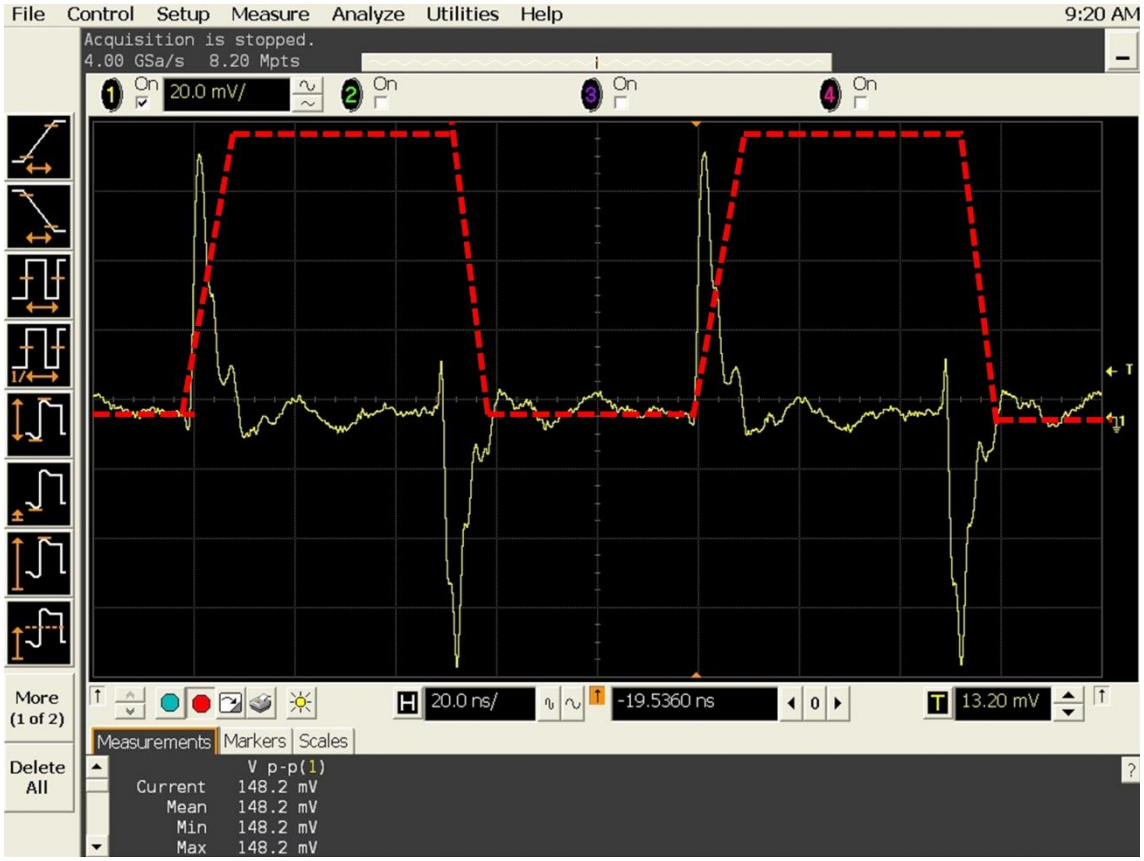

Figure 61. The electric field probe output voltage yellow curve when electric field probe connected to oscilloscope and oscilloscope input impedance is 50 Ω. The EMI-source output voltage shown as a red dotted line.

Figure 62 contains the spectrum analyzer measurement result from the electric field probe. As we can see the magnitudes of harmonics are not comparable with far field from Figure 56. However the spotted frequencies are comparable (same frequencies can be seen in far field and near-field) and this is the purpose of using a near-field probe that we can see the problematic interfering frequency from the PCB or the EUT cables. Spectrum analyzer can be configured to one frequency so an interesting frequency can be investigated.

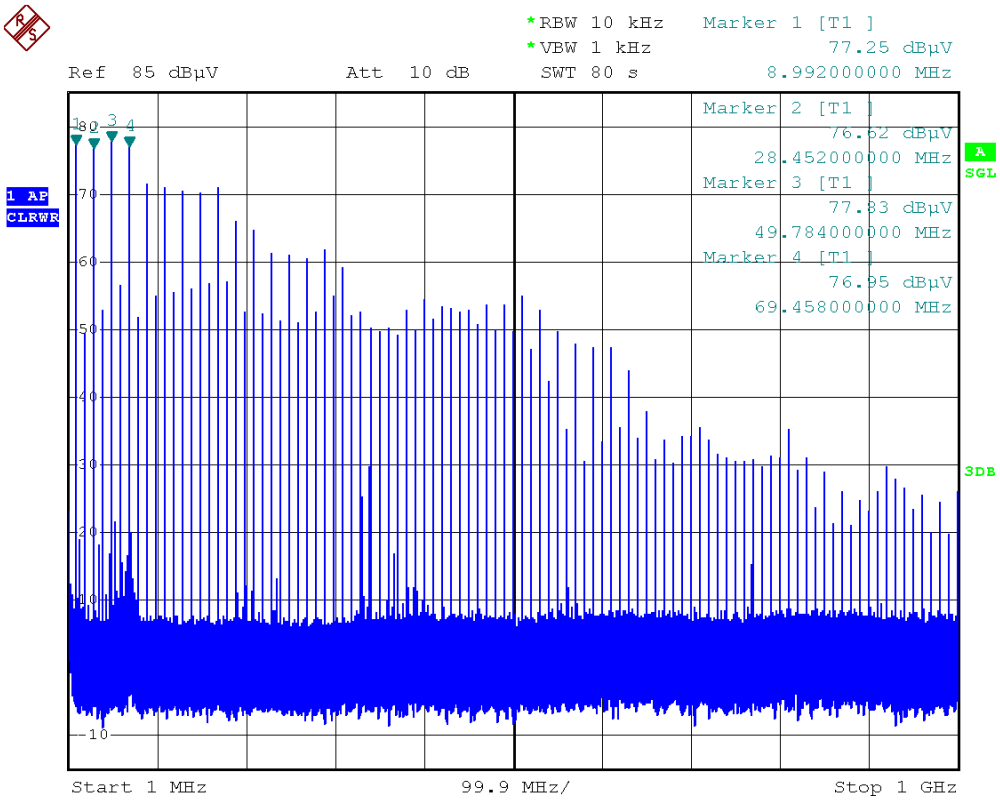

Figure 62. The electric field probe output voltage harmonics when electric field probe connected to spectrum analyzer and analyzer input impedance is 50 Ω.

Table 12 shows the result when the distance between electric field probe and the antenna is increased. In the results we can see that the magnitude of peak to peak voltage drops quite fast when the distance is increased.

Table 12. Electric field probe voltage at different distances.

Distance [mm]	Output peak to peak voltage [mV]
1	148
20	42
100	17

Table 13 shows how electric field probe radiation resistance R_a and reactance X_a behaves if we handle the electric field probe as a dipole antenna. According to Table 13 the usable frequency range for an electric field probe would be approximately 300 MHz - 1000 MHz. The first line of Table 13 can be read as antenna length is 0.2 times wavelength of used frequency f, when $c = 300 \cdot 10^6$ m/s, $f = 300 \cdot 10^6$ m/s then $L = 0.2(c/f) = 0.2$ m. Each line will give the same length for the antenna, $L = 0.2$ m.

Table 13. Electric field probe radiation resistance and reactance

λ multiplier	**f [MHz]**	**R_a [Ω]**	**X_a [Ω]**
0.2	300	10	-730
0.25	375	15	-590
0.3	450	22	-460
0.35	525	30	-330
0.4	600	40	-190
0.45	675	55	-70
0.5	750	73	44
0.55	825	98	160
0.6	900	132	290

5.4 Shielded magnetic field probe (loop antenna)

Doug Smith provides on his homepage very good instructions for how to build the one square inch shielded magnetic field probe. This chapter shows detailed instructions with Figures that show how a shielded magnetic field probe can be manufactured. I chose this loop because there were good instructions available. (D.C. Smith Consultants)

5.4.1 Shielded magnetic field probe equivalent circuit

Real loop antenna contains several serial impedances which are shown in Figure 63. The voltage generator V_{OC} is the voltage caused by external flux. (McGraw-Hill Professional. Loop antennas)

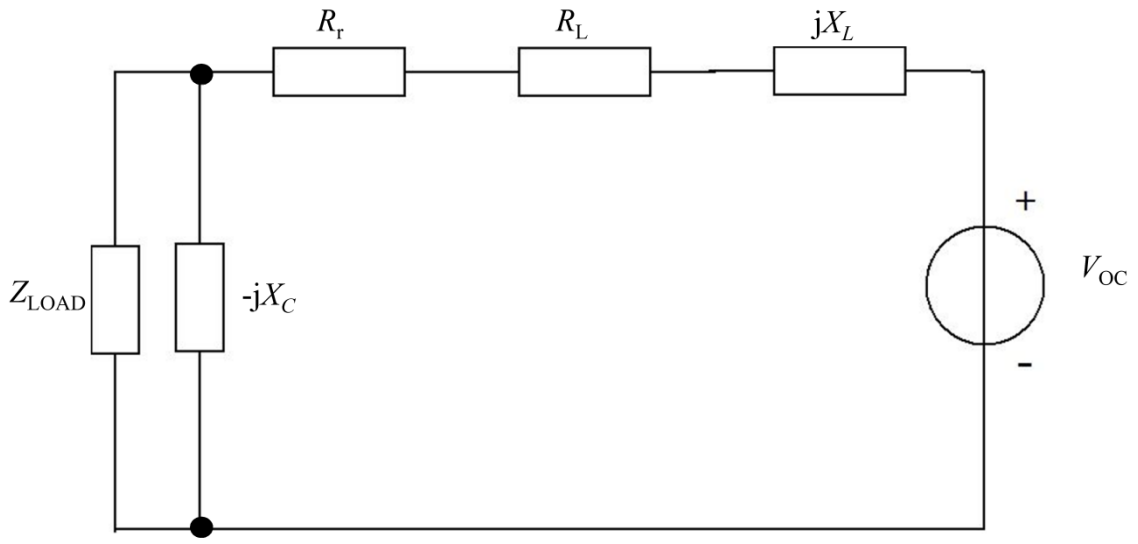

Figure 63. Magnetic field probe (loop antenna) equivalent circuit.

The loop external inductance for square loop can be approximated by using equation 37 and the value of external inductance L_e for one inch square loop is about 70 nH and this inductance causes reactance part X_L in the Figure 63, where s is side length of the magnetic field probe, d_{wire} is diameter of magnetic field probe wire and equation is (Miron 2006: 32):

$$L_e = \frac{2\mu_0}{\pi} s\left[\ln\left(\frac{2s}{d_{wire}}\right) + \frac{d_{wire}}{2s} - 0.774\right]. \quad (37)$$

The capacitance of the loop antenna is related to Figure 62 X_C and the capacitance is estimated from circle loop equation 38 where the capacitance is extremely small 0.108 pF. The diameter for magnetic field probe d_{loop} is estimated 0.0254 m and equation is

$$C = \frac{d_{loop}^2}{(0.98\,c)^2\, L_e}. \quad (38)$$

Radiation resistance R_r can be calculated according to equation 39 (Miron 2006: 33):

$$R_r = \frac{8\pi^3 \eta_0}{3}\left(\frac{Sf^2}{c^2}\right)^2. \quad (39)$$

Losses R_L can be calculated with equation 40. The conductivity σ_{CU} for copper is 57 MS/m and the wire radius r is 0.4 mm (Edminister 1993: 305):

$$R_L = \frac{2s\sqrt{\pi f \mu_0 \sigma_{CU}}}{\pi r \sigma_{CU}}. \quad (40)$$

The Table 14 contains open circuit V_{OC} values for one square inch loop antenna at different frequencies when the incident wave is a plane wave and its frequency range 30 MHz – 1000 MHz. Values are calculated by using equations 38-40. Calculated series resonance frequency is about 1.7 GHz which is far beyond the needed maximum 1000 MHz frequency. At each used frequency 30 MHz – 1000 MHz the reactance value X_C is quite big compared to the reactance X_L so this capacitive part can be ignored. Radiation resistance R_r is very small compared to the reactance X_L and can also be ignored. The ohmic resistance R_L can be ignored because losses are smaller than the radiation resistance where values for losses are 58 mΩ at 30 MHz and 336 mΩ at 1000 MHz. The equivalent circuit in Figure 63 reduces to equivalent circuit in Figure 64 which is much more convenient. We can see from Table 14 that inductive reactance X_L increases when frequency is increased.

Table 14. Magnetic field probe (loop antenna) parameters as function of frequency.

f **[MHz]**	***S*** **[cm^2]**	***E*** **[V/m]**	***H*** **[A/m]**	X_L **[Ω]**	R_r **[Ω]**	X_C **[Ω]**
30	6.45	10	0.0265	13	1.30E-06	49122
100	6.45	10	0.0265	44	1.60E-04	14737
230	6.45	10	0.0265	101	4.48E-03	6407
500	6.45	10	0.0265	220	1.00E-01	2947
650	6.45	10	0.0265	286	2.86E-01	2267
1000	6.45	10	0.0265	440	1.60E+00	1474

After ignoring some components from Figure 61 equivalent circuit the new equivalent circuit looks like in Figure 62. Now the circuit is just a simple voltage divider. (D.C. Smith Consultants)

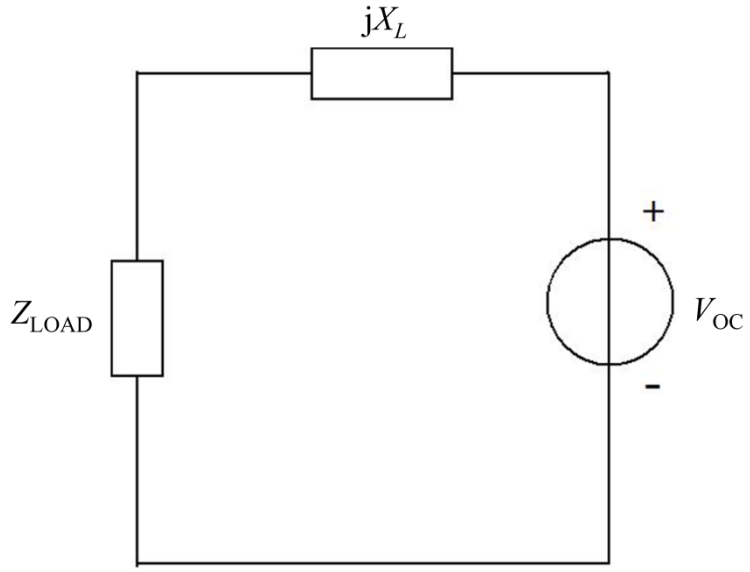

Figure 64. Simplified magnetic field probe (loop antenna) equivalent circuit.

Table 15 shows values for voltage division circuit. We can see that the output voltage V_{LOAD} remains approximately at the same value even though the reactance X_L increases as a function of frequency. This is because V_{OC} increases as well. Z_{LOAD} is now a measuring device like an oscilloscope or a spectrum analyzer whose input resistance is equal to 50 Ω.

Table 15. Simplified magnetic field probe parameters as a function of frequency.

f **[MHz]**	***S*** **[cm^2]**	***E*** **[V/m]**	***H*** **[A/m]**	V_{OC} **[mV]**	V_{LOAD} **[mV]**	X_L **[Ω]**
30	6.45	10	0.0265	4.1	3.21	13
100	6.45	10	0.0265	13.5	7.19	44
230	6.45	10	0.0265	31.1	10.28	101
500	6.45	10	0.0265	67.5	12.51	220
650	6.45	10	0.0265	87.8	13.07	286
1000	6.45	10	0.0265	135.1	13.79	440

The real measurement situation will be that there is a transmission line between the loop antenna and the measurement device like in Figure 65. Transmission line characteristic impedance Z_0 is selected to 50 Ω and Z_{LOAD} is 50 Ω resistive so there is no mismatch between the transmission line and the load. The transmission line between the antenna

and the load in Figure 65 will not change the values of V_{LOAD} in Table 15 because the voltage which goes to transmission line will be calculated in the same manner as the load voltage in Figure 64. The losses caused by the transmission line will be very low because the cable length is only two meters and the cable is a high quality coaxial cable.

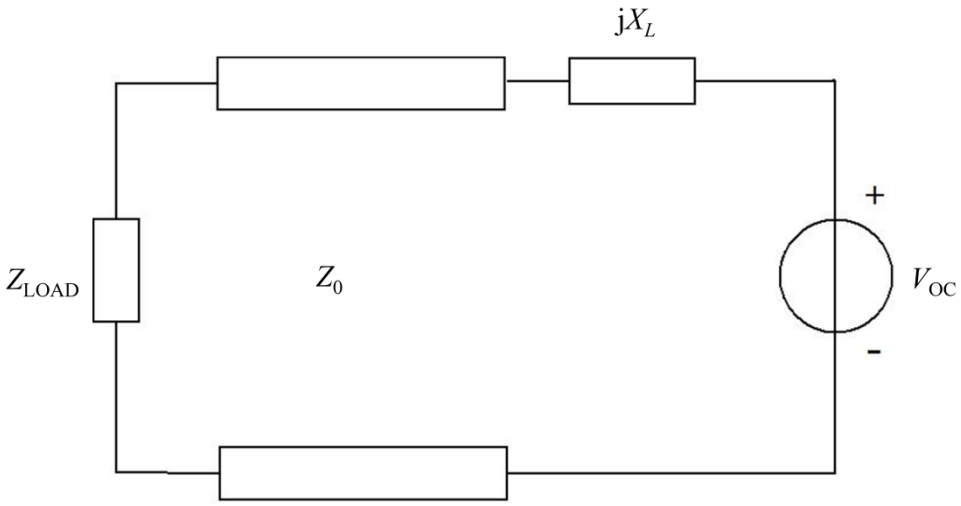

Figure 65. Measurement equivalent circuit.

The load voltage in Figure 66 is a function of frequency and we can see from the curve that at higher frequencies the reactance X_L increases and the induced voltage V_{OC} increases as well.

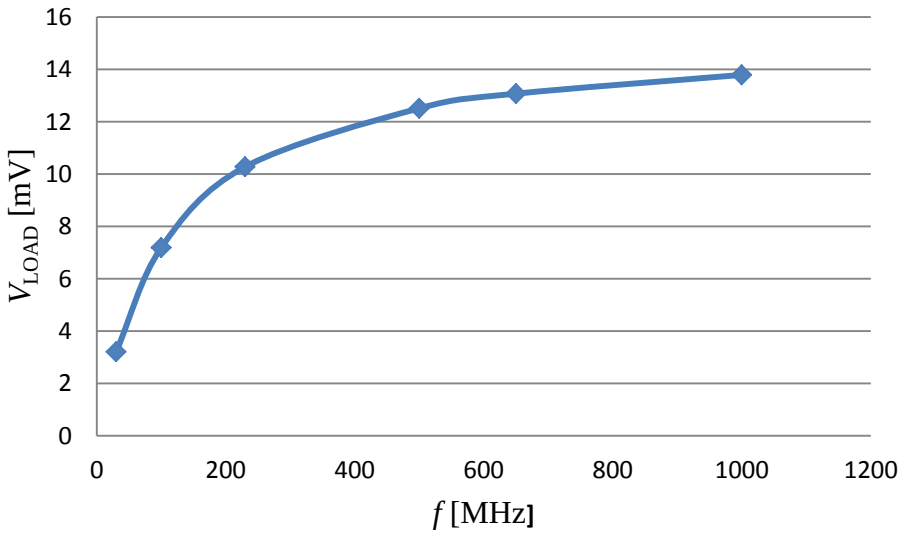

Figure 66. Measurement device voltage as a function of frequency.

5.4.2 Construction of shielded magnetic field probe

Figure 67 shows the loop where blue line is copper shield, red line is inner wire, black line is outer insulator. An important aspect is the loop connection point where the red line and the blue line are connected together.

The shielding of the loop means that the loop wire is surrounded by copper shield and this shield is called a Faraday connection because the copper tape forms a Faraday shield. (Carr 2001: 318)

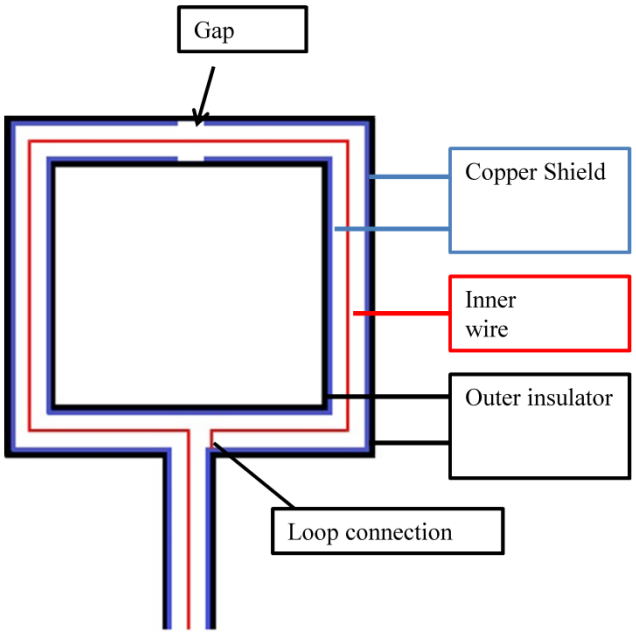

Figure 67. Magnetic field probe (loop antenna).

Figure 68 shows the copper wire which is 160 mm long and the diameter is 0.8 mm. This copper wire is insulated by a blue shrinking tube and the left end is exposed for about 30 mm and the right end for about 10 mm. The BNC female to female connector has been used to construct the probe.

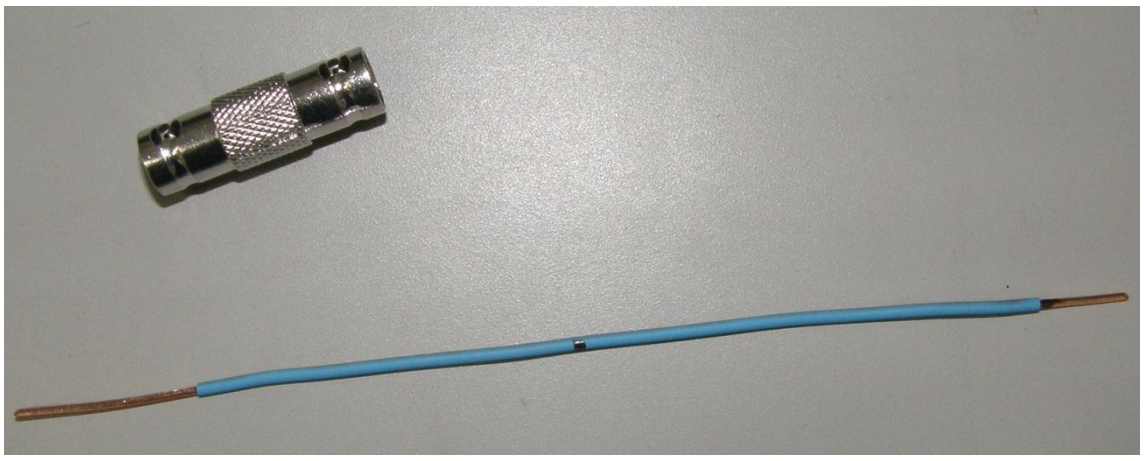

Figure 68. BNC-connector and copper wire.

In Figure 69 the copper tape is placed around the wire and the copper tape left end is connected to the copper wire. The black mark in the middle means the center point of the loop where a small gap is needed.

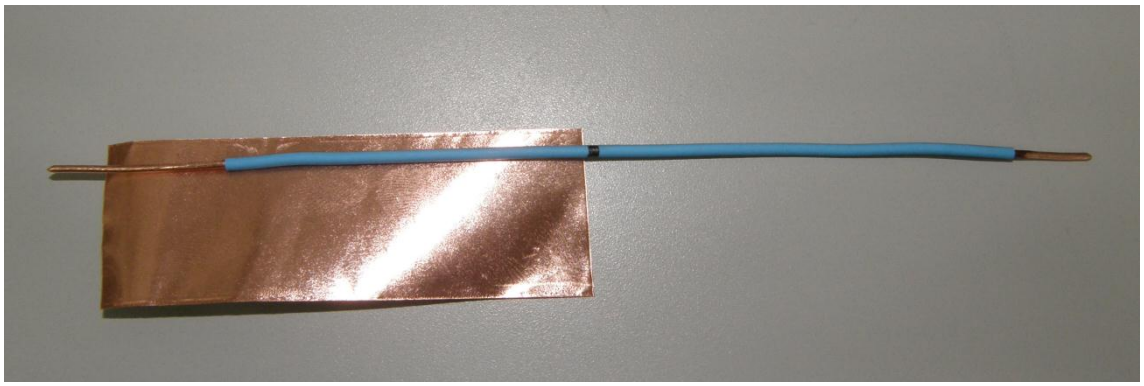

Figure 69. Copper wire, blue insulator and copper tape (copper tape adhesive is electrically conductive).

Then the copper tape is rolled around the insulated wire and the small gap can be seen in Figure 70.

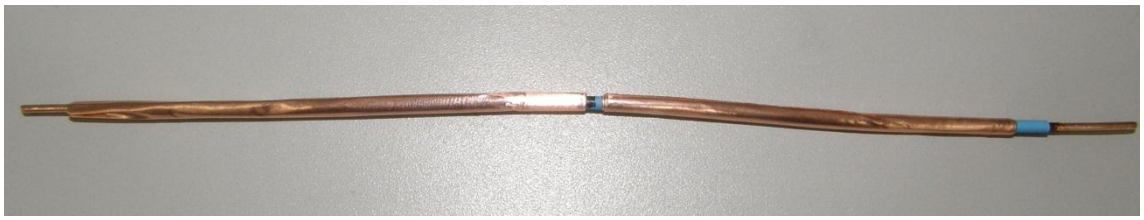

Figure 70. Outer copper tape and copper wire connected electrically at the left end.

Shrinking tube is used around the antenna section and then the loop is formed as in Figure 71.

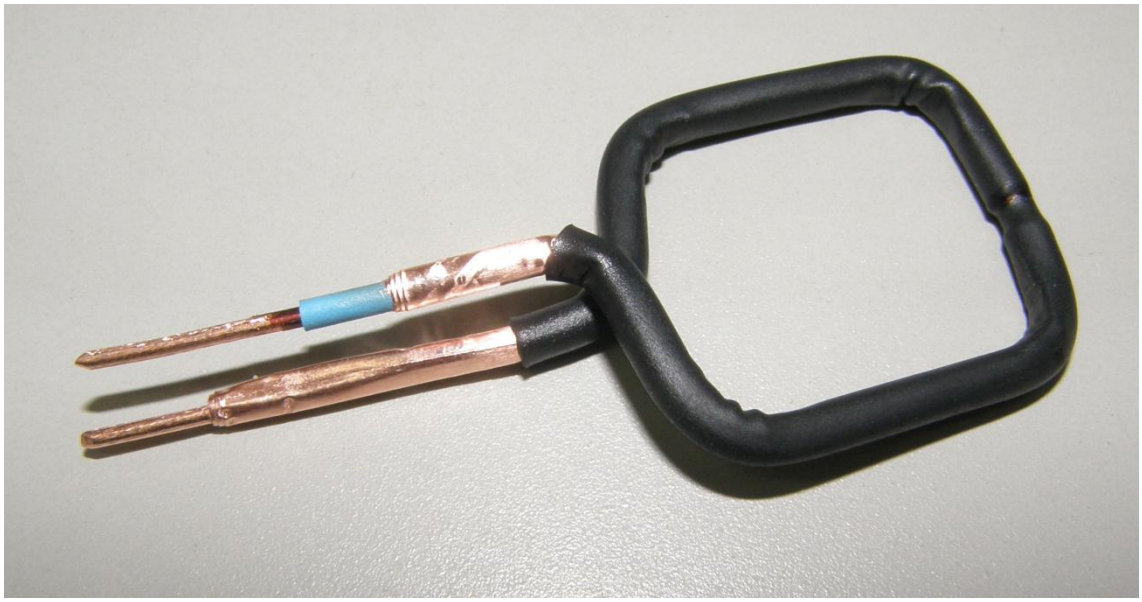

Figure 71. Magnetic field probe (loop antenna), where outer copper tape insulated by using shrinking tube.

Figure 72 shows how the loop is soldered to the female BNC-connector.

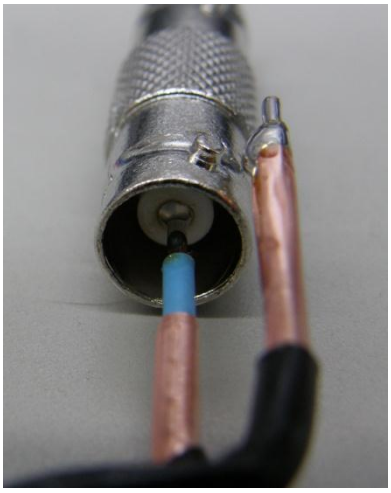

Figure 72. Magnetic field probe (loop antenna) electrical connection to BNC-connector.

Then another wire is soldered to the BNC-connector chassis as in Figure 73.

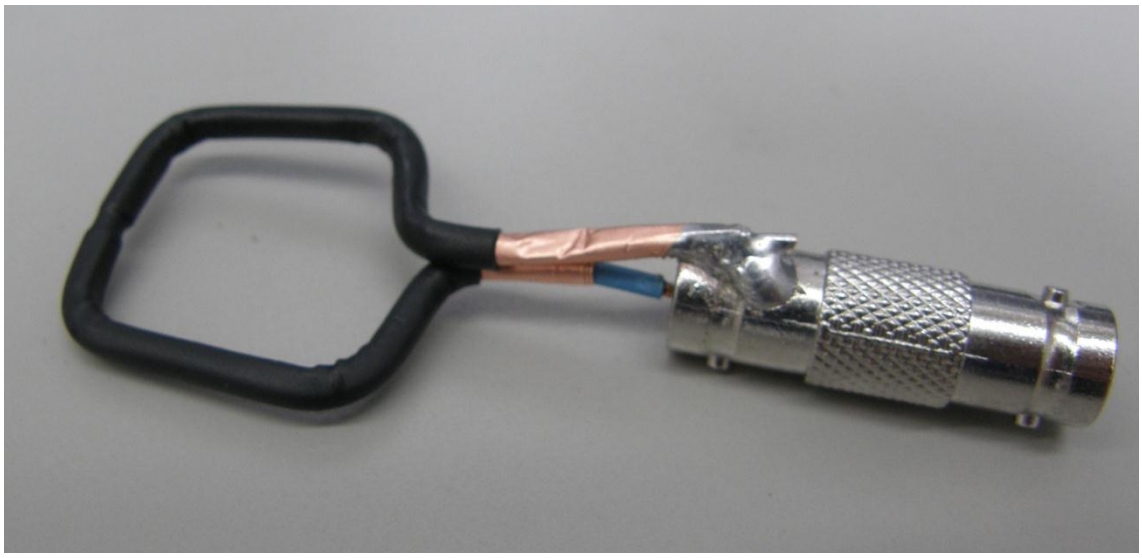

Figure 73. Magnetic field probe (loop antenna) electrical connection to BNC-connector.

Figure 74 shows how the copper tape is added around the BNC-connector to form a Faraday shield.

Figure 74. Copper tape around magnetic field probe (loop antenna) and BNC-connector.

Figure 75 shows how the copper tape connection to the loop Faraday shield is ensured by soldering the tape at the root of the loop.

Figure 75. Copper tape soldered to magnetic field probe.

Figure 76 shows the finished shielded magnetic field probe.

Figure 76. Finished insulated magnetic field probe (loop antenna).

Figure 77 contains the real measurement arrangement. The loop is connected to the spectrum analyzer by using Sucoflex104PE $Z_0 = 50\ \Omega$ coaxial cable. The EMI-source is

connected through a one meter RG58 cable to the load (metal film) resistor R_L = 47 Ω and the load end is exposed (black and red wire) for about 100 mm. Measurements have been done with a spectrum analyzer and an oscilloscope. When the oscilloscope is used the oscilloscope channel one is connected to the load resistor R_L and the oscilloscope channel one input impedance is one mega ohm.

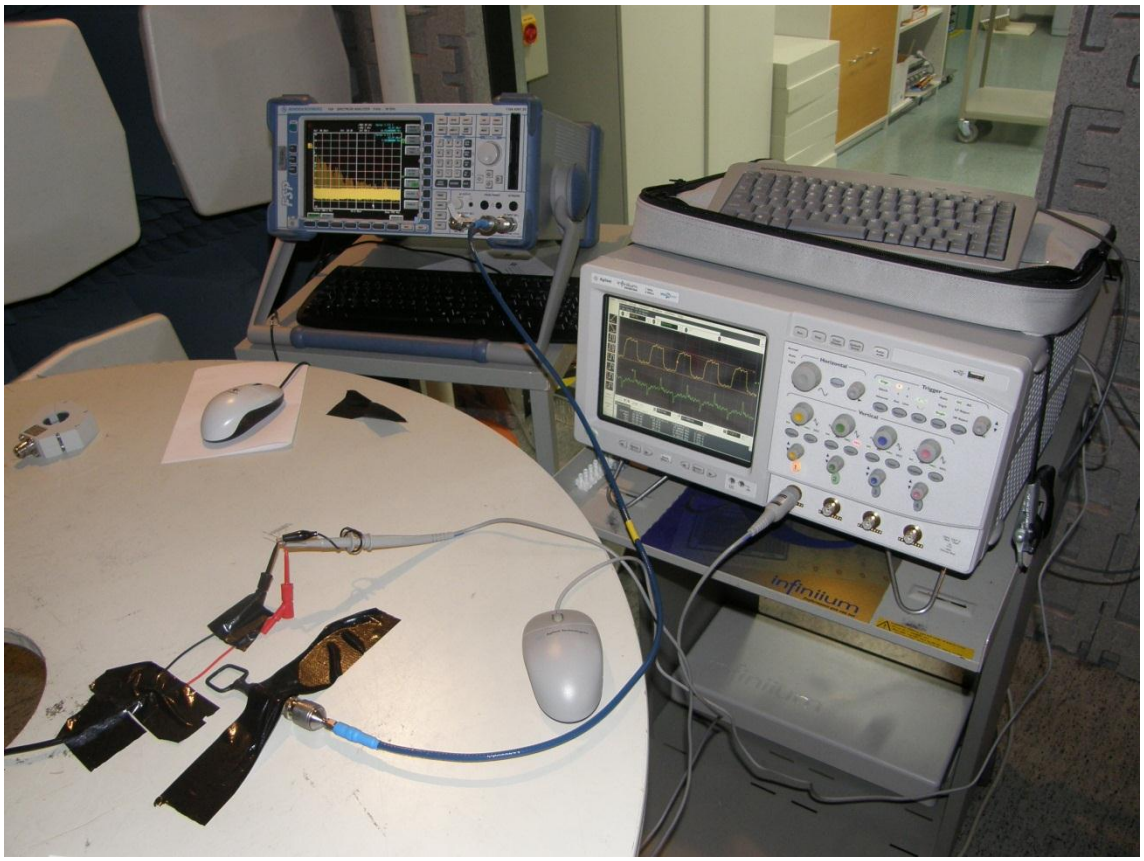

Figure 77. Conductor (red wire) time varying current causes circulating and changing magnetic field which can be measured by using magnetic field probe (loop antenna) at the distance of 10 mm.

Figure 78 shows the measurement situation when the loop probe is at close distance from a current carrying cable. The oscilloscope channel one is connected to the load 47 Ω resistor (oscilloscope channel one input impedance one mega ohm). The loop is connected to the oscilloscope channel two (oscilloscope channel two input impedance is 50 Ω). The distance between the loop and the wire is about 2 mm because of insulators.

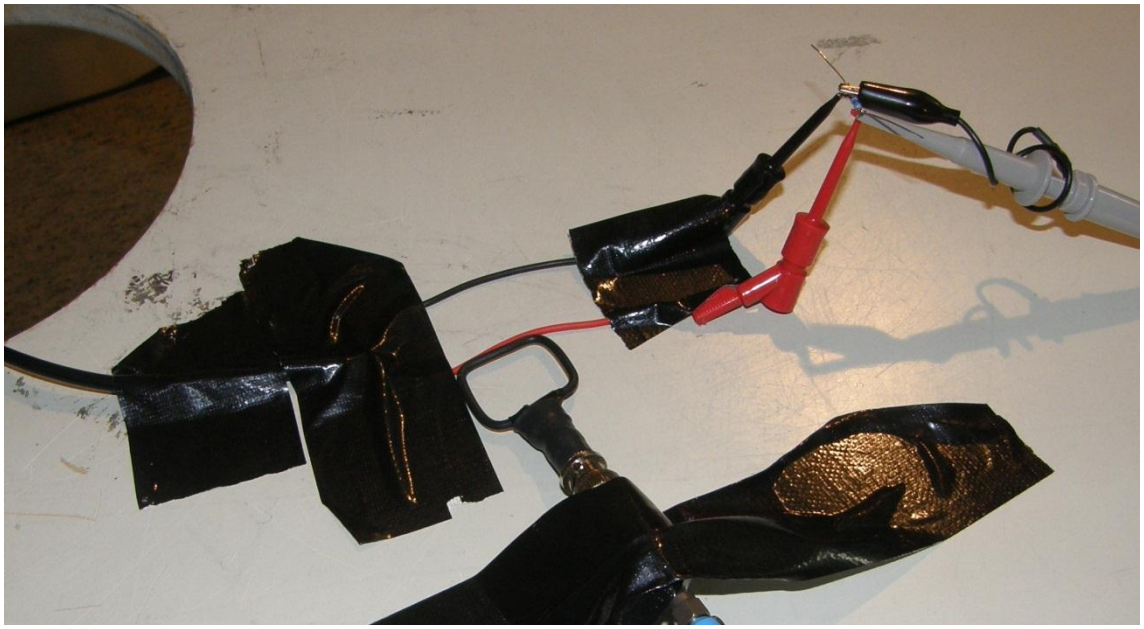

Figure 78. Conductor (red wire) time varying current causes circulating and changing magnetic field which can be measured by using magnetic field probe (loop antenna) at the distance of 2 mm.

Figure 79 shows that only rising and falling edges can be seen on the loop output.

Figure 79. Time varying magnetic field induces voltage to magnetic field probe terminals and this voltage can be seen in oscilloscope (oscilloscope input impedance is 50 Ω).

Figure 80 shows spectrum the analyzer measurement result.

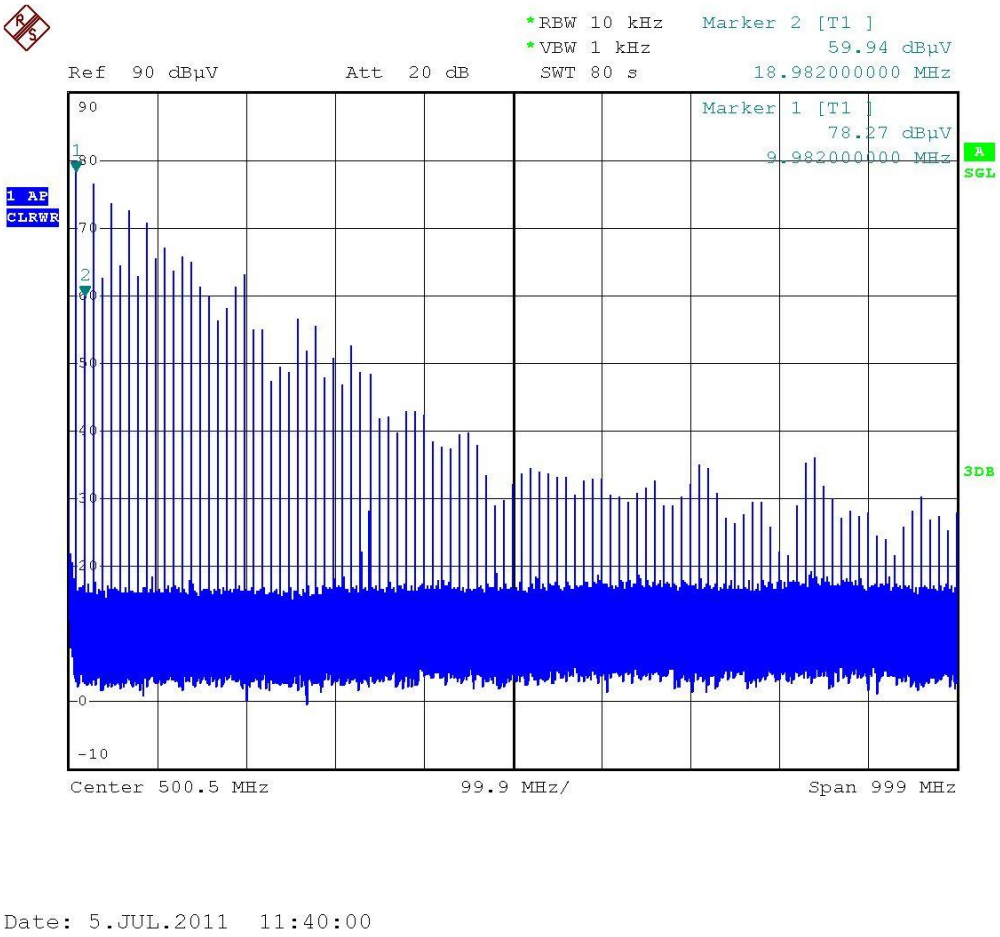

Figure 80. Magnetic field probe output voltage spectrum, where frequency range 10 MHz – 1 GHz.

Table 16 shows how the loop output voltage drops when the distance is increased.

Table 16. Magnetic field probe (loop antenna) measurements at different distances.

Distance [mm]	**Output peak to peak voltage [mV]**
1	106
10	39
20	22

Figure 81 shows the result when the loop is turned by 180 degrees and it can be seen that now the output voltage of the loop is inverted when compared to Figure 79. This is because the current direction in the loop changes.

Figure 81. Time varying magnetic field induces voltage to magnetic field probe terminals and this voltage can be seen in oscilloscope. Magnetic field probe turned by 180° degrees.

Figure 82 shows the situation when the loop is turned by 90 degrees and according to the theory there should not be any output voltage from the loop, because the magnetic field is now parallel to the loop.

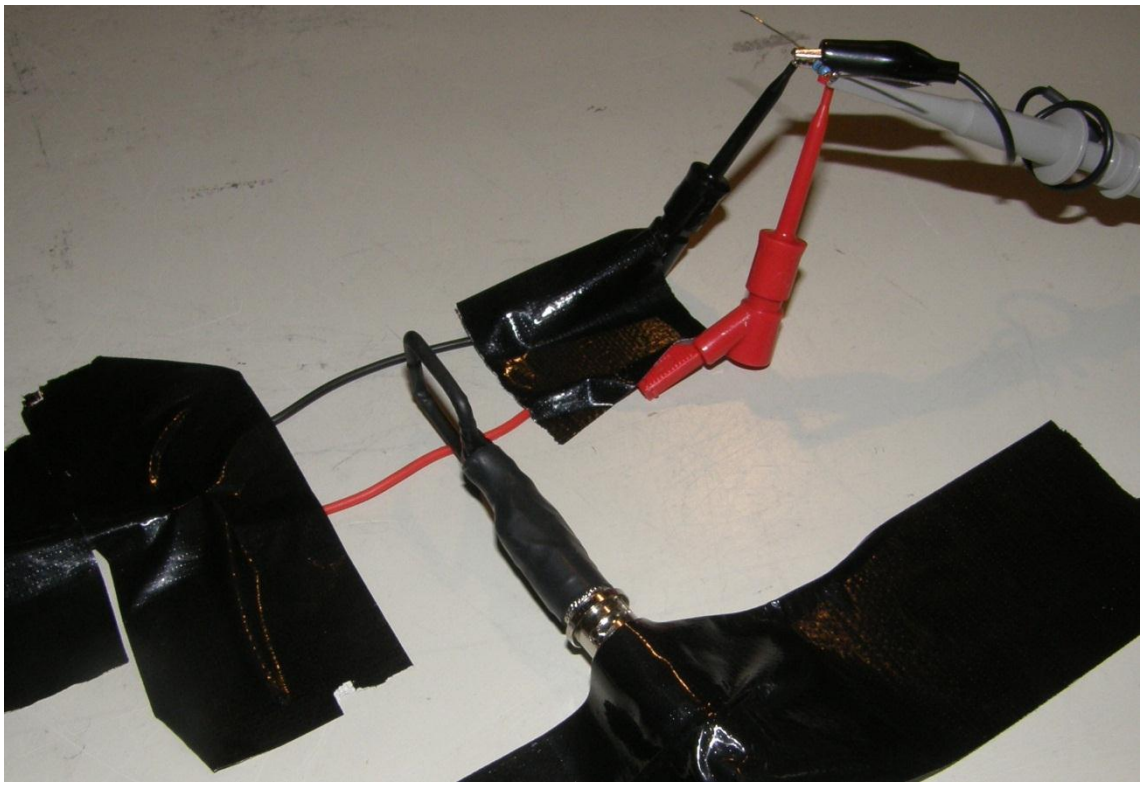

Figure 82. Conductor (red wire) time varying current causes circulating and changing magnetic field, which cannot penetrate the probe perpendicularly, because the probe is turned by 90 degrees.

Figure 83 shows the results when the loop is turned by 90 degrees and as we can see the output voltage is about ten times lower. The very small output voltage of the loop can be seen because of a non-uniform electric field. (D.C. Smith Consultants)

Figure 83. Time varying magnetic field should not induce voltage to the magnetic field probe terminals because of probe alignment. Magnetic field probe is turned by 90 degrees.

5.5 High-frequency current probe

The common-mode current is the most problematic interference radiation source from EUT cables in the frequency range 30 MHz – 250 MHz. This common-mode current acts like an antenna current which radiates to the environment. The standardized test in the anechoic chamber shows that because of this common-mode current the EUT cannot pass the test. When common-mode current is higher than five micro amperes in the EUT cables and by using CIPR22 commercial limit for electric field then the test cannot be passed. The standardized test is very expensive because of expensive equipment and therefore it is wise to first measure common-mode current with cheaper equipment like a high-frequency current probe Rohde Schwarz EZ-17-2 or Fisher custom communication F-33-1 together with a spectrum analyzer. When common-mode current is below five micro amperes then the product developer can be quite sure that the standardized test can be passed. (Ott 2009: 7 690-691)

5.5.1 Common-mode current approximation

The common-mode-current from the cables can be reduced by reducing harmonics content of digital circuit currents, by reducing the frequency of the analog circuit or by reducing the EUT cable length. The CISPR22 radiation limits for commercial equipment are 30 dBμV/m (31.6 μV/m) when the frequency range is 30 MHz - 230 MHz and 40 dBμV/m (100 μV/m) for industrial equipment when the distance between the EUT and the measuring antenna is r = 10 m. With equation 41 the maximum common-mode current (RMS value of current) I_{CM} can be calculated for cables $l < \lambda/4$ which means that the maximum usable frequency for equation 41 can be used when $f \leq c/4l$. Otherwise equation 42 should be used. For equations 41 and 42 the factors $k_1 = 0.8 \cdot 10^6$ [Am/Vs] and $k_2 = 10.6 \cdot 10^{-3}$ [A/V] (Ott 2009: 478,479):

$$I_{\mathrm{CM}} = k_1 \frac{Er}{fl} \quad \text{and} \tag{41}$$

$$I_{\mathrm{CM}} = k_2 Er\,. \tag{42}$$

According to these equations we can estimate the radiation in far field and make limit lines for common-mode current I_{CM}. Table 17 shows these calculated limit lines. The maximum frequency for a one meter cable is 75 MHz and for a three meter cable is 25 MHz so equation 42 can be used directly to estimate the three meter cable common-mode current when the used frequency range is 30 MHz - 1000 MHz. The common-mode currents are shown in Table 17 in both units [A] and [dBµA].

Table 17. Maximum allowable common-mode currents for device.

	CISPR22							
	I_{CM} [µA]	I_{CM} [dBµA]	I_{CM} [µA]	I_{CM} [dBµA]	I_{CM} [µA]	I_{CM} [dBµA]	I_{CM} [µA]	I_{CM} [dBµA]
f [MHz]	Class A Cable 1m	Class A Cable 1m	Class B Cable 1m	Class B Cable 1m	Class A Cable 3m	Class A Cable 3m	Class B Cable 3m	Class B Cable 3m
30	26.7	28.5	8.4	18.5	10.6	20.5	3.3	10.5
40	20.0	26.0	6.3	16.0	10.6	20.5	3.3	10.5
50	16.0	24.1	5.1	14.1	10.6	20.5	3.3	10.5
60	13.3	22.5	4.2	12.5	10.6	20.5	3.3	10.5
70	11.4	21.2	3.6	11.2	10.6	20.5	3.3	10.5
75	10.7	20.6	3.4	10.6	10.6	20.5	3.3	10.5
200	10.6	20.5	3.3	10.5	10.6	20.5	3.3	10.5

In Figure 84 we can see that at low frequencies the one meter cable common-mode current can be higher than the common-mode current in the three meter cable so the longer cable is a better radiator.

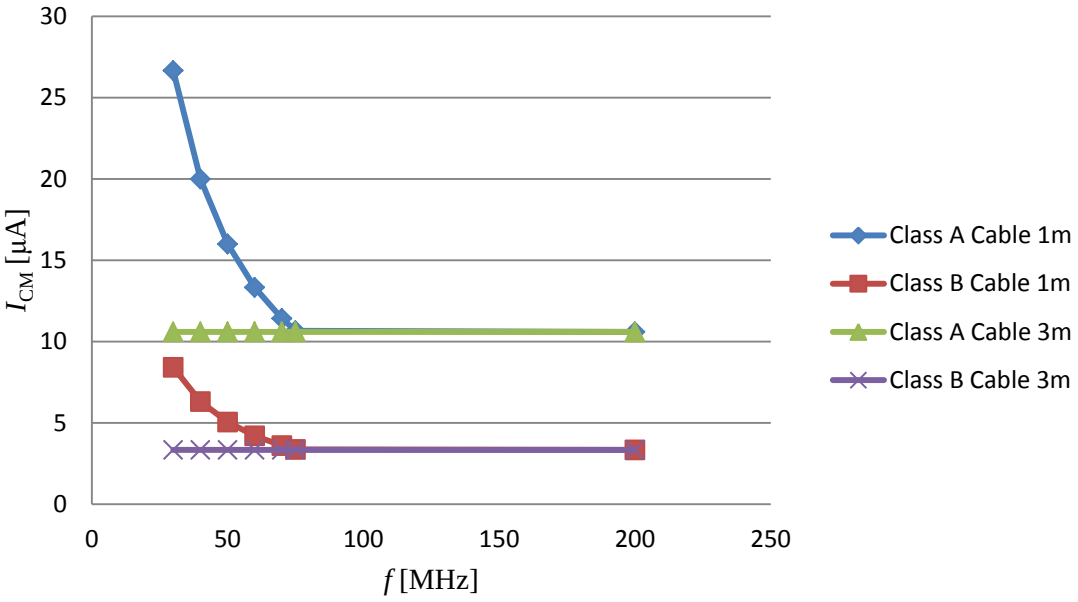

Figure 84. Common-mode current limits for different EUT-cable lengths.

5.5.2 Design of high-frequency current probe

Amperes law in equation 43 shows that when we have a conduction current density $\boldsymbol{J}_C$ or a displacement current density $\boldsymbol{J}_D$ which penetrates the surface $\boldsymbol{S}$ then the magnetic field can be induced around a conductor. Displacement current needs a time changing electric field $\boldsymbol{E}$ so if we don't have this $\boldsymbol{E}$ field at all then only the conduction current density is present which will cause a magnetic field. If the conduction current density is independent then the equation 43 can be put as $|i| = J_C S$ and the external magnetic field around the conductor is $|H| = i/2\pi r$, where ε_r is relative permittivity and equation for current is (Clayton 2006: 518):

$$i = \oint \boldsymbol{H} \cdot \mathrm{d}\boldsymbol{l} = \int_{\boldsymbol{S}} \left(\boldsymbol{J}_C + \boldsymbol{J}_D\right) \cdot \mathrm{d}\boldsymbol{S} = \int_{\boldsymbol{S}} \left(\boldsymbol{J}_C + \frac{\partial \boldsymbol{D}}{\partial t}\right) \cdot \mathrm{d}\boldsymbol{S} = \int_{\boldsymbol{S}} \left(\boldsymbol{J}_C + \frac{\partial \varepsilon_0 \varepsilon_r \boldsymbol{E}}{\partial t}\right) \cdot \mathrm{d}\boldsymbol{S}. \qquad (43)$$

The common-mode current appears as conduction current which causes a circulating magnetic field $\boldsymbol{H}$ according to Amperes law. We want to measure this common-mode current and the Faraday law in equation 44 tells that a voltage can be induced to the loop if a time changing magnetic field penetrates the surface S. The common-mode cur-

rent is a time changing current which causes a time changing magnetic field where μ_r is relative permeability and equation is

$$V_{\mathrm{OC}} = \int_{\boldsymbol{S}} \left(-\frac{\partial \boldsymbol{B}}{\partial t} \right) \cdot \mathrm{d}\boldsymbol{S} = \int_{\boldsymbol{S}} \left(-\frac{\partial \mu_0 \mu_{\mathrm{r}} \boldsymbol{H}}{\partial t} \right) \cdot \mathrm{d}\boldsymbol{S} = -\frac{\partial \phi}{\partial t}. \tag{44}$$

Figure 85 shows that a magnetic field $\boldsymbol{H}$ is induced around a current carrying cable (at the time when the direction of the current in the cable is forward as in Figure 85). The reason why ferrite material is used is because the flux ϕ is related to the magnetic flux density $\phi = B/S = \mu_0 \mu_{\mathrm{r}} H/S$ and ferrite material has a high relative permittivity μ_r so more flux can flow through the winding turns. According to Faradays law the voltage is higher if we have more flux through a surface. The minus sign in Faradays law states that the voltage induced in the clamp winding (and the current in the clamp winding because of induced voltage) by the magnetic flux (caused by the current in the cable) has a polarity such that this induced voltage (in the clamp winding) causes a current (in the clamp winding) which causes a magnetic field which opposes the magnetic field produced by the current carrying cable.

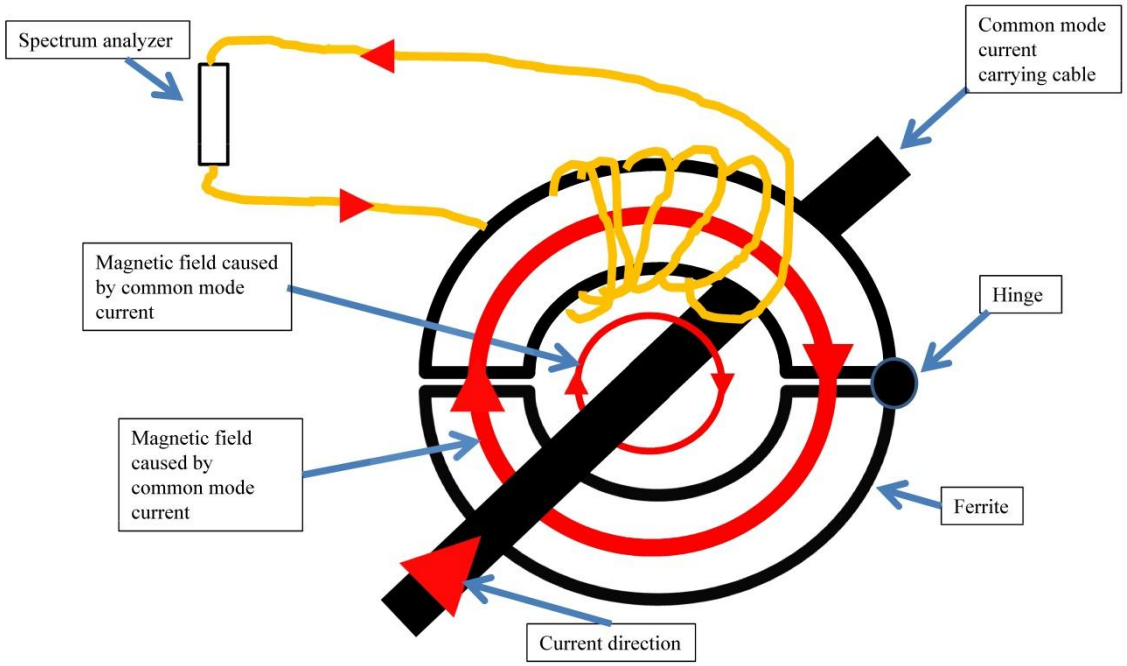

Figure 85. Principle of common-mode current probe, where time varying current flows in investigated cable. This current causes a strong circulating magnetic field inside the ferrite core and this magnetic field penetrates the winding perpendicularly and a voltage is induced to the winding terminals. The winding terminal voltage can be measured by using a spectrum analyzer.

The self-made current probe uses a Wurth elektronik ferrite core which has the code 7427135 and the datasheet for the ferrite is in Appendix 2. There are five rounds of copper wire around the ferrite upper half and the wire is connected to a BNC-connector. Defined air gaps have been made with insulating tape which cannot be seen in Figure 86.

Figure 86. Self-made common-mode current probe.

Figure 87 shows the situation when the self-made current probe is connected to the EMI-source.

5.5.3 Measurements

Figure 85 shows the EMI-source and a one meter low cost $Z_0 = 50\ \Omega$ coaxial cable.

Figure 87. Low cost coaxial cable connected to the EMI-source.

Figure 88 shows the test results which are measured in a full anechoic chamber.

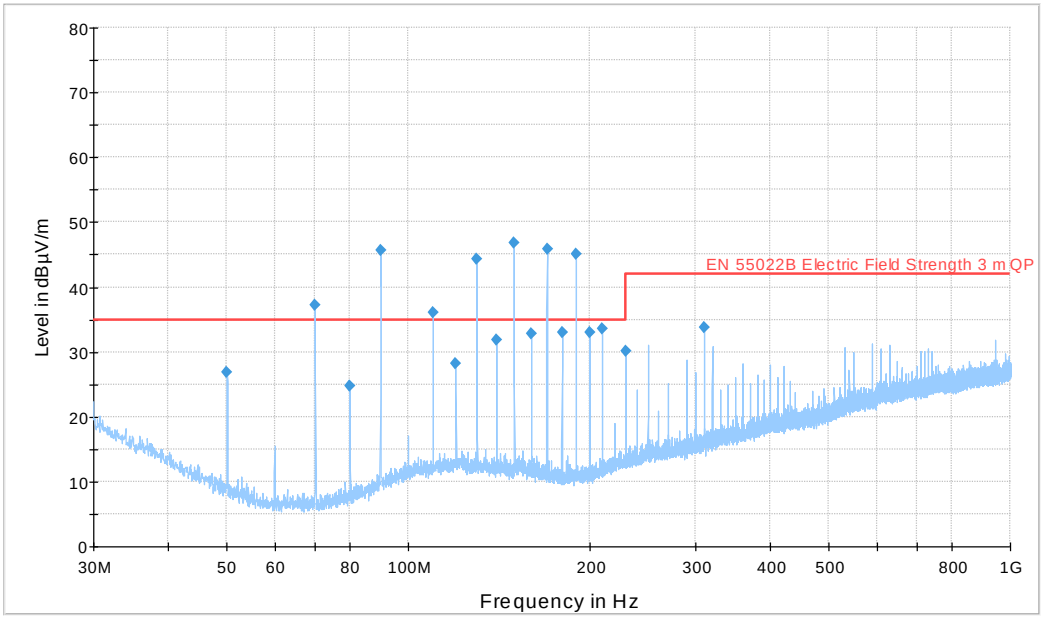

Figure 88. Results for one meter coaxial cable.

Table 18 shows results and we can see clearly that even and odd harmonics are present.

Table 18. Results for one meter coaxial cable.

Frequency (MHz)	QuasiPeak (dBµV/m)	Meas. Time (ms)	Bandwidth (kHz)	Antenna height (cm)	Polarity	TurnTable position (deg)	Corr. (dB)	Margin (dB)	Limit (dBµV/m)
49.980000	26.9	1000.00	120.000	155.0	H	-2.0	8.0	8.1	35.0
70.020000	37.2	1000.00	120.000	155.0	H	-2.0	5.7	-2.2	35.0
79.980000	24.7	1000.00	120.000	155.0	H	-2.0	7.1	10.3	35.0
90.000000	45.7	1000.00	120.000	155.0	H	-2.0	9.1	-10.7	35.0
109.980000	36.0	1000.00	120.000	155.0	H	-2.0	11.5	-1.0	35.0
120.000000	28.3	1000.00	120.000	155.0	H	-2.0	12.1	6.7	35.0
130.020000	44.3	1000.00	120.000	155.0	H	-2.0	11.6	-9.3	35.0
139.980000	31.8	1000.00	120.000	155.0	H	-2.0	11.2	3.2	35.0
150.000000	46.7	1000.00	120.000	155.0	H	-2.0	10.8	-11.7	35.0
160.020000	32.8	1000.00	120.000	155.0	H	-2.0	10.3	2.2	35.0
169.980000	45.9	1000.00	120.000	155.0	H	-2.0	9.7	-10.9	35.0
180.000000	33.0	1000.00	120.000	155.0	H	-2.0	9.1	2.0	35.0
190.020000	45.1	1000.00	120.000	155.0	H	-2.0	9.4	-10.1	35.0
199.980000	33.1	1000.00	120.000	155.0	H	-2.0	9.6	1.9	35.0
210.000000	33.5	1000.00	120.000	155.0	H	-2.0	10.3	1.5	35.0
229.980000	30.0	1000.00	120.000	155.0	H	-2.0	11.6	5.0	35.0
310.020000	33.7	1000.00	120.000	155.0	H	-2.0	14.3	8.3	42.0

The measurement has been done very close to the EMI-source. Some frequencies might get even higher values if measured from the center of the cable because of current distribution. (Ott 2009: 693)

The manufacturer Rohde & Schwarz gives transfer impedance values as a function of frequency for EZ-17-3 current probe, because then the current values can be calculated according to equation 45 which is actually Ohms law $I = U/Z$, but using relative dB units, where Z_T is transfer impedance and equation is

$$I\,[\mathrm{dB\mu A}] = U\,[\mathrm{dB\mu V}] - Z_T\,[\mathrm{dB\Omega}]. \quad (45)$$

Table 19 shows values for transfer impedance and some measured values which are the even and odd harmonics of the EMI-source. Datasheet for Rohde & Schwarz EZ-17-3 current probe is in Appendix 3.

Table 19. Transfer impedance values for EZ-17-3 current probe.

***f* [MHz]**	***U* [dBµV]**	**Z_T [dBΩ]**	**I_{CM} [dBµA]**
30	31.8	17	14.8
40	12.2	16.9	-4.7
50	37.5	16.7	20.8
60	17.4	16.5	0.9
70	40.4	16.7	23.7
80	23.5	16.4	7.1
90	41.7	16	25.7
100	7.5	15.9	-8.4
110	31.4	15.4	16
120	16.7	15.1	1.6
130	27.9	14.8	13.1
140	13.1	14.4	-1.3
150	29.8	13.9	15.9
160	18.6	12.5	6.1
170	31.2	11.7	19.5
180	20.6	11.3	9.3
190	34.7	11.1	23.6
200	24.8	8.3	16.5

The common-mode currents are measured with Rohde Schwarz EZ-17-3 and the results are excellent in Figure 89. All the odd harmonics are above the limit line which is also the same in far field measurement in Figure 88.

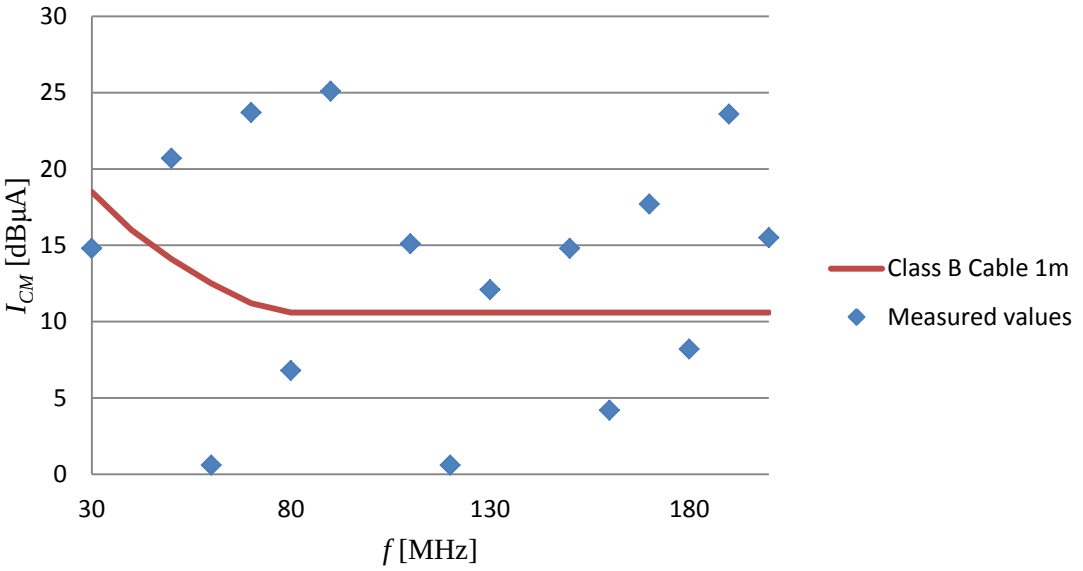

Figure 89. Common-mode current values for one meter coaxial cable, when coaxial cable connected to the EMI-source.

Figure 90 shows the situation when the Rohde Schwarz EZ-17-3 current probe is connected to the EMI-source.

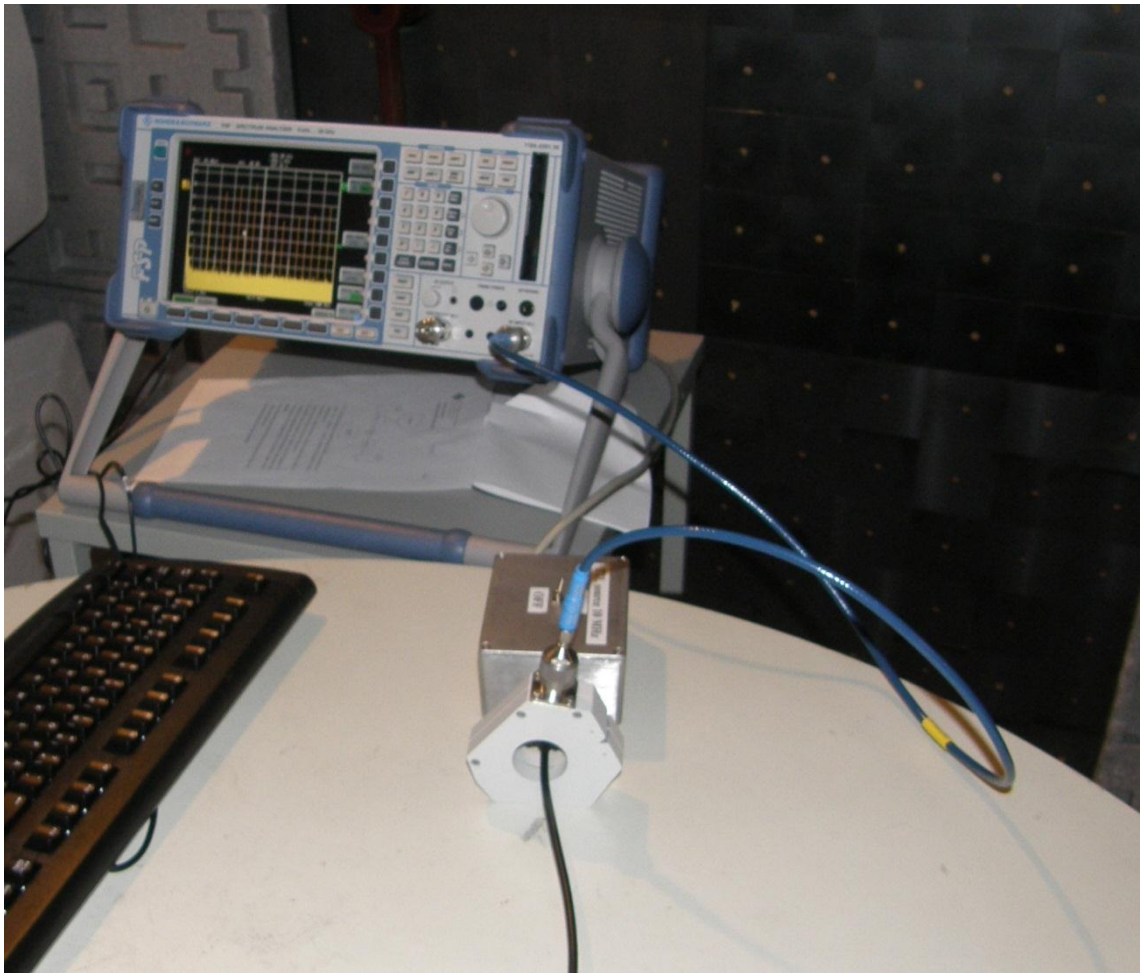

Figure 90. Common-mode current measurement by using Rohde Schwarz current probe EZ-17-3 and a spectrum analyzer.

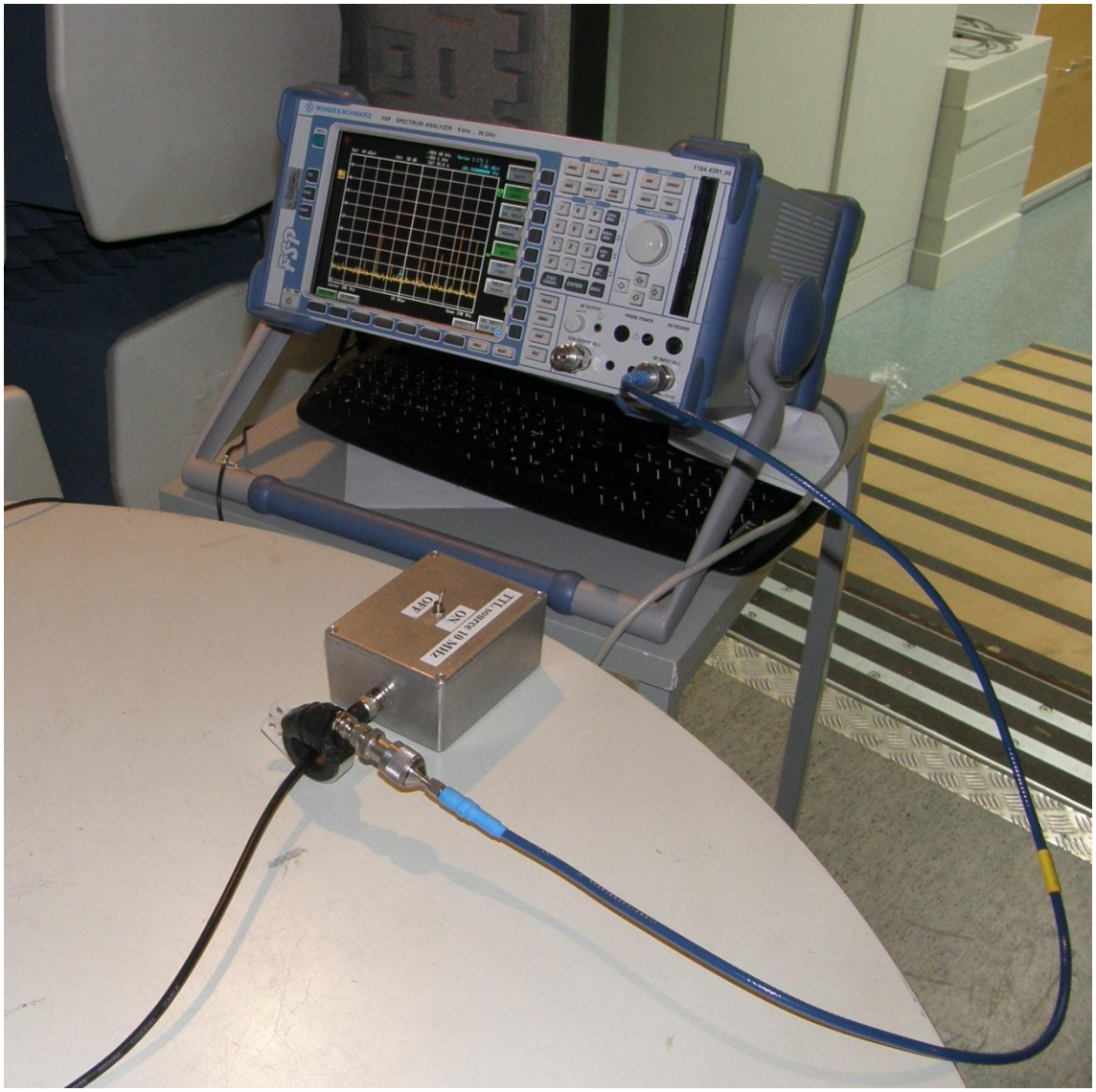

Figure 91. Common-mode current measurement by using the self-made current probe CP and a spectrum analyzer.

The comparison between EZ-17-3 and the self-made current probe CP can be seen in Figure 92. The results show that CP gives higher current values than the professional EZ-17-3 probe. The measurement compares output voltage values between these two current probes and no correction factors or transfer impedance correction is used in this measurement. Figure 92 shows that the CP can be used for comparative measurements and it can be used to find an interfering cable if a far field measurement has been done before measuring with the CP. The next task would be to define the transfer impedance

for the CP and it can be defined when a known current passes through probe and the voltage is measured from the secondary winding. (Clayton 2006: 519)

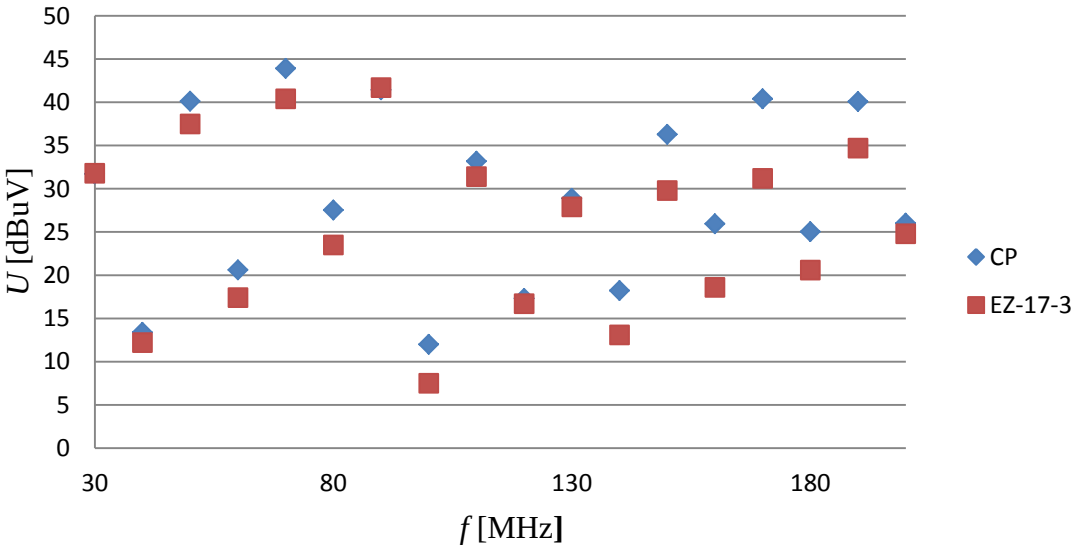

Figure 92. Comparison between the self-made current probe CP and the professional current probe Rohde Schwarz EZ-17-3.

6 DISCUSSION

The results have shown that the designed and manufactured electric field probe, magnetic field probe and the high-frequency current probe can be used to search for problematic radiation sources from an electronic device. The high-frequency current probe has to be improved from this CP version in order to measure common-mode current accurately, but still it can be used to make comparative measurements and it shows efficiently the source of a radiating cable. This study was very challenging because both issues theory and practical aspects have to be done. I think that electromagnetic compatibility (EMC) is one of the most difficult phases during electronic device design. With field theory the magnitude of electric field or magnetic field can be calculated, but for concrete device we need to make measurements in order to spot problematic electronic components, PCB traces, cables or enclosures.

Before this thesis I had only basic knowhow about antennas but no knowhow about near-field measurements. Now I have little bit deeper understanding of both issues, but still much more study is needed about antenna theory and near-field measurement techniques. Research should be continued in the future and more experience about near-field measurement is needed for the author. Research should be continued for high-frequency current probe to achieve better measurement accuracy.

7 CONCLUSIONS

Any equipment (EUT) which contains electronics is electro-magnetically very complex, because equipment can contain hundreds of active and passive components in the PCB. The verification of radiation (emission) is always a result of empirical testing. For electronic equipment the near-field measurements and common-mode current measurements are necessary to find radiation sources, because otherwise the EUT designer spends many hours by searching the source of radiation in expensive anechoic room. In general, the empirical test results can be explained by field theory, but many devices are so complex, that the simple field theory based explanation is challenging to find, because many variables in the electromagnetics like inductance, capacitance, radiation resistance, ohmic resistance of an antenna, skin depth are all frequency dependent.

In this thesis the antenna calculations are done and calculations show clearly that even a small common-mode current or a differential mode current will cause the EUT to fail in emission test. The intent was to design and manufacture an electric field probe, a magnetic field probe and a high-frequency current probe for near-field measurements and these probes are working well according to the measurement results. The designed high-frequency current probe cannot be used to measure high-frequency current accurately. The designed and manufactured high-frequency current probe can be used effectively after EUT far-field measurements are done to pin-point the cable or the wire which causes the radiation by using comparative measurements.

The expectations for this thesis were fulfilled from the author’s perspective, because most of the near-field probes worked without problems and only the high-frequency current probe should be improved. The author needs to make many more measurements from electronic devices with near-field probes to gain experience.

8 REFERENCES

Agilent technologies (2006). Spectrum Analysis Basics [online][referred 2.8.2011], Available: <http://cp.literature.agilent.com/litweb/pdf/5952-0292.pdf>.

Analab (1998). History of EMC [online][referred 2.8.2011], Available: <http://www.analab1.com/emc.html>.

Bk Precision (1996). Instruction manual Near-field "sniffer" probe model PR-261; 16 p.

Carr Joseph J (2001). Practical antenna handbook; 583 p. ISBN 0-07-138931-8.

CISPR22 ed6.0 (2008) Information technology equipment – Radio disturbance characteristics - Limits and methods of measurement; 164 p.

Clayton Paul (2006). Introduction to electromagnetic compatibility. Second edition; 983 p. ISBN 978-0-471-75500-5.

Com-power Corporation (2010). Near-field Probes PS-400 [online][referred 2.8.2011] Available: <http://www.com-power.com/ps-400_near_field_probes.html>.

Conformity (2007). Standards and Certification [online][referred 2.8.2011] Available: <http://www.conformity.com/artman/publish/printer_208.shtml>.

Crowell Benjamin (2010). Electricity and Magnetism. Light and Matter; 219 p. ISBN 0-9704670-4-4.

D.C. Smith Consultants (1999). Signal and noise measurement techniques using magnetic field probes [online][referred 2.8.2011], Available: <http://www.emcesd.com/pdf/emc99-w.pdf>.

Edminister Joseph A (1993). Electromagnetics. Second edition; 338 p. ISBN 0-07-018993-5.

Em scan. [online][referred 2.8.2011], Available: <http://www.emscan.com/emscan/AboutEMSCAN.cfm>.

ETS-Lindgren. Near-Field Probe Set [online][referred 2.8.2011], Available: <http://www.ets-lindgren.com/manuals/7405.pdf>.

High-frequency Design (2007). Basic Principles of Electrically Small Antennas [online] [referred 2.8.2011], Available: <http://www.highfrequencyelectronics.com/Archives/Feb07/HFE0207_tutorial.pdf>.

Huang Yi & Boyle Kevin (2008). Antennas from theory to practice, ISBN 978-0-471-75500-5.

HyperJeff Network (2010). Sketching the History of Classical Electromagnetism, [online][referred 1.5.2011], Available: <http://history.hyperjeff.net/electromagnetism>.

IEC 61000-6-2 ed2.0 (2005). Electromagnetic compatibility (EMC) – Part 6-2: Generic standards – Immunity for industrial environments; 38 p.

Institute of telecommunication sciences. Glossary of Telecommunication Terms [online][referred 2.8.2011], Available: <http://www.its.bldrdoc.gov/fs-1037/dir-008/_1097.htm>.

Lehto Arto (2006). Radioaaltojen maailma. Otatieto Oy; 301 p. ISBN 951-672-350-0.

McGraw-Hill Professional. Loop antennas [online][referred 2.8.2011], Available: <http://www.mhprofessional.com/downloads/products/0071475745/0071475745_chap05.pdf>.

Miron Douglas (2006). Small Antenna Design; 283 p, ISBN 978-0-7506-7861-2.

Nasa (1995). Electronic Systems Failures and Anomalies Attributed to Electromagnetic Interference. [online][referred 29.4.2011], Available: <http://hdl.handle.net/2060/19960009442>.

National Semiconductor (1996). Eliminating EMI in Microcontroller Applications [online][referred 26.5.2011], Available: <http://www.national.com/an/AN/AN-1050.pdf>.

Nikolova Natalia (2010). Introduction into the Theory of Radiation [online][referred 26.5.2011], Available: <http://www.ece.mcmaster.ca/faculty/nikolova/antenna_dload/current_lectures/L02_EMbasics.pdf>.

Orfanidis Sophocles J. (2008). Electromagnetic Waves and Antennas [online] [referred 1.5.2011], Available: <http://www.ece.rutgers.edu/~orfanidi/ewa>.

Ott Henry W (2009). Electromagnetic compatibility engineering, ISBN 978-0-470-18930-6.

Renesas (2007). Microcontrollers Enrich our Lives [online][referred 26.5.2011], Available: <http://www2.renesas.com/csr/en/pdf_2007/csrreport_2007_en_03.pdf>.

Sepponen Raimo (2011). Piirilevyn häiriöiden syntymekanismit sekä piirilevyn häiriöiden rajoittaminen (seminar publication).

STM Microelectronics (2000). EMC guidelines for Microcontroller based applications [online][referred 26.5.2011], Available: http://www.st.com/stonline/books/pdf/docs/4967.pdf>.

Tukes. Sähkömagneettinen yhteensopivuus (EMC) [referred 28.4.2011], Available: <http://www.tukes.fi/fi/Toimialat/Sahko-ja-hissit/EMC>.

UNC School of Medicine. Sources of Electromagnetic Interference (EMI) [online][referred 26.5.2011], Available: <http://www.med.unc.edu/medicine/card/fellows/patientinstructions/EMI.pdf>.

University of Toulouse (2007). Towards an EMC roadmap for Integrated Circuits [online][referred 29.4.2011], Available: <http://www.lesia.insa-e.fr/~emccompo/topics/EMC_Compo07_Towards_Roadmap_v5.pdf>.

Vesapuisto Maarit (2009). Antennit [online][referred 26.5.2011], Available: <http://lipas.uwasa.fi/~mave/SAH104/DynAntenneista091203.pdf>.

Willis Tim (2007). EMC for product designers. Fourth edition; 498 p. ISBN 0-7506-8170-5.

Appendix 1 Loop antenna as receiver

In appendix 1 figure ab right side blue arrows are external flux ϕ perpendicular (normal) against loop and loop is placed to origin of cylindrical coordinate system**,** V_{OC} is induced voltage which is caused by change in external flux ϕ (in this case uniform magnetic flux density $\boldsymbol{B}$ perpendicular through loop, which absolute value can be calculated $|B_0| = \phi/S$ where S is loop surface area and environment is vacuum where $|B_0| = \mu_0|H|$), red arrow is current I which has a such direction that it creates the flux which opposes the external flux. The differential loop surface area d$\boldsymbol{S}$ can be calculated according the equation in Figure ab left side.

Given values:

$\boldsymbol{B} = B_0 \sin(\omega t)(-\boldsymbol{e}_Z)$

$d\boldsymbol{S} = dl_1 dl_2 \boldsymbol{e}_Z = \rho d\phi d\rho \boldsymbol{e}_Z$

$B_0 = \mu_0 H$

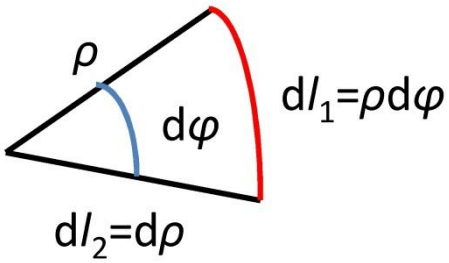

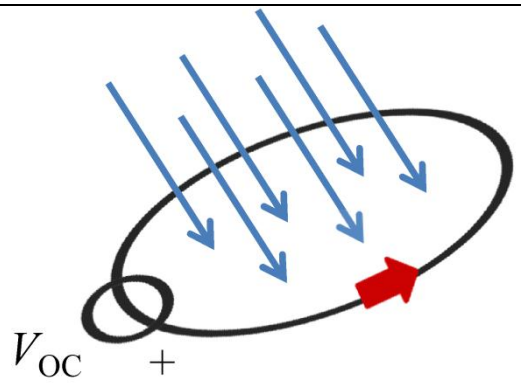

Figure ab. Receiving loop antenna.

According to Faradays law the induced voltage can be calculated

$$V_{OC} = \oint \boldsymbol{E} \cdot d\boldsymbol{l} = \int_S \left(-\frac{\partial \boldsymbol{B}}{\partial t} \right) \cdot d\boldsymbol{S}$$

$$V_{OC} = \int_S \left(-\frac{\partial \boldsymbol{B}}{\partial t} \right) \cdot d\boldsymbol{S}$$

$$V_{OC} = \int_S \left[\left(-\frac{\partial (B_0 \sin(\omega t)(-\boldsymbol{e}_Z))}{\partial t} \right) \cdot \rho d\varphi d\rho \boldsymbol{e}_Z \right]$$

$$V_{OC} = -\frac{\partial}{\partial t}\int_0^{2\pi}\int_0^{a}\left(B_0 \sin(\omega t)(-\boldsymbol{e_z})\cdot \rho \,\mathrm{d}\rho \mathrm{d}\varphi(\boldsymbol{e_z})\right)$$

$$V_{OC} = \frac{\partial}{\partial t}\int_0^{2\pi}\int_0^{a}\left(B_0 \sin(\omega t)\rho \,\mathrm{d}\rho \mathrm{d}\varphi\right)$$

$$V_{OC} = \frac{\partial B_0 \sin(\omega t)}{\partial t}\int_0^{2\pi}\int_0^{a}\left(\rho \,\mathrm{d}\rho \mathrm{d}\varphi\right)$$

$$V_{OC} = \frac{\partial B_0 \sin(\omega t)}{\partial t}\left(\left[\rho^2\right]_0^a 2\pi\right)$$

$$V_{OC} = \frac{\partial B_0 \sin(\omega t)}{\partial t}\left(2\pi\frac{a^2}{2}\right)$$

$$V_{OC} = \frac{\partial B_0 \sin(\omega t)}{\partial t}\left(\pi a^2\right)$$

$$V_{OC} = B_0\left(\pi a^2\right)\frac{\partial \sin(\omega t)}{\partial t}$$

$$V_{OC} = B_0\left(\pi a^2\right)\cos(\omega t)\omega$$

$$V_{OC} = B_0\left(\pi a^2\right)\cos(2\pi\, ft)2\pi\, f$$

$$V_{OC} = B_0(S)\cos(2\pi\, ft)2\pi\, f$$

$$V_{OC} = 2\pi\, f\, B_0 S\cos(2\pi\, ft)$$

$$\left|V_{OC}\right| = 2\pi\, f\, SH\,\mu_0$$

The result shows that induced voltage has a directional proportion to the frequency *f* and to the incoming magnetic field *H* and to the surface area *S* (in calculations the variable *a* is loop radius). The loop area should be kept small in PCBs in order to reduce induced voltage.

Appendix 2 Wurth ferrite 7427135 datasheet

Spezifikation für Freigabe / specification for release

Kunde / customer :_____

Artikelnummer / part number : **7427135**

Bezeichnung : **FERRITRING MIT NYLONHALTER**

description : **SPLIT FERRITE WITH NYLON CLAMP**

compliant RoHS WÜRTH ELEKTRONIK

WÜRTH ELEKTRONIK

DATUM / DATE : 2007-01-30

A Mechanische Abmessungen / dimensions:

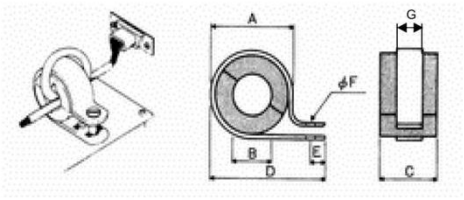

A	**44,6 ± 1,0**	mm
B	**27,5 ± 0,5**	mm
C	**15,0 ± 0,5**	mm
D	**55,3 ± 1,0**	mm
E	**6,3 ± 0,8**	mm
F	**5,1 ± 0,4**	mm
G	**-**	mm

B Elektrische Eigenschaften / electrical properties:

Eigenschaften / properties	Testbedingungen / test conditions		Wert / value	Einheit / unit	Tol.
Impedanz @ 1 Wg./ impedance @ 1 turn	**25 MHz**	Z	**48**	Ω	**± 25%**
Impedanz @ 1 Wg./ impedance @ 1 turn	**100 MHz**	Z	**98**	Ω	**± 25%**
Impedanz @ 2 Wg./ impedance @ 2 turn	**25 MHz**	Z	**197**	Ω	**± 25%**
Impedanz @ 2 Wg./ impedance @ 2 turn	**100 MHz**	Z	**382**	Ω	**± 25%**

C

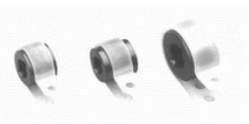

D Prüfgeräte / test equipment:

HP 4191 B für/for Z und/and material

16092A - Klemme / clamp

AWG26 - Ø 0,5mm - Länge/length: 165 mm

E Testbedingungen / test conditions:

Luftfeuchtigkeit / humidity: 33%

Umgebungstemperatur / temperature: + 20°C

F Werkstoffe & Zulassungen / material & approvals:

Basismaterial / base material: 4 W 620

Kunststoff / plastic material: PA 6.6

UL-Zulassungen / UL-approval: UL94-V2

UL file no: E140736(M)

Klebeband / adhesive tape: 3M 5386

G Eigenschaften / general specifications:

Curietemperatur / curie temperature: + 150°C

Kabeldurchmesser / cable diameter [mm]: ≤ 26,5

Lagertemperatur / storage temperature: -40°C ~ + 85°C

Betriebstemp. / operating temperature: -25°C ~ +105°C

Freigabe erteilt / general release: **Kunde / customer**

Datum / date — Unterschrift / signature

Würth Elektronik

Geprüft / checked — Kontrolliert / approved

Name	Änderung / modification	Datum / date
KSC	Version 4	07-01-30
LF	RoHS update	04-10-11
LF	Clip	03-08-14
JH	Neugestaltung	00-12-06

Würth Elektronik eiSos GmbH & Co. KG

D-74638 Waldenburg · Max-Eyth-Strasse 1 - 3 · Germany · Telefon (+49) (0) 7942 - 945 - 0 · Telefax (+49) (0) 7942 - 945 - 400

http://www.we-online.com

Spezifikation für Freigabe / specification for release

Kunde / customer : _____

Artikelnummer / part number : **7427135**

Bezeichnung : **FERRITRING MIT NYLONHALTER**

description : **SPLIT FERRITE WITH NYLON CLAMP**

compliant RoHS WÜRTH ELEKTRONIK

WÜRTH ELEKTRONIK

DATUM / DATE : 2007-01-30

H Impedanzverlauf / impedance curve:

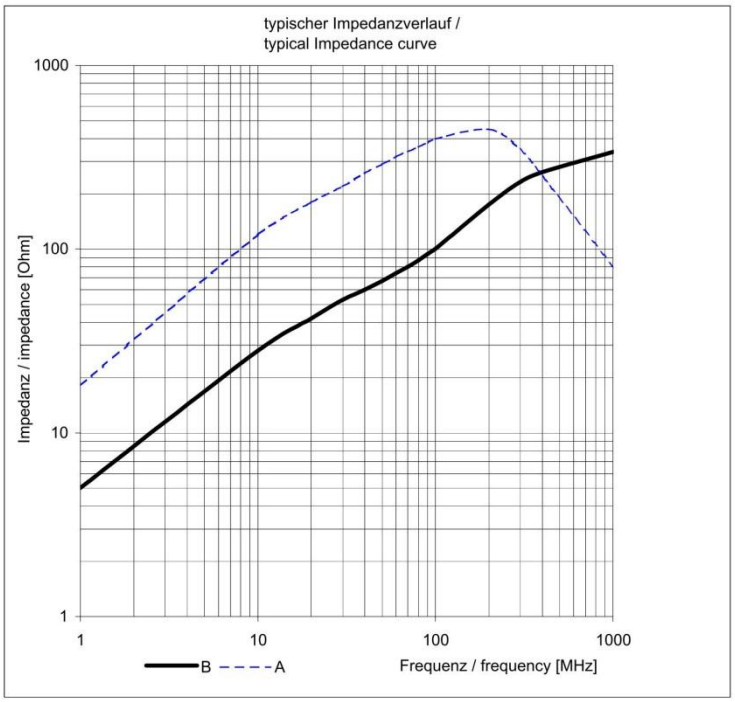

A: 2 x durch Bohrung Ferrit / 2 x times through ferrite

B: 1 x durch Bohrung Ferrit / 1 x times trough ferrite

Freigabe erteilt / general release:	Kunde / customer			
Datum / date	Unterschrift / signature	KSC	Version 4	07-01-30
	Würth Elektronik	LF	RoHS update	04-10-11
		LF	Clip	03-08-14
		JH	Neugestaltung	00-12-06
Geprüft / checked	Kontrolliert / approved	Name	**Änderung / modification**	Datum / date

Würth Elektronik eiSos GmbH & Co. KG

D-74638 Waldenburg · Max-Eyth-Strasse 1 - 3 · Germany · Telefon (+49) (0) 7942 - 945 - 0 · Telefax (+49) (0) 7942 - 945 - 400

http://www.we-online.com

Appendix 3 Rohde & Schwarz EZ-17-3 high-frequency current probe

Data sheet

Version 03.01

March 2005

Current Probe R&S®EZ-17

Electromagnetic emission and susceptibility measurements in the range 20 Hz to 100 (200) MHz

- Wide frequency range
- High sensitivity
- High load capacity for DC and AC currents (300 A)
- Small dimensions in spite of large inner diameter (30 mm)
- Simple clamping thanks to spring-loaded mechanism
- Calibrated to CISPR 16-1-2

ROHDE&SCHWARZ

- Model 02 for emission measurements in the range 20 Hz to 100 (200) MHz
- Model 03 for emission and susceptibility measurements in the range 20 Hz to 100 (200) MHz

Description

RF currents carried on supply and control lines of equipment and systems can be measured with the aid of current probes clamped on to the conductors. The current probe itself forms a transformer, the current-carrying conductor being its primary winding. A voltage proportional to the primary current is measured at the RF output of the current probe.

Fields of application

Current probes are used in particular where other coupling networks, such as line-impedance stabilization networks, are either not available or not suitable for practical reasons. Current probes are however also used to measure the electromagnetic susceptibility of equipment and systems. With the aid of the current probe, sinewave or pulse-shaped RF current is injected into lines or cable harnesses. The shielding effectiveness of RF cables can also very easily be measured with the aid of current probes. The Current Probes R&S®EZ-17 comply with the following standards:

- CISPR 16-1 and VDE 0876 Part 1/ Part 161 for standards stipulating maximum values for RFI current
- MIL-STD-461 A, B and C CE 01 and 03 as well as MIL-STD-461D/E CE 101
- VG 95373 Part 20 and VG 95377 Part 14
- DEF STAN 59-41 DCE 01 and 02
- GAM EG 13
- RTCA/DO 160 C and ED-14-C

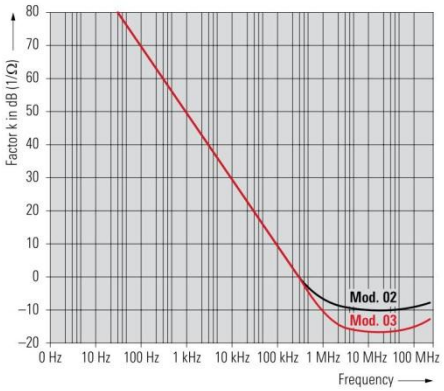

Transducer factor k of the three models of the Current Probe R&S®EZ-17

Three models to suit different applications

The models 02 and 03 of the Current Probe R&S®EZ-17 are suitable for the following applications in the frequency range 20 Hz to 100 MHz:

- Model 02 with its flat frequency response above 1 MHz and output impedance of 50 Ω is ideal for emission measurements as well as for measuring the shielding effectiveness
- Due to its small transducer factor in the range from 1 MHz to 200 MHz, model 03 is particularly suitable for emission measurements with stringent requirements placed on sensitivity (e.g. VG 95 373 limit class 1) and, due to its high load capacity, also recommended for EMS measurements (bulk current injection tests)

Owing to their high magnetic overload capacity, the Current Probes R&S®EZ-17 can be used on three-phase power lines with currents up to 300 A without any adverse effect on the result of the RF current measurement. The small dimensions – despite the large inner diameter – and the simple clamping mechanism allow the current probes to be used even where space is at a premium.

Specifications

	Model 02	Model 03
Frequency range	20 Hz to 100 (200)[1] MHz	20 Hz to 100 (200)[1] MHz
Range with constant transducer factor (–3 dB)	1 MHz to 100 MHz	2 MHz to 100 MHz
Transducer factor reduced by 20 dB/decade in range	20 Hz to 1 MHz	20 Hz to 2 MHz
RF connector	N female	N female
Output impedance	50 Ω (f ≥ 10 MHz)	reactive
VSWR	<2 (f > 10 MHz)	—
Insertion impedance	≤0.8 Ω	≤1 Ω
Transfer impedance Z_t		
In range with constant transducer factor	3.16 Ω	7.1 Ω
Transducer factor k[1] in range with flat frequency response	–10 dB (1/Ω)	–17 dB (1/Ω)
Effect by external magnetic fields		
Suppression of indication from current-carrying conductors next to probe	>40 dB	>40 dB
Load capacity (RF current measurement)		
Max. DC current or peak AC current	300 A (f < 1 kHz)	300 A (f < 1 kHz)
RMS value of RF current	2 A (f > 1 MHz)	1 A (f > 1 MHz)
Load capacity (EMS measurement)		
AC (RMS value)	6 A (f < 1 kHz)	6 A (f < 1 kHz)
Dropping to	0.2 A (up to 1 MHz) 2 W (f > 1 MHz)	0.45 A (up to1 MHz) 10 W (f > 1 MHz) (50 W for max. 15 min)
General data (all models)		
Operating temperature range	–10 °C to +55 °C	
Storage temperature range	–25 °C to 70 °C	
Permissible core temperature	80 °C	
Mechanical stress	shock-tested to MIL-STD-810D (shock spectrum, 40 g), vibration-tested to MIL-T-28800D, class 5; EN 60068-2-6	
Dimensions		
L × W × H	95 mm × 84 mm × 26 mm	
Inner diameter	30 mm	
Weight	0.6 kg	

[1] The manual contains a table specifying the transducer factor from 20 Hz to 200 MHz.
The transducer factor k is calculated as $k = 20 \log (1/Z_t)$, where Z_t is the transfer impedance.

Ordering information

Current Probe		
Model 02: 20 Hz to 100 MHz	R&S®EZ-17	0816.2063.02
Model 03: 20 Hz to 100 MHz	R&S®EZ-17	0816.2063.03
Accessories supplied		
Model 02	RF connecting cable with N connectors (1 m), coding connector	
Model 03	RF connecting cable with N connectors (1 m)	
Both models	operating manual with information on relevant transducer factor	

More information at
www.rohde-schwarz.com
(search term: EZ-17)

Certified Quality System ISO 9001 DQS REG. NO 1954 QM

Certified Environmental System ISO 14001 DQS REG. NO 1954 UM

ROHDE&SCHWARZ

www.rohde-schwarz.com
Europe: Tel. +49 1805 12 4242, e-mail: customersupport@rohde-schwarz.com · North America: Tel. +1 410-910-7988, e-mail: customer.support@rsa.rohde-schwarz.com
Asia: Tel. +65 68463710, e-mail: customer-service@rssg.rohde-schwarz.com

ROHDE & SCHWARZ

Conversion factor for

Current Probe EZ-17

Model Number: 816.2063.02/03

Serial Number: 841.384/016

Calibrated (DD/MM/YY): 11. 1. 96

Frequency	Conv.Factor/dB	Frequency	Conv.Factor/dB
20 Hz	80,1 dB	500 kHz	- 5,6 dB
100 Hz	66,4 dB	1 MHz	- 10,8 dB
200 Hz	60,5 dB	2 MHz	- 14,7 dB
500 Hz	52,8 dB	5 MHz	- 16,8 dB
1 kHz	47,0 dB	10 MHz	- 17,2 dB
2 kHz	41,3 dB	20 MHz	- 17,1 dB
5 kHz	33,5 dB	50 MHz	- 16,7 dB
10 kHz	27,7 dB	100 MHz	- 15,9 dB
20 kHz	21,7 dB	125 MHz	- 15,1 dB
50 kHz	13,9 dB	150 MHz	- 13,9 dB
100 kHz	7,9 dB	175 MHz	- 11,8 dB
200 kHz	2,0 dB	200 MHz	- 8,3 dB